# International Geology Review



Vol. 1, No. 4 April 1959



- complete table of contents inside -

*published by the*
**AMERICAN GEOLOGICAL INSTITUTE**

The American Geological Institute operates under the National Academy of Sciences. It is governed by an Executive Committee and a Board of Directors composed of two directors from each of the fourteen Member Societies.

International Geology Review is published monthly by the American Geological Institute with the assistance of an initiating grant from the National Science Foundation. The journal will report in English on significant developments in pure and applied geologic research which appear in foreign language journals, especially those published in the U.S.S.R.

The editors of International Geology Review will give consideration to full English translations, condensations and reviews submitted voluntarily for publication. Translators will be appropriately credited. Original papers of international significance will also be considered for publication.

Readers are invited to direct to the editors their comments and discussions of articles published in the International Geology Review. Readers are encouraged also to submit suggestions as to published foreign literature considered worthy of translation and publication. Such suggestions should relate to materials of broad, general interest, rather than materials of limited reader interest.

*Address editorial and subscription inquiries to*

**AGI TRANSLATIONS OFFICE**
**AMERICAN GEOLOGICAL INSTITUTE**
**2101 Constitution Avenue, N.W., Washington 25, D. C.**

The basic subscription rate for International Geology Review is $55 per year, 12 issues. A special subscription rate of $15 per year is available to members of AGI Member Societies who are on the GEOTIMES mailing list and who will pledge to restrict the journal to their personal use. The $15 per year subscription rate is also available to educational institutions and personnel. Foreign postage: No additional charge to Canada and Mexico; to Pan American Union countries add $0.50 per year; to all other foreign countries add $1.00 per year. Single copy price $5.00 ($1.50 to subscribers qualifying for special rates). Second class postage paid at Washington, D. C.

# International Geology Review

*published monthly by the*
AMERICAN GEOLOGICAL INSTITUTE

Vol. 1, No. 4. April 1959

CONTENTS



REVIEW SECTION



INTERNATIONAL SCIENTIFIC MEETINGS

## IGR TRANSLITERATION OF RUSSIAN[1]

The AGI Translation Center has adopted the essential features of Cyrillic Transliteration recommended by the U. S. Department of the Interior, Board of Geographical Names, Washington, D. C.

| Alphabet | | transliteration |
|---|---|---|
| А | а | a |
| Б | б | b |
| В | в | v |
| Г | г | g |
| Д | д | d |
| Е | е | e, ye (1) |
| Ё | ё | ё, yё |
| Ж | ж | zh |
| З | з | z |
| И | и | i (2) |
| Й | й | y |
| К | к | k |
| Л | л | l |
| М | м | m |
| Н | н | n |
| О | о | o |
| П | п | p |
| Р | р | r |
| С | с | s |
| Т | т | t |
| У | у | u |
| Ф | ф | f |
| Х | х | kh |
| Ц | ц | ts |
| Ч | ч | ch |
| Ш | ш | sh |
| Щ | щ | shch |
| Ъ | ъ | " (3) |
| Ы | ы | y |
| Ь | ь | ' (3) |
| Э | э | e |
| Ю | ю | yu |
| Я | я | ya |

However, the AGI Translation Center recommends the following modifications:

1. Ye initially, after vowels, and after ъ, ь. Customary usage calls for "ie" in many names, e.g., SOVIET KIEV, DNIEPER, etc.; or "ye", e.g., BYELORUSSIA, where "e" follows consonants. "e" with dieresis in Russian should be given as "yo".

2. Omitted if preceding a y, e.g., Arkhangelsky (not iy; not ii).

3. Generally omitted.

NOTE: The well-known place and personnel names that have wide acceptance in international literature will be here adopted. However, German-type transliteration e.g., J for Y will not be used.

---

[1] Due to the individual training and tastes of the translators and reviewers whose work is published in this issue of IGR., it has been impossible to follow the above recommended system. In the near future, however, an effort will be made to standardize transliteration procedures.

# PRINCIPAL FEATURES OF THE TECTONIC STRUCTURE OF TURKMEN SSR

## Subtitle: On the Problem of the Oil- and Gas-Bearing Character of the Western Regions of Central Asia[1]

*by*

*Yu. N. Godin, N. P. Luppov, Yu. I. Sytin, and P. K. Chikhachev*

*• translated by Theodore Shabad •*

### INTRODUCTION

The Western part of Soviet Central Asia is of interest to researchers as an undoubtedly potential oil and gas-bearing region. This expectation is based on the geographical location of the area in the over-all regional tectonic pattern and on the structural and facies characteristics of the sedimentary deposits; and it is confirmed by the actual existence of many oil and gas shows and commercial oil and gas deposits.

A comparison of the geological structure of western Central Asia with that of neighboring regions known to be oil-bearing shows, on the one hand, and similar structural features among the various regions, on the other hand, points to the fact that the sedimentary facies associated with commercial oil deposits in neighboring regions also occur in the western parts of Central Asia. All this supports the conclusion that the presence of large new oil and gas deposits can be expected within the area under study.

However, our geological knowledge of the western part of Central Asia is still not sufficient to enable us to say specifically what areas offer the greatest promise for prospecting and exploration for oil and gas, what sediments in any given area would be associated with commercial oil and gas deposits, or under what tectonic conditions and at what depths such deposits may be found. The following results of a study of the deep-seated tectonics of the western parts of Central Asia represent one more step toward the solution of the complex and topical problems.

### PRINCIPAL STAGES OF THE GEOLOGICAL DEVELOPMENT OF WESTERN CENTRAL ASIA

The present tectonic structure of the studied area arose in the course of the long and complex history of its geologic development. That history may be divided into several major stages, each of which corresponds to the development of a structural phase that differs in its structural feature from that formed during the preceding historical stage.

If we exclude Precambrian time, for which we have no data within the studied area, we find that the two most important stages in the geologic development of western Central Asia were the Paleozoic and the Mesozoic-Cenozoic. In addition there seems to have been a transitional stage covering the late Paleozoic and early Mesozoic (Permian and Triassic). Finally, the second major stage may be divided in turn into two second-order stages, one of which covered the Jurassic and Cretaceous periods and the Paleocene, and the second the Neocene [Ed. note: Neocene is taken to be generally equivalent to Miocene-Pliocene. ] and the Quaternary. We thus have four stages of geologic history and four corresponding structural stages.

Characteristic features of the Paleozoic stage are the existence of geosynclinal conditions over a large part of the area and the occasional occurrence of intensive volcanic activity. The existence of geosynclinal conditions led to the accumulation of thick sediments, mainly of marine origin, in facies that are characteristic for geosynclines.

The Paleozoic sediments, which have been intensively dislocated over a large part of the area, and are more or less metamorphosed and intruded by igneous rocks, outcrop only in a few places, chiefly in the east, where they constitute the hills of the Kyzyl-Kum and show up in outliers of the Zeravshan and Gissar ranges. Over most of the study area the Paleozoic sediments lie at great depths, constituting the basement on which Mesozoic and Cenozoic sediments now rest.

The Permian-Triassic stage of geologic development is characterized by occasional downwarping against a general background of uplifting. The thick Permian and Triassic sediments that accumulated in these occasional depressions are of both marine and continental origin. These zones of sediment accumulation

---

[1]Translation of Osnovnye osobennosti tektonicheskovo stroyenya territorii Turkmenskoy SSR. (K probleme neftegazonosnostizapadnykh oblastey Sredney Azii): Sovetskaga Geologiya, 1958, no. 1, p. 3-24.

are most evident in the Emba oil-bearing region, in the Mangyshlak and in Tuarkyr. Possibly they also exist in other areas where they have been buried by younger sediments. Judging from the single case of the Tuarkyr area and from data on more easterly parts of central Asia, the accumulation of sediments was associated with volcanic activity.

Permian-Triassic sediments in Mangyshlak and Tuarkyr were later also subjected to folding. They thus form a distinct structural stage that differs in degree of dislocation and metamorphism both from the lower structural stage and from the upper stages.

Over a large part of the studied area there was evidently no accumulation of sediments during the Permian-Triassic stage. The beginning of the stage was marked by folding and probably the entry of intrusions, followed by a long process of peneplanation. This process eliminated the Permian-Triassic stage over most of the area; the subsequent stage thus rests directly on the Paleozoic, as can be seen most clearly in the Kyzyl-Kum. On the basis of geophysical data, we can expect the same situation in the Trans-Unguz Karakum, in the Kara-Bogaz-Gol area and in the Krasnovodsk peninsula.

The third geologic stage, covering the Jurassic, Cretaceous and Paleocene, which is the most important from the standpoint of the oil and gas-bearing problem, is characterized by renewed subsidence extending more or less over the entire studied area. These downwarps, starting in various times (during the Jurassic in most of the western areas, and during the Cretaceous in the Kyzyl-Kum), led to renewed sediment accumulation over vast areas.

One of the most characteristic features of this stage is the differentiation of the studied area into a more mobile geosynclinal zone along the southern margin and a more stable cratonic zone in the rest of the area. This division existed throughout this stage and led to considerable differences in the thickness and facies of sediments.

The conditions under which sediments accumulated in various parts of these zones were not uniform and changed with time, producing an alternation of marine, lagoon and continental facies. Volcanism during this stage was restricted to Badkhyz, in the extreme south, where it occurred in the Paleocene.

Crustal movements from time to time interrupted the depositional process over substantial parts of the area. Occasionally folding of moderate intensity took place. These crustal movements were most evident in the Late Jurassic and at the border between the Cretaceous and the Paleocene. However, these movements did not result in any significant structural changes and did not affect the overall process of sediment deposition. From the structural standpoint, therefore, the entire sequence of Jurassic, Cretaceous and Paleocene sediments must be regarded as one series forming a single structural stage.

While affirming the structural unity of the Jurassic-Paleocene series, we must, however, bear in mind that there may not be complete conformity among the various component members of the stratigraphic cross section, as may be found in detailed geophysical surveys and by drilling. This factor may be significant in exploring any specific structures for oil and gas. This consideration does not alter the basic proposition that the entire Jurassic-Cretaceous-Paleocene complex has common structural characteristics distinguishing it clearly from both older and younger geologic formations.

The last historical stage, covering the Neocene and Quaternary, is characterized by tectonic movements of the Alpine cycle. Starting as early as the late Paleocene, the movements became more intense in the early Neocene and continued till the Quaternary. Evidences of these movements can be observed through almost the entire studied area, though different sections were affected to varying degrees.

In the geosynclinal zone these movements were relatively more intense and of longer duration. They led to a reshaping of the earth's crust, producing a folded region in place of the geosyncline. Sediment accumulation was limited to downwarps and to the periphery of the uplifted ranges, which were subjected to intensive erosion. Sediment deposition continued through the period of tectonic movements, resulting in more or less considerable dislocation of sediments and the presence of unconformities.

In the cratonic zone, the more intensive movements were restricted to the initial stages of the Alpine cycle, when gentle folds were formed in sediments of the Jurassic-Paleocene stage and parts of the lower structural stages were uplifted in some places and outcropped in the form of hilly areas. This initial period was followed by the accumulation of relatively thin sedimentary beds over vast areas, interrupted now and then by local uplifting. These slight tectonic movements dislocated areas of Neocene and Quaternary deposition and produced gentle downwarps of the sediments themselves. These downwarps are evident mainly in the older members of the stratigraphic cross section (in the Miocene), and are virtually absent in younger strata. In general the Neocene-Quaternary stage of the cratonic zone has been only slightly affected by dislocations.

A characteristic feature of this stage is the

occurrence of tectonic depressions formed through more or less intensive downwarping of the earth's crust. These depressions became sites of heavier deposition of Neocene and Quaternary sediments than was the case in the rest of the studied area. The most marked depressions occurred within the geosynclinal zone and along its border with the cratonic zone.

The above-mentioned differences in the structure of the various stages point to different degrees of oil and gas-bearing prospects. Of greatest interest is the third (Jurassic-Paleocene) stage, whose structural features and facies favor oil and gas accumulation in various parts of the studied area depending on local conditions.

The upper structural stage in most of the studied area functions as an overburden over sediments and structures that may be associated with oil deposits. The only exception is provided by the young tectonic depressions, where the existence of oil deposits in sediments of the upper stage is quite possible, and has actually been proven in the south. The lower structural stages, at the present state of our knowledge, cannot be regarded as being of immediate interest for oil and gas exploration in view of their great depth and intensive dislocation and metamorphism.

This situation is subject to change if special regional seismic and core-drill surveys disclose areas of less dislocated and unmetamorphosed Paleozoic and Triassic sediments. Such a case has already been established in the Northern Ustyurt, on the northern margin of the studied area, where structural conditions and the character of the sediments favor the presence of oil deposits in the Paleozoic.

## DIAGRAM OF THE TECTONIC STRUCTURE OF TURKMENISTAN AND ADJOINING AREAS

The delimiting of tectonic regions in western Central Asia represents the first step in establishing structural features that favor oil and gas deposition. Because of inadequate geologic data for the studied area and in view of the very uneven distribution of deep core holes, any present delimitation of regional zones whose structure and facies favor oil and gas accumulation must be based mainly on geophysical data.

Since geophysical surveys in the past covered mainly the western and some central sections of Turkmenia, the first tectonic maps were restricted to that part of Central Asia. It was only in 1956, after magnetic air surveys had been conducted in most of western Central Asia and after gravity-meter surveys had been made along the Amu Darya and in southeastern Turkmenia, that it became possible to compile the first version of a tectonic map for the vast area extending from the Paleozoic hills of the Kyzyl-Kum west and southwest to the Caspian Sea. This area contains most of the prospective oil and gas sites of western Central Asia.

The attached diagrammatic map of the tectonics of Turkmenistan and adjoining areas is based on geologic and geophysical work done in the studied area up to 1957. The limited scope of the present paper does not permit detailed discussion of the methodology used in compiling the tectonic regions on the map. Since the methodology is important in itself, all the principles that guided us in the complex analysis of the geologic and geophysical data at our disposal will be discussed in a separate paper.

In compiling the map we made use of data supplied by the former Ministry of the Petroleum Industry, the Ministry of Geology and Mineral Conservation, and the Academy of Sciences of the U. S. S. R.

Coordinated analysis of geophysical data covering the western part of Central Asia permits division of the entire area into two fundamentally distinct sections: a cratonic section and a geosynclinal section. There is apparently no clearly definite boundary between the two, but an intermediate zone can be identified with sufficient certainty. This zone extends from the Krasnovodsk peninsula and the Bolshoi Balkhan through the Kopet-Dag foreland trough to Kaakhka, and then turns south following approximately along the Soviet frontier.

### A. The Cratonic Section of Turkmenistan and Adjoining Areas.

The cratonic section of the studied area is made up of a number of relatively stable tectonic zones that have developed under steady cratonic conditions since the middle Paleozoic, and perhaps even since the Precambrian. These zones, hereafter called inner blocks, are bounded by mobile belts of tectonically more active sectors that are clearly distinguished in terms of their geophysical fields and form a frame around the stable zones. We have distinguished four such inner blocks (see map):

(1) the Northern Ustyurt block;
(2) the Krasnovodsk-Karabogaz block;
(3) the Southern Ustyurt block;
(4) the Kara-Kum block

The Northern Ustyurt inner block (I on the map) is situated in the northern part of the studied area and covers the greater part of the Ustyurt. On the northwest this block is bounded by the mobile zone of the South Emba cratonic uplifts, which is probably associated with a region of ancient, deep-seated fractures, judging from geophysical data and deep borings. It is also possible that this zone is associated

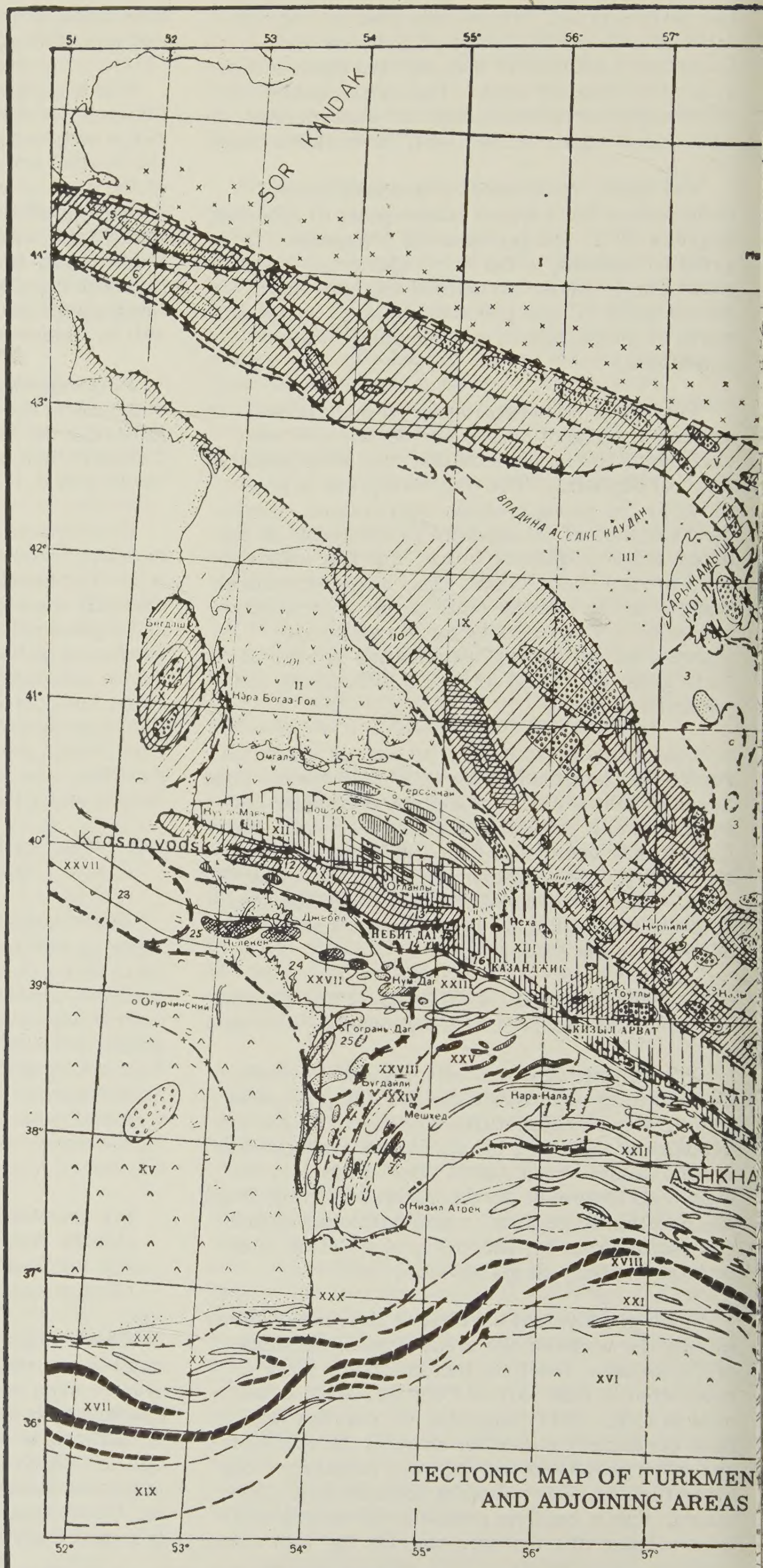
SOR KANDAK
Krasnovodsk
TECTONIC MAP OF TURKMEN
AND ADJOINING AREAS

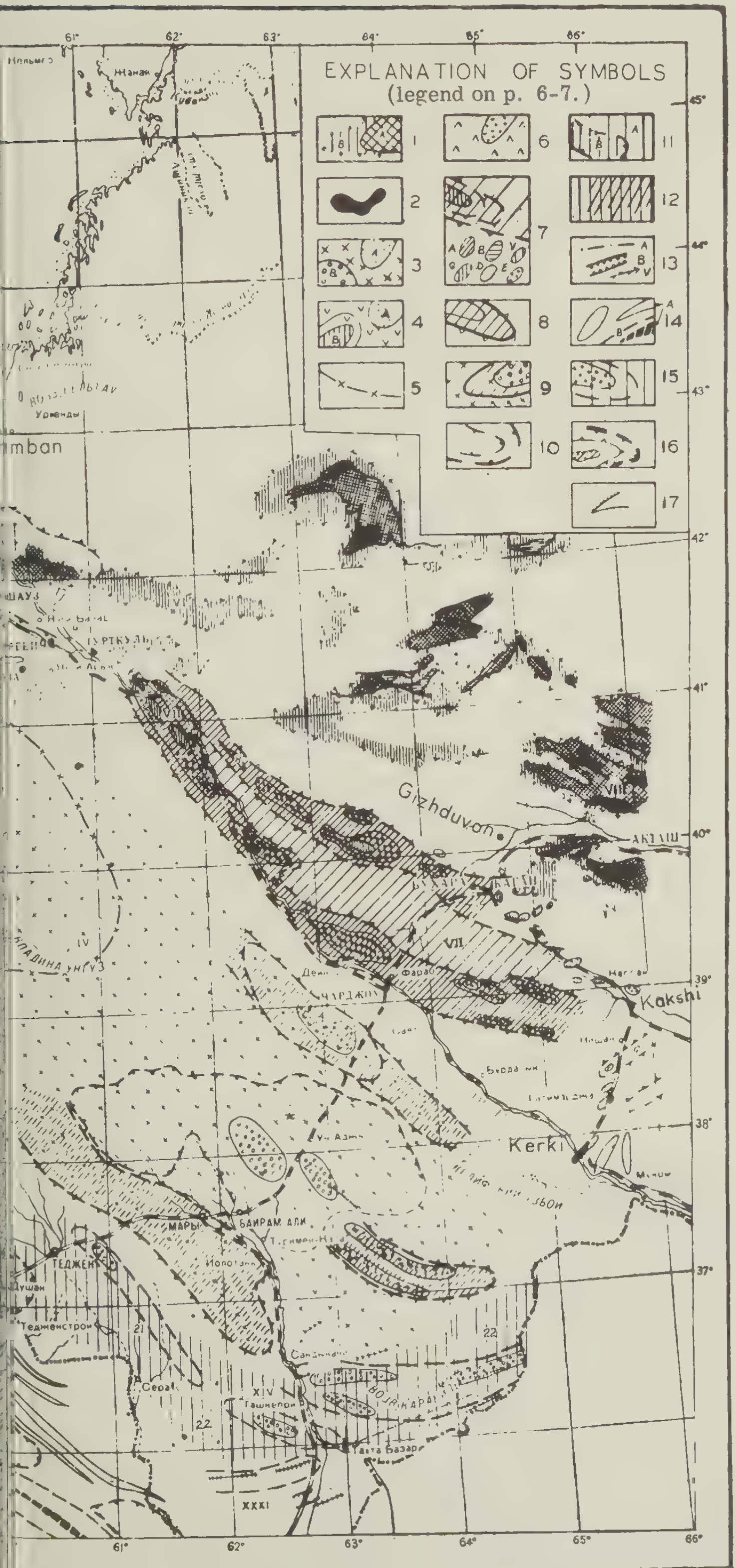
EXPLANATION OF SYMBOLS
(legend on p. 6-7.)
Gizhduvon
Kakshi
Kerki
mban
61°
62°
63°
64°
65°
66°
45°
44°
43°
42°
41°
40°
39°
38°
37°

Map Legend

Tectonic Map of Turkmenistan and Adjoining Areas.

Compiled from Geophysical Data, Making Use of the Materials of Geologic Surveys and Core Drilling (from Yu. N. Godin and Yu. I. Sytin).

Conventional Symbols: /upper right-hand corner/

1 - Hercynian folded structures
   A - outcrops
   B - covered by thin mantle of Cretaceous sediments

2 - Intrusions

3 - Inner blocks of the Hercynian folded basement and related dome-like uplifts in the cratonic mantle
   A - detected in Neocene beds
   B - tentatively identified from gravimetric data

4 - Inner blocks of the Hercynian folded basement related to a rise in the Mohorovičić surface
   A - detected in Neocene beds
   B - detected in Cretaceous beds

5 - Outlines of arch-like uplifts of the basement in the inner blocks

6 - Inner blocks in Alpine depressions (corresponding to uplifts in the Mohorovičić surface) and associated dome-like uplifts

7 - Belts of Hercynian folding reflected in the cratonic mantle by a linear zone of uplifts consisting in the arch sections of:
   A - Permian-Triassic rocks
   B - Jurassic
   V - Cretaceous
   G - Paleocene
   D - Neocene
   E - tentatively identified from gravimetric data

8 - Fault-block uplifts in the transition zone

9 - Areas of cratonic uplifts in the marginal sections of an inner block

10 - Outlines of major troughs and synclines

11 - Marginal troughs
   A - outer zones where the thickness of the cratonic mantle is 3 to 6 kilometers
   B - inner zones where the thickness of the sedimentary cover is more than 6 kilometers

12 - Transverse uplifts in marginal troughs

13 - Recent tectonic elements in southeastern Turkmenia
   A - axes of uplifts
   B - areas of submergence
   V - surface ridges

14 - Alpine folded structures
   A - outcrops of major anticlines
   B - anticlines identified from geophysical data under a mantle of slightly dislocated Neocene and Quaternary sediments reaching a thickness of 0.5 to 2.0 kilometers
   V - boundary between folded zones

15 - Large uplifts in areas of marginal troughs identified tentatively from gravimetric data

16 - Alpine troughs corresponding to "ditches" in the Mohorovičić surface with large inversion structures in their axial sections

17 - faults

Major Tectonic Elements:
  Cratonic Areas:
    A - Inner blocks
      I - North Ustyurt
      II - Krasnovodsk-Karabogaz
        I - North Balkhan marginal section
      III - South Ustyurt

- IV - Kara-Kum
    - 2 - Trans-Unguz arch uplift
    - 3 - North Kara-Kum marginal section
        - a - Upper Uzboy depression
        - b - Sarykamysh uplift
        - v - Khiva depression
            - v' - Takhta uplift zone
            - v'' - Kunya-Darya internal trough
    - 4 - South Kara-Kum marginal section
        - g - Mary uplift zone
        - d - Repetek uplift zone
        - e - Taryshly uplift zone
        - zh - Uch-Adzhi depression zone

B - Hercynian folded belts reflected in the cratonic mantle by a linear zone of uplifts

- V - Mangyshlak-Ustyurt
    - 5 - Central Mangyshlak uplift zone
    - 6 - Beke-Bashkuduk uplift zone
    - 7 - Central Ustyurt uplift zone
- VI - Sultan-Uiz-Dag
- VII - Amu-Darya
    - 8 - Bukhara uplift zone
    - 9 - Darganata-Chardzhou uplift zone
- VIII - Nura-Tau
- IX - Tuarkyr-Kaplankyr
    - 10 - Tuarkyr-Karbakshi uplift zone
    - 11 - Kaplankyr-Yerbent uplift zone
- X - Bekdash-Krasnovodsk

Transition zone areas:

A - Fault-block uplifts

- XI - Kubadag-Bolshoi Balkhan
    - 12 - Kubadag uplift
    - 13 - Bolshoi Balkhan uplift

B - Marginal troughs

- XII - North Balkhan
- XIII - Kopet-Dag
    - 14 - Balkhan intermontane trough
    - 15 - Ayda structural salient
    - 16 - Kazandzhik depression
    - 17 - Kyzyl-Arvat structural salient
    - 18 - Bami-Ashkhabad depression
    - 19 - Akhsu-Artyk structural salient
    - 20 - Kaakhka depression
- XIV - East Turkmen
    - 21 - Tedzhen depression
    - 22 - Tashkepri depression

Alpine geosynclinal areas

A - Inner blocks

- XV - South Caspian
- XVI - Iranian

B - Meganticlinoria and folded zones

- XVII - Elburz meganticlinorium
- XVIII - Aladag-Binalud meganticlinorium
- XIX - South Elburz folded zone
- XX - North Elburz folded zone
- XXI - Jaghatai folded zone of the southern Aladag
- XXII - Kopet-Dag meganticlinorium
- XXIII - Malyy Balkhan-Danata folded zone
- XXIV - Messerian-Khodzhakala folded zone
- XXV - Ezet-Karagez folded zone
- XXVI - Eastern Kopet-Dag folded zone

V - Troughs and depressions

- XXVII - Apsheron-Balkhan depression zone
    - 23 - Central Caspian depression
    - 24 - Balkhan foreland depression
    - 25 - West Cheleken uplift
- XXVIII - Shakhman foreland trough
- XXIX - Quchan-Meshed superimposed trough
- XXX - Gorgan foreland trough
- XXXI - Badkhyz-Karabil depression zone

with the folded structure of the basement (of Caledonian or early Hercynian age), which in turn is linked genetically with the above-mentioned fractures. (The existence of a folded basement in the Ustyurt area is confirmed by recent boring data. Borehole No. 4 in the Tugarakchan area has reached Devonian sediments at 3000 meters dipping up to $50^{\circ}$ and overlain by slightly dislocated Carboniferous formations.) On the east the block is bounded by East Urals Hercynian formations that have been detected in the Aral Sea area by magnetic surveys. Finally, in the south, the Central Ustyurt block is bounded by the Mangyshlak-Ustyurt mobile belt separating that relatively mobile section of the craton from the consolidated blocks of Central Turkmenistan.

The Mangyshlak-Ustyurt mobile belt (V on the map) consists in the west of a series of elongated anticlinal zones striking WNW-ESE and separated by depressions. The central part of the Mangyshlak peninsula contains the Central Mangyshlak zone (5), which consists of an uplift of Mesozoic rocks having folded Permian-Triassic formations in its core. This uplift, which is broken into three distinct blocks -- the Karatauchik, Western Karatau and Eastern Karatau ranges -- is submerged below recent sediments both in the west (Tyubkaragan peninsula) and in the east (Tanasha-Karamain area). South of and parallel to the Central Mangyshlak zone is the relatively narrow, 200-kilometer-long Beke-Bashkuduk zone (6), which also corresponds to a clearly marked anticlinal structure. Both these anticlinal zones and the intervening depressions have been formed as a result of the disjunctive tectonics that have been widely developed in Mangyshlak.

According to geophysical data, the Mangyshlak-Ustyurt mobile belt is distinguished by a chain of intensive gravity maximums striking WNW-ESE, and bounded on the north by elongated linear zones of positive magnetic anomlies. The nature of the magnetic and gravity fields of this zone and their association with the fields of the Central Ustyurt suggest the possible existence of deep-seated fractures. However, the deep-seated structure of the Mangyshlak zone itself and its eastern Ustyurt extension is somewhat different, judging from the character of its magnetic field.

The Mangyshlak area contains large anticlinal structures that consist of Jurassic, Cretaceous and Paleocene sediments which have been greatly dislocated by faulting. The eroded cores of some of the more elevated anticlines disclose large outcrops of intensively faulted Permian-Triassic sediments that are separated from the upper formations by an angular and azimuthal unconformity. The Neocene sediments that cover the older formations transgressively form relatively gentle uplifts of the cratonic type that repeat the dislocations of the lower strata in extenuated form. It should be noted that the intensive dislocations of the Permian-Triassic are limited to a relatively narrow zone less than 80 kilometers wide. In adjoining areas to the north and south seismic surveys have established gentle structures of the cratonic type. The same surveys, conducted by VNIGRI, have established the interesting fact that the Permian-Triassic sediments, which reach a thickness of 8 to 10 km in the central part of Mangyshlak, are pinched out toward the south.

The wide development of faulting in the Mangyshlak structures, their block-like character, and the relatively narrow zone affected by the intensive dislocations suggest that the Mangyshlak-Ustyurt mobile belt within the Mangyshlak area is genetically linked with a zone of deep-seated fractures. Greater activity in the zone of the deep-seated fractures toward the end of the Hercynian and the start of the Alpine stage, led at the end of Paleozoic and the start of Mesozoic times to intensive local downwarping, the accumulation of thick Permian and lower Mesozoic sediments, and a subsequent local inversion of conditions in the fracture zone; this in turn led to the formation of complex, faulted, block-like structures. The Mangyshlak is thus a typical example of the characteristics of deep-seated structures and the tectonic development of mobile belts within cratons.

The same type of gravitational field has been established east of the Mangyshlak by the work of VNIIGeofizika. Here we also find intensive local gravity maximums similar to the local anomalies of the Mangyshlak that correspond to the large Permian-Triassic anticlinal structures. This suggests that the Central Ustyurt also contains buried anticlines similar to the Mangyshlak structures, or somewhat older, and that these anticlines are again associated with inherited, gentler upper Mesozoic and Cenozoic structures. The large tectonic elements of this area include the north Ustyurt zone of linear uplifts (7 on the map), which is situated in the same tectonic line as the uplifts of the Central Mangyshlak. Its association with the gravity maximums of the gentle Sarmatian anticline -- which is reflected in the present relief, and was first identified by N. P. Lupov and A. L. Yanshin as the Central Ustyurt anticline -- once again confirms the reliability of the geophysical data used in delimiting the tectonic regions on the map.

Moreover, as was already noted, the magnetic field of the eastern part of the Mangyshlak-Ustyurt belt has far more clearly marked anomalies than the western part. This points not only to the greater complexity of the deep-

seated structure of the eastern part, but specifically to the fact that the deep-seated fractures play a more important role here than in the Mangyshlak. Undoubtedly the fractures in the basement of the eastern section are filled with magnetically more active rocks, apparently basics or ultrabasics. The presence of large basic or ultrabasic intrusions, with a specific gravity of 2.8-3.0 grams per cubic centimeter, can also explain the existence of a belt of intensive positive gravity anomalies. In the east, in the lower reaches of the Amu-Darya, the Mangyshlak-Ustyurt mobile belt adjoins the Sultan-Uiz-Dag Hercynian anticlinorium, which strikes NW-SE.

The Sultan-Uiz-Dag mobile belt (VI on the map) is one of the tectonic elements linking the folded mountains of the Urals with the Tien Shan. The folded structure of the Sultan-Uiz-Dag dates apparently from the Caledonian stage, although the structure was greatly changed and further developed in Hercynian times. The structure consists of heavily metamorphosed rocks, more than 8 km thick, made up of biotite paragneisses, marbles, black siliceous slates and greenstone extrusives. The age of the black siliceous slates can be correlated with that of the Lower Gotlandian sediments of the Tamdy-Tau and the Nura-Tau, and the upper bed of extrusives with Devonian sediments. The lower gneisses and marbles apparently date from the Proterozoic. All these ancient rocks are covered in spots by Cretaceous formations.

The Sultan-Uiz-Dag anticlinorium is also clearly reflected in geophysical data. On gravimetric maps it appears as intensive, positive anomalies bounded on the southwest by zones of increased gravity gradients, which may reflect the existence of disjunctive dislocations in the Paleozoic basement. The magnetic field of the area is marked by clearly expressed linear anomalies oriented NW-SE, which have a tendency to strike N-S at the northern extremity.

The older structure of the Sultan-Uiz-Dag evidently predetermined the structural arrangement of the eastern part of the Mangyshlak-Ustyurt belt since the tectonic lines of that belt adopt a parallel NW-SE strike as they approach the Sultan-Uiz-Dag. The same strike is followed in this area by some magnetic anomalies, apparently reflecting major fractures in the basement that are filled with basic or ultrabasic rocks.

South of the Sultan-Uiz-Dag, in the Turtkul area, in a tectonic zone that links the Paleozoic outcrops in the lower reaches of the Amu-Darya with similar outcrops in the Tamdy-Tau and Nura-Tau hills (VIII on the map), we find the Amu-Darya mobile belt, which is clearly reflected in gravimetric and magnetic data.

Within the Amu-Darya mobile belt (VII on the map), complex analysis of gravimetric and magnetic data indicates the existence of the Bukhara (8) and Darganata-Chardzhou (9) anticlinal zones of the Paleozoic basement, diverging at a slight angle southeastward from Turtkul and associated with echelon-like Mesozoic-Cenozoic structures of the cratonic type. On a gravimetric map these zones correspond to linear belts of intensive relative gravity maximums, and on a magnetic map to negative anomaly zones.

The contours of the anomaly zones on the gravimetric and magnetic maps coincide almost exactly.

Attempts to determine the depths of the disturbing formations on the basis of magnetic air survey data have shown that the disturbing formations approach the surface of the earth in areas that we have identified as Paleozoic anticlinal zones. Most probably these zones occur in the relief of the top of the Paleozoic basement. However, it is also possible that the top of the Paleozoic rocks is an erosion surface and that the anticlinoria, which may even be displaced with respect to each other, occur within the Paleozoic formations.

The absence of geophysical data over a large part of the right bank of the Amu-Darya makes it impossible to determine exactly how the Amu-Darya mobile belt connects with the Sultan-Uiz-Dag anticlinorium. However, attention is drawn to the extreme complexity of the junction of structural elements of the Mangyshlak-Ustyurt, Amu-Darya and Sultan-Uiz-Dag tectonic zones. Without going into details pending the receipt of additional geophysical and geologic data, we may note that all these tectonically active regions apparently form a single mobile belt bordering on the consolidated blocks of Central Turkmenistan on the north and northeast.

The Krasnovodsk-Karabogaz inner block (II on the map), which includes the gulf Kara-Bogaz-Gol and the northern part of the Krasnovodsk plateau, is a separate part of the larger Central Caspian block. On the northeast the Krasnovodsk-Karabogaz block is bordered by the Tuarkyr-Kaplankyr mobile belt, on the south by the zone of the Kubadag-Bolshoi Balkhan dislocations, and on the west probably by an area of deep-seated fractures and associated uplifts striking north-south. On a gravimetric map the block is clearly reflected as a regional gravity maximum, apparently related to the higher position of the peridotite layer within Turkmenia and adjoining territories.

The Tuarkyr-Kaplankyr mobile belt (IX on

the map), which separates the Krasnovodsk-Karabogaz block from the South Ustyurt block, is a structurally complex tectonic zone 500 km long and 120 km wide. Striking NW-SE, it includes the Tuarkyr, Kumsebshen and Karashor areas and a large part of the Kara-Kum lowlands.

On gravimetric maps the Tuarkyr-Kaplankyr mobile belt appears as two zones of intensive gravity maximums striking NW-SE, clearly separated by an area of minimums. On magnetic maps the zone appears as a regular alternation of narrow, elongated positive and negative anomalies of the same NW-SE strike.

Morphologically this tectonic zone corresponds to the structurally complex arch-like uplift that has been designated on older structural maps as the Karabogaz-Yerbent ridge and contains a local trough in its axial (Uchtagan) section. The uplift is clearly defined throughout except for the northeastern limb of its eastern pericline, where it merges with the flat-lying section of the Central Kara-Kum.

According to magnetic data that have been confirmed in some areas by seismic work, the crystalline basement in the area of the Tuarkyr-Kaplankyr belt lies at a depth of 2 to 3 km and is submerged to more than 3.5 km only in a few places, such as Uchtagan trough and the southern slope of the Tuarkyr-Karabakshi anticlinal zone. Within the local uplifts the depth of the crystalline rocks is seldom more than a few hundred meters, or one kilometer (Tuarkyr, Kumsebshen).

The complexity of the deep-seated structure of the Tuarkyr-Kaplankyr belt has determined the distinctive character of the geophysical fields in this belt. Gravity and magnetic anomalies are related here mainly to major structural units (anticlinoria) of the folded and heavily metamorphosed Paleozoic, complicated by deep-seated fractures. The latter clearly appear on magnetic maps as isolated, narrow, elongated, peak-like anomalies.

The Mesozoic and Cenozoic structures that have been mapped in geologic and seismic surveys have been inherited from older large structures (anticlinoria) of the basement or are associated with deep-seated fractures. The inherited character of the Mesozoic and Cenozoic structures is confirmed by an analysis of the thicknesses of specific stratigraphic series. According to seismic and boring data, certain beds thin out toward the arches of the structures and toward zones of gravity maximums. This explains quite convincingly the characteristic correlation between gravity and magnetic anomalies, and Mesozoic and Cenozoic structures in mobile belts. Thus in interpreting the geophysical data obtained within the mobile zones of the cratonic part of the studied area, we can gain a picture of the detailed structural arrangement of these zones.

In the Tuarkyr-Kaplankyr zone, specifically, we can thus distinguish two main areas of Mesozoic and Cenozoic structures striking NW-SE that are associated with anticlinoria of the Paleozoic basement and possibly with deep-seated fractures:

The first of these two areas -- the Tuarkyr-Karabakshi area (10 on the map) -- is more than 500 km long and is in turn clearly divided into two anticlinal zones, each of which is structurally complex. One of these anticlinal zones -- the Tuarkyr in the northwest -- is known from geologic surveys; and only its southeastern pericline has been mapped by geophysical methods. The second anticlinal zone -- the Karabakshi in the southeast -- has been studied entirely on the basis of interpretation of geophysical data, specifically on the basis of the results of recomputation of the gravitational field by modern methods of transformation.

The second area of Mesozoic and Cenozoic structures -- the Kaplankyr-Yerbent area (11 on the map) -- is separated from the Tuarkyr-Karabakshi area by a depression zone. Like the Tuarkyr-Karabakshi area, and possibly even with greater justification, the Kaplankyr-Yerbent area can be divided into separate Kaplankyr and Yerbent anticlinal zones. The area of greater submergence, as shown by the gravity effect, is much larger in this area than between the Tuarkyr and Karbakshi zones, and its existence is probably related to the presence of disjunctive dislocations striking E-W. The presence of these dislocations is yet to be fully demonstrated; however, they do appear quite clearly on maps of variations in the gravitational field that have been compiled by the recomputation of observed fields by various methods. In some places these dislocations are also confirmed by irregularities in the seismic horizons that have been constructed by the correlation method of refracted waves.

Of considerable importance is the question of juncture between the Tuarkyr-Kaplankyr and Mangyshlak-Ustyurt mobile belts. The Jurassic-Paleocene structural stage of the Tuarkyr folds has much in common with that of the Mangyshlak structure, the only difference being a somewhat lesser intensity of dislocation and lesser development of disjunctive structures in the Tuarkyr. In the lower structural stage, however, there are substantial differences between the two zones. In the Mangyshlak, that stage consists of an 8-to-10-kilometer-thick heavily dislocated series of Permian-Triassic sediments, while in the Tuarkyr these sediments are much thinner and less dislocated.

It can be assumed that the Mangyshlak underwent a long and deep submergence at the end of the Paleozoic and the start of the Mesozoic, followed at the end of the Triassic by rather intensive folding. At the same time, the Paleozoic block of the Tuarkyr area, having been dislocated by Hercynian movements, was only partly submerged in Permian and Triassic times and was not affected by any subsequent intensive folding.

All these facts, as well as the presence of a relatively negative gravitational anomaly separating the Tuarkyr-Kaplankyr and Mangyshlak-Ustyurt mobile belts, show that there can hardly be any connection between the two zones. It is much more plausible to assume the possibility of a change in the strike of the Tuarkyr-Kaplankyr belt from NW-SE to WNW-ESE, bringing the tectonic lines of the two tectonic zones parallel to each other, or to assume that the folding movements died out in the northwestern part of the Tuarkyr-Kaplankyr mobile belt.

Seismic work carried on in 1956 by VNIGRI in the Mangyshlak peninsula points to the existence in the southern part of the peninsula of a geologic situation similar to the one in the Tuarkyr. The seismic data show a sharp thinning-out of the Permian-Triassic beds in a southerly direction; although the beds are not totally pinched out, they do become extremely thin along the coast. This would support the first assumption, especially since, on the basis of aeromagnetic data, the strike of magnetic anomalies quite definitely points to a connection between the Tuarkyr-Karabakshi mobile zone and the tectonic zone of the southern Mangyshlak.

The South Ustyurt inner block (III on the map), situated east of the Krasnovodsk-Karabogaz block, is bounded on the north by the Mangyshlak-Ustyurt mobile belt, on the southwest by the Tuarkyr-Kaplankyr mobile belt and on the east by the complex area of the Upper Uzboy dislocations, which are part of the North Kara-Kum marginal section of the Kara-Kum inner block. The character of the geophysical fields in Central Turkmenistan and the morphologic position of the South Ustyurt block suggests that the latter is actually part of the Kara-Kum block, having been separated by a deep-seated fracture.

The Kara-Kum inner block (IV on the map) occupies a large area in Eastern Turkmenistan, including the Trans-Unguz and southeastern parts of the Kara-Kum. It is clearly reflected in geophysical data by the mosaic-like character of the gravitational and magnetic fields and is rather complex in its structural arrangement. Because of the limited amount of geophysical work done in the area of this block, we are unable to list the detailed structural elements and must restrict ourselves to the more general features.

The largest structural element of the Kara-Kum block is the Trans-Unguz uplift (2 on the map) in the northwest. This uplift is apparently the most stable part of the block, having been affected much less by the tectonic movements that involved the areas bordering on the mobile belts. The intensity of these tectonic processes was probably quite insignificant in the marginal sections of the block. However, during stages of predominant downwarping, the movements in the active mobile zones also brought about some submergence of the margins of the inner block. Similarly, during periods of folding, the marginal sections of the block were to some extent affected by uplifting movements. Both the intensity of downwarping and the extent of uplifting in the marginal sections of the inner block were quite insignificant. However, these forms are clear enough, on the one hand, to be identified as part of the relatively stable area of the inner block and, on the other hand, to indicate the effect of the adjoining mobile belts on their strike.

By generalizing individual areas of submergence along the margins of the Kara-Kum block, we can distinguish the North Kara-Kum and the South Kara-Kum marginal sections. The North Kara-Kum marginal section (3 on the map) consists of the Upper Uzboy and Khiva depression zones and the intervening Sarykamysh ridge-like uplift. The Upper Uzboy depression zone (a), which separates the Kara-Kum block from the South Ustyurt block, is associated with a deep-seated fracture; it has developed as a direct result of the activated tectonic life of this section of the earth's crust because of the existence of this fracture. The Sarykamysh ridge-like uplift (b) is a Paleozoic structure striking NW-SE that stands out quite clearly against the gravitational and magnetic anomalies characteristic of the area of consolidated blocks. The existence of this structure has been confirmed by seismic work.

The Khiva depression zone (v), bordering the Kara-Kum block on the north and northeast, has been identified on the basis of complex analysis of gravitational, magnetic and seismic data in its northwestern section and only magnetic data in its southeastern section. The depression contains individual troughs and uplifts, but pending receipt of additional data these elements cannot all be located exactly.

The Kunya-Darya internal trough (v'') and the Takhta uplift (v') can be identified with somewhat greater certainty than the other elements. The Takhta uplift, incidentally, has been identified only in its extreme northwest section. There is a wide variety of opinions

in regard to its southeasterly extent, including even the suggestion that it may connect with the Repetek tectonic zone, which has been identified in the extreme southeast of the Kara-Kum block.

The South Kara-Kum marginal section (4) consists of the Mary, Taryshly and Repetek uplift zones and a large area that we have called the Uch-Adzhi depression.

The Mary uplift zone (g) is probably made up of several local structural forms whose outlines are unclear and cover a large area. These structures may be genetically related to the Klych-Damly and Akhchakaya structures, which have been identified on the western margin of the block on the basis of geologic data.

The Repetek zone (d), in contrast to the other marginal uplifts of the inner block, is reflected in a rather intensive gravitational anomaly, comparable in value to the anomalies of the Amu-Darya mobile belt. However, it has been classified as a marginal part of the inner block because it displays a combination of an intensive gravitational anomaly and an indistinct magnetic anomaly that is not typical of a mobile belt. Additional data, particularly those derived from a seismic traverse along the Mary-Chardzhou line, may shed further light on the position of this zone in the overall structural arrangement of the Hercynian craton.

The Taryshly uplift (e) is less distinct than the two preceding structures. This is explained, first, by the fact that the structure is situated in a zone where no geophysical work has been done, except for aeromagnetic surveys and small-scale gravimetric surveys designed to set up a base network. Secondly, the identification of structures of the Paleozoic basement on the southern limb of the inner block is made difficult by the fact that the gravitational effect here begins to be distorted by beds in the upper part of the stratigraphic cross section that have been affected by Alpine tectonic movements.

The presence of the gravitational effect produced by the Mesozoic and Cenozoic beds greatly complicates the interpretation of gravitational maps; and the indistinct contours of the magnetic field in this area do not supply the necessary corrections needed for a geologic interpretation of geophysical data.

The Uch-Adzhi depression (zh) is shown only tentatively and needs confirmation even more than the other tectonic elements. The distribution of gravitational and magnetic fields typical of depression zones within inner blocks is not clearly evident here, and the observed combination of weak relatively negative gravitational and magnetic anomalies may be caused not only by the existence of an area of submergence but by other factors, such as the existence of large acidic intrusions.

B. Transition Zone Predominating in Marginal Depressions.

In addition to areas that are typical of cratonic or geosynclinal conditions of development, the western part of Central Asia also contains areas that can be assigned neither to one nor the other type. Those areas that lie near the geosynclinal region usually contain forms reflecting intensive folding. At greater distances from the geosynclinal region, the effect of folding weakens, and structures adopt cratonic characteristics.

While the cratonic and geosynclinal regions cannot be simply outlined we can separate these two types of contrasting tectonic regions by an area whose structural forms are intermediate in character; we shall call this area a transition zone.

On the basis of special seismic surveys and an analysis of the gravitational and magnetic fields, the width of this zone can be placed between 30-40 and 70-80 kilometers.

The transition zone contains the following major structural elements: the Kubadag-Bolshoi Balkhan fault-block uplift, the North Balkhan marginal trough, the Kopet-Dag marginal trough, and the East Turkmen marginal trough.

The Kubadag-Bolshoi Balkhan fault-block uplift (XI on the map), made up of Mesozoic sediments from the surface to the Lower Jurassic inclusive, borders the West Turkmen depression on the north and the Kazandzhik depression on the west. The uplift is associated with the mobile belt that skirts the Krasnovodsk-Karabogaz block on the south, and with a zone of major, deep-seated fractures related to the sharp submergence of the Mohorovičić surface. The position of the structure, which was formed mainly in pre-Miocene and post-Miocene times, along a seam in the earth's crust has determined its distinctive fault-block character. The uplift falls into two separate anticlinal structures -- the Kaba-Dag (12) and Bolshoi Balkhan (13) anticlines -- separated by a small saddle.

The North Balkhan marginal trough (XII on the map), covering the southern part of the Krasnovodsk plateau and the Chilmamed-Kum desert, is apparently not connected with the depression zone of the Kopet-Dag foreland and can be regarded as a separate element. Available data are, however, inadequate to determine the exact position of this trough and its structural details.

The Kopet-Dag marginal trough (XIII on the map) appears on gravitational maps as large

closed gravity minimums separated by relative maximums. Seismic surveys have shown that the minimums correspond to intensive submergence of the seismic horizons and, consequently, to a sharp increase in the thicknesses of Tertiary and Mesozoic sediments.

On the basis of the sum total of gravitational, magnetic and seismic data, we can distinguish the following tectonic elements in this marginal trough: the Balkhan intermontane trough, the Kazandzhik depression, the Kyzyl-Arvat structural salient, the Bami-Ashkhabad depression, the Akhsu-Artyk structural salient and the Kaakhka depression.

The Balkhan intermontane trough (14 on the map), separating the Bolshoi Balkhan and the Malyy Balkhan, appears clearly on gravimetric maps in the form of an elongated semi-closed gravity minimum merging in the west with the gravitational minimum of the Balkhan foreland depression. In the east this trough connects through a narrow neck with the gravimetric minimum of the Kazandzhik depression.

According to seismic data, the trough is sharply asymmetric with a gently dipping northern limb and an abrupt southern limb, complicated by a thrust fault. The depth of the eroded surface of Cretaceous limestones in the axial part of the trough is estimated at 2,500 meters.

Most of the Balkhan intermontane trough constitutes a separate structural unit that we have called the Ayda structural salient (15 on the map), which is an irregularity in the southern limb of the Bolshoi Balkhan. This salient separates the Balkhan foreland depression and the Balkhan intermontane trough proper from the Kazandzhik depression.

The Kazandzhik depression (16 on the map) appears clearly on gravimetric maps as a closed gravity minimum extending southeast along the northwestern outliers of the Kopet-Dag. According to seismic and gravity data, the Kazandzhik depression, like the Balkhan intermontane trough, has a sharply asymmetric structure, with a gentle northern limb and a steep southern limb complicated by a system of regional thrust faults. The steep dip of the southern limb, sometimes complicated by normal and thrust faults, is evident from seismic and gravimetric data in the area of the Kyzylbair bridge linking the Malyy Balkhan with the Kyuren-Dag, and can be traced farther to the east. A refracting horizon within the Cretaceous sandstone and limestone series shows that the central part of the Kazandzhik depression is closed neatly toward the east as it approaches the Kyzyl-Arvat salient. The horizon rises by more than 1,500 meters from the center of the depression to the Kyzyl-Arvat salient.

We can distinguish an inner and an outer zone in the Kazandzhik depression on the basis of seismic data. The inner (geosynclinal) zone covers the center and the southern limb of the depression. It is marked by a steep dip and greater thicknesses of Cretaceous and Cenozoic deposits. The great thickness of Neocene and Quaternary sediments in the center of the depression, reaching about 2,000 meters, and lying nonconformably on the Paleocene, points to intensive submergence of the Kazandzhik depression in Neocene and Quaternary times.

The outer (cratonic) zone is associated with the northern limb of the depression. According to seismic data it is marked by gentle dips, the pinching out of some beds, and a general reduction of stratigraphic thicknesses toward the north. Detailed geophysical surveys have uncovered several gently sloping local structures in the depression.

The Kyzyl-Arvat structural salient--(17 on the map) a transverse uplift--is clearly defined by a regional bend of the gravity lines in the Kyzyl-Arvat area and by the characteristic position of magnetic anomalies. The position of the salient is shown equally well by seismic data, which point to gentler dips of the beds along a N-S section, compared with the Kazandzhik and Bami-Ashkhabad depressions, and to a rise of the seismic beds in the center of the salient. Stratification of the seismic cross sections shows that the top of the Cretaceous at a point 20 km north of Kyzyl-Arvat lies at a depth of less than 1200 meters. This is confirmed by drilling carried out by Turkmenburneft (the Turkmen Petroleum Drilling Organization), which established the absence of Miocene and a large part of the Paleocene sediments thus proving that the Akchagyl formation lies directly on the lower Paleocene beds. On the basis of magnetic and seismic data, the depth of the metamorphosed rocks of the basement here is placed at 3 to 4 kilometers.

The Bami-Ashkhabad depression (18 on the map), on the basis of geophysical data, is clearly outlined in the west in the Kyzyl-Aryat area, bounded in the south by the structures of the Central Kopet-Dag, and passes gradually in the north in the Kara-Kum craton. This depression is much larger than that of Kazandzhik. Its center, according to seismic and gravimetric data, lies near Ashkhabad and is marked by the deep submergence of Mesozoic formations.

This depression has also been subdivided into inner (geosynclinal) and outer (cratonic) zones whose characteristics conform to the zones of the Kazandzhik depression. The depression contains some local structures, such as the ones of Archman and Izgant.

The Akhsu-Artyk structural salient (19 on the map) is shown mainly by gravimetric and magnetic data. Irregular anomaly lines at the southeastern end of the Bami-Ashkhabad depression suggest that instead of being one consolidated cratonic salient, the Akhsu-Artyk structure actually consists of two, separated, transverse uplifts. On the basis of generalized data, the Akhsu-Artyk structure can be compared with similar salients noted in the northwestern sections of the Kopet-Dag marginal trough. Pending the completion of seismic work along the Ashkhabad-Kaakhka line, nothing more definite can be said about this structure.

The Kaakhka depression (20 on the map) is the southeasternmost element of the Kopet-Dag marginal trough. Judging from the configuration of the gravitational field, the maximum submergence is found in the Kaakhka -Dushak area and the southeastern closure is located west of Dushak. In view of the complex shape of the Akhsu-Artyk salient separating the Kaakhka from the Bami-Ashkhabad depression, we can expect to find a small, separate trough in the northwest section of the Kaakhka depression.

The East Turkmen marginal trough (XIV on the map), which includes the Tedzhen river basin and part of the Badkhyz and Karabil hills, differs structurally somewhat from the two previous tectonic elements of the transition zone. This is due to the characteristics of formation of depression zones in the marginal cratonic areas, whose basement consists of stable, consolidated sections. The proximity of these stable cratonic zones (which cause a sharp southward bend of the tectonic lines of the Kopet-Dag), and the existence in adjoining areas of two contrasting lines of folding, (the Hercynian and the Alpine) have combined to determine the structural arrangement of the East Turkmen trough.

The distinctive feature of this tectonic zone is that most of its structures are not clearly defined. However, the internal structure of individual elements appears to be quite complex since these elements have been affected by tectonic processes that resulted in folding both in Hercynian and Alpine times. Some elements show greater evidence of the effects of Hercynian folding, and others of Alpine folding. The former, for example, include an area in the Tedzhen river basin called the Tedzhen depression (21), and the latter, the entire southern part of the trough, known as the Tashkepri depression (22).

In conclusion it should be noted that the strike of the structural elements of southeastern Turkmenia conforms characteristically to the trend of the tectonic lines that can be traced in the Mesozoic and Cenozoic sediments.

## C. Alpine Geosynclinal Region

As in the case of the craton, the geosynclinal region contains areas that have been relatively stable through time. The distribution of these stable areas and the configuration of the southern cratonic slope have determined the strike of the mobile belts and the Alpine folded systems in the geosynclinal region.

The geosynclinal region contains two relatively stable sections. One of them, called the South Caspian inner block, covers most of the Southern Caspian and part of the southwestern Keymir-Chikishlyar area of the West Turkmen lowland. The other, situated entirely in Iran, is called the Iranian inner block.

The South Caspian inner block (XV on the map) appears clearly in gravimetric data as a regional gravity maximum, confirmed on the basis of a few isolated seismic E-W cross sections as an anomalous westward rise of deeply submerged reflecting beds. The position and configuration of this block has affected not only the position of bordering mobile belts but also the strike of Tertiary structures and regional fractures in the Central Caspian and Balkhan foreland depressions and in the Keymir-Chikishlyar area. As a relatively rigid obstacle, the South Caspian block caused the Kopet-Dag to branch out into southwesterly and southerly outliers and produced the characteristic arching Hercynian and Alpine strikes in the south and southwest of the studied area (Elburz, Kopet-Dag and Aladag-Binalud meganticlinoria).

On the south the South Caspian inner block is bounded by the folded region of the Elburz meganticlinorium (XVII on the map), formed in the course of pre-Cretaceous and pre-Eocene folding. The mountains of this meganticlinorium consist chiefly of Jurassic rocks, and the cores of individual anticlinoria of Paleozoic formations. In the north and south, the Elburz is adjoined by younger folded zones, dating from the Eocene and consisting chiefly of Upper Cretaceous and Tertiary rocks. The Elburz meganticlinorium is separated from the South Caspian inner block by the large Gorgan foreland trough (XXX on the map).

East of the South Caspian block we find a tectonically very active mobile belt formed during various phases of the Alpine period. Among the distinctive features of this belt are the almost total absence of extrusives, and of evidence of Alpine intrusive activity, and certain characteristics of the facies of Mesozoic sediments. Morphologically and structurally, this mobile belt can be divided prior to the end of the Neocene into three distinct zones: a western lowland corresponding to the West Turkmen depression, a central mountain, including the folded area of the Kopet-Dag, and an eastern plateau, covering the southern part of

the Badkhyz and Karabil hills.

In the western zone, a mantle of recent homogeneous sediments that are almost flat over a large part of the area covers a multilevel, deep-seated structure that is complex and tectonically quite variegated. In the northern part of the West Turkmen lowland, geophysical data point to the presence of the Balkhan foreland depression (24), which is separated by the West Cheleken transverse uplift (25) from the Central Caspian depression (23). Both these depressions are part of the parageosyncline of the Apsheron-Balkhan mobile belt, which can be clearly traced on gravitational maps as a narrow zone (70 to 150 kilometers wide) of intensive gravity minimums (100-200 mgl or more). According to deep seismic sounding and gravimetric data, the Apsheron-Balkhan belt corresponds to a deep trough in the Mohorovičić surface. The depth of the bottom of the earth's crust in the axial part of the trough is 45 to 50 kilometers.

The Apsheron-Balkhan mobile belt includes a variety of tectonic zones, judging from the upper part of a cross section onthe Mohorovičić surface. In some stages of the Alpine cycle these zones passed through identical conditions of development produced by deep-seated processes. These processes produced troughs in the substratum and deep-seated fractures with associated inversion (or fault-block) uplifts.

The mobile belt contains areas distinguished by the heavy accumulation of sediments, the development of regional faults and the existence of large, buried anticlinal structures and domes up to 60 kilometers across and 3 to 5 kilometers high, which are associated with the axial section of the depression zones. The basic difference between such areas and typical geosynclines lies in the incomplete inversion of individual sectors during continuing intensive submergence and the absence of evidence of magmatic activity; although the latter is not completely excluded on the basis of geologic and geophysical data.

In looking at the geologic structure of the western part of the Alpine geosynclinal zone, it should be noted that its development starting with the Paleocene was uniform through most of its territory. Typical of that period was the intensive submergence of the entire basin and the accumulation of sediments to a thickness of 5 to 6 kilometers. Differences in the deep-seated structure of individual sections are reflected in the surface relief and in the structural characteristics of Neocene uplifts. For example, in the Balkhan foreland depression, the largest anticlinal structures occur in the axial section, which is also the most mobile. These types of uplifts include the structures of the Cheleken, Kotur-Tepe, Nebit-Dag and Monzhukly.

These structures have much in common with other uplifts in the axial part of the southeastern closure of the Balkhan depression -- the Gogran-Dag, Karadashli and part of the Kamyshldzha. It is also noteworthy that all these structures have a tendency to change in character toward the south; as they approach a salient of the South Caspian block that penetrates into the Keymir-Chikishlyar area, the amplitude of individual uplifts decreases noticeably and the area occupied by the structures increases. The Okarem-Keymir structure, which lies in the southern continuation of this zone, is already part of the marginal section of the inner block.

The axial part of the depression is also associated with most of the regional faults, whose strike as a first approximation coincides with the alignment of the margin of the inner block. East of the zone of uplifts associated with the axial part of the depression, we find structures that are smaller in size and elevation and form an eastern belt of anticlinal uplifts.

The structural arrangement of the central part of the Alpine geosynclinal zone, including the folded mountains of the Kopet-Dag and the Khorasan, was probably predetermined by the rigid edge of the Kara-Kum craton in the northeast (specifically, the salient of the Kara-Kum inner block), and the South Caspian and Iranian inner blocks in the west and the south.

These stable sections caused the branching off of outliers in the western and eastern Kopet-Dag and the arching strike of the tectonic lines that border the south Caspian and Kara-Kum blocks on the south and the Iranian block on the north.

The central tectonic element of the Kopet-Dag and the Khorasan is the Aladag-Binalud meganticlinorium (XVIII on the map). Formed by pre-Cretaceous and pre-Eocene folding and consisting of predominantly Jurassic rocks, this meganticlinorium is the oldest folded element of the entire system. The cores of individual anticlinoria consist of Paleozoic rocks.

The Aladag-Binalud structure is adjoined in the north by the Kopet-Dag meganticlinorium (XXII on the map). It was formed predominantly by pre-Miocene folding and consists of Lower Cretaceous rocks. In the east, the Aladag-Binalud meganticlinorium is separated from the Kopet-Dag structure by the Quchan-Meshed superimposed trough (XXIX). The Jaghatai folded zone (XXI), farther south, is an intermediate link between the Aladag-Binalud meganticlinorium and the Iranian inner block (XVI). This folded zone, made up chiefly of Upper Cretaceous and Tertiary rocks, arose in the Neocene.

On the northwest, the Kopet-Dag meganticlinorium is adjoined by the folded region of

the Western Kopet-Dag, formed chiefly by pre-Akchagyl folding. This region, whose elements are made up of Cretaceous and Tertiary formations, falls into three structurally distinct zones: the Malyy Balkhan-Danata zone (XXIII) in the northwest, the Messerian-Khodzhakala zone (XXIV) in the south, and the separate Ezet-Karagez zone (XXV).

The Malyy Balkhan-Danata zone, the structure of whose central part was established in recent years through gravimetric and seismic surveys, was formed by pre-Akchagyl folding. It includes the westernmost outliers of the Kopet-Dag, which border the Danata corridor on the southeast (Kyuren-Dag), and the Kyzylbair bridge of the Malyy Balkhan.

The Messerian Khodzhakala zone is the region of the western submergence of the folds of the Kopet-Dag, covered by the Pliocene and Recent sediments of the Western Turkmen depression. Compared with most of the rest of the depression, the Messerian-Khodzhakala zone was subjected to relatively slight submergence in the Neocene. The structure of this zone dates from the pre-Akchagyl folding phase. The Messerian-Khodzhakala zone is separated from the South Caspian block by the narrow Shakhman foreland trough (XXVIII). In the northeast this trough adjoins the Ezet-Karagez folded zone, which, unlike the two other zones of the Western Kopet-Dag, experienced intensive post-Akchagyl folding.

The southeastern part of the Kopet-Dag meganticlinorium contains the eastern folded zone of the Kopet-Dag (XXVI), which was probably formed in the pre-Akchagyl and post-Akchagyl folding phases and consists chiefly of Upper Cretaceous and Paleocene rocks. As we noted above, the presence of a rigid obstacle in the form of the marginal southeastern part of the Kara-Kum inner block produced structural forms in the eastern Kopet-Dag whose strike differs substantially from that of the central Kopet-Dag. The absence of adequate geologic and geophysical data for eastern Turkmenistan does not make it possible at this time to regard this area as a separate tectonic zone. However, the existence in the Tedzhen river basin of distinctive strikes of gravitational anomalies, of elements of recent tectonic processes, and of individual outcrops of Paleocene and Cretaceous rocks point to the fact that separation of this area as a separate tectonic zone would make sense.

The easternmost element of the Alpine mobile belt is the plateau-like section of the Badkhyz and Karabil hills (XXXI). This part of the mobile belt is a region of substantial submergence, where the thickness of Neocene sediments reaches several hundred meters. E-W and even ESE-WNW strikes of gravitational anomalies, the conforming strike of recent tectonic elements, and isolated outcrops of bedrock in some places point to the presence of buried anticlinal uplifts. These uplifts are evidently linked, on the one hand, with the submerged folds of the Eastern Kopet-Dag in the west, and, on the other hand, with the buried anticlinoria of the Gissar range in the east. Detailed regional classification of this territory and interpretation of the geologic situation in the Gaurdak-Kugitang area, where the Alpine and Hercynian mobile zones join, must await the gathering of additional geologic and geophysical data.

## REFERENCES


Arkhangelsky, A. D. GEOLOGICHESKOYE STROYENYE I GEOLOGICHESKAYA ISTORYA SSSR [THE GEOLOGICAL STRUCTURE AND GEOLOGICAL HISTORY OF THE U. S. S. R.]: GNGI, 1941.

Beloussov, V. V. OSNOVNYE VORPROSY GEOTEKTONIKI [BASIC PROBLEMS OF GEOTECTONICS]: Gostekhizdat, 1954.

Godin, Yu. N. KOMPLEKSNYE GEOFIZICHESKYE ISSLEDOVANYA GLUBINNOGO STROYENYA ZEMNOY KORY NA PRIMERE ZAKASPYA [COMPLEX GEOPHYSICAL STUDIES OF THE DEEP-SEATED STRUCTURE OF THE EARTH'S CRUST AS EXEMPLIFIED BY BY THE TRANS-CASPIAN REGION]: Paper delivered at the 20th International Congress, Mexico City, 1956.

Kalugin, P. I. SKHEMA TEKTONIKI PEREDOVOGO KHREBETA KOPET-DAGA [TECTONIC DIAGRAM OF THE KOPET-DAG FRONTAL RANGE]: Trudy Turkmii FAN, no. 2, 1942.

Kropotkin, V. N. SOVREMENNYE GEOFIZICHESKYE DANNYE O STROYENII ZEMLI I PROBLEMA PROIZKHOZHDENYA BAZALTOVOY I GRANITNOY MAGMY [CONTEMPORARY GEOPHYSICAL DATA ON THE STRUCTURE OF THE EARTH AND THE PROBLEM OF THE ORIGIN OF BASALTIC AND GRANITIC MAGMA]: Akademiya Nauk SSSR, Izvestiya, Seriya Geologicheskaya, 1953, no. 1.

Luppov, N. P. GEOLOGICHESKAYA KARTA SSSR MASHTABA 1:1,000,000 (LIST K-40, NUKUS) [GEOLOGICAL MAP OF THE U. S. S. R. AT 1:1,000,000 AND ITS EXPLANATORY NOTE (SHEET K-40 NUKUS)]: Gosgeolizdat, 1946.

Muratov, N. V. TEKTONICHESKAYA STRUKTURA ZAPADNOY TURKMENII I POLOZHENYE BOLSHOGO BALKHANA [THE TECTONIC STRUCTURE OF WESTERN TURK-

MENIA AND THE POSITION OF THE BOLSHOI BALKHAN]: Akademiya Nauk SSSR, Izvestiya, Collection of papers in honor of the 90th Anniversary of Academician V. A. Obruchev, 1954.

Petrushevsky, B. A., I. A. Rezanov, V. A. Rastvorova, and I. N. Leonov. O TEKTONIKE ZAPADNOY TURKMENII [ON THE TECTONICS OF WESTERN TURKMENIA]: BM OIN, 1954, no. 4.

Shatskiy, N. S. O GLUBOKIKH DISLOKATSYAKH, OKHVATYVAYUSHCHIKH PLATFORMY I SKLADCHATYE OBLASTI (POVOLZHYE I KAVKAZ) [ON DEEP-SEATED DISLOCATIONS COVERING CRATONS AND FOLDED REGIONS (VOLGA VALLEY AND THE CAUCASUS]: Akademiya Nauk SSSR, Izvestiya, Seriya Geologicheskaya, 1948, no. 5.

Yanskin, A. L. VZGYLADA A. D. ARKHANGELSKOGO NA TEKTONICHESKY KHARAKTER YUGO-VOSTOCHNOGO OBRAMLENYA RUSSKOY PLATFORMY I SOVREMENNOYE PREDSTAVLENYE PO ETOMU VOPROSU [A. D. ARKHANGELSKY'S VIEWS ON THE TECTONIC CHARACTER OF THE SOUTHEASTERN MARGIN OF THE RUSSIAN CRATON AND PRESENT IDEAS ON THAT PROBLEM]: Collection of papers in memory of Academician A. D. Arkhangelsky, 1951.

# STRATIGRAPHY OF PRECAMBRIAN ROCKS OF THE WESTERN SECTION OF THE SANGILEN HIGHLAND (TUVA)[1]

*by*

*A. V. Ilin*[2]

*• translated by L. Drashevska •*

ABSTRACT

The stratigraphic sequence of the Precambrian complex of the western Sangilen Highlands, Tannu Tuva, include schists, schistose sandstones, fine-gravel conglomerates, micaceous and ferruginous quartzites, graphitic marbles, and gneisses of the Teskhem, Mugur, Balyktyghkem, Chartyss, and Naryn formations, which grade upward into one another without break. Deposits containing Lower Cambrian fossils are also known in the area. The ferruginous quartzites, associated with the upper Mugur, mark the principal boundary in Precambrian sedimentary accumulation and indicate the change from terrigenous sediments to calcareous marine sedimentation.

The degree of metamorphism varies considerably, both horizontally and vertically. Terrigenous deposits correspond to the green-schist facies. Local variations in the metamorphism of calcareous deposits apparently result from the variability of original components. Also important is the superimposed injection metamorphism associated with Proterozoic intrusions. --Editor.

* * *

The western section of the Sangilen Highland is the territory lying to the west of meridian 96$^{\circ}$ East and occupying the basin of the Erzin and Naryn rivers.

Investigations carried on here by the author and V. M. Moralev during the last five years have confirmed A. I. Levenko's ideas [2] that Precambrian rocks predominate in this area. In the western section of the Sangilen Highland, these rocks were the subject of a rather detailed investigation when prospecting was carried out in connection with the discovery in 1953 of bedded deposits of ferruginous quartzites. These quartzites are associated with a certain section of the geologic profile; usually they are well exposed, and, if not, they can be easily detected by using a portable magnetometer, or even a compass. Due to these peculiarities, it was possible to use ferruginous quartzites as marker beds in mapping and subdividing the Precambrian rocks in great detail. In addition, new data were collected about facies changes of the separate formations, their thicknesses and the character of their metamorphism. The review and analysis of these data will be the subject of the present work.

Two complexes are clearly distinguished among the Precambrian rocks of the Sangilen: the lower - terrigenous, and the upper - calcareous. The lower complex, which corresponds to A. I. Levenko's Teskhem beds and to A. P. Bozhinsky's Emiy beds, we subdivided into two formations: the lower - properly Teskhem formation, and the upper - Mugur formation. The upper complex includes the Balyktygkhem, Chartyss, and Naryn formations (fig. 1). Deposits of all five formations gradually pass upward into another; there are no disconformities and regional hiatuses inside the geologic column.

Deposits containing Lower Cambrian fossils are known in the area of the junction of the Sangilen Highland with the Eastern Tannuola ridge. The contact of these deposits with the Precambrian rocks goes along the zone of the great regional sublatitudinal fracture. Some indirect indications, the discussion of which is beyond the subject of this work, make it possible to assume the existence of a hiatus between the Lower Cambrian and the Precambrian in the western Sangilen.

In 1956-57, organic remnants were found in deposits of the calcareous complex. In the Naryn formation they are represented by the algae from the Osagia group. In the opinion of V. P. Maslov and I. K. Korolyuk, the algae of the Naryn formation are allied to those of the Uluntuy formation of the triple Baikal complex. Due to this similarity, the Naryn formation, as well as the Baikal complex [4] are correlated with the Siniy deposits; the underlying Precambrian rocks of Sangilen are inferred to be upper Proterozoic.

In the general contemporary structural framework of southeastern Tuva and the adjacent portions of Mongolia, the Sangilen massif is a large horst-anticlinorium. However, the ancient structure of the massif itself is synclinal. In a west to east direction, the general plunge of the structure is clearly observed.

---

[1] Translation of Stratigrafya Dokembryskikh otlozheny zapadnoy chasti Nagorya Sangilen (Tuva): Sovetskaya Geologiya, 1958, no. 4, p. 33-42.

[2] All-Union Aerogeological Trust. Ministry of Geology and Mineral Industries, U.S.S.R..

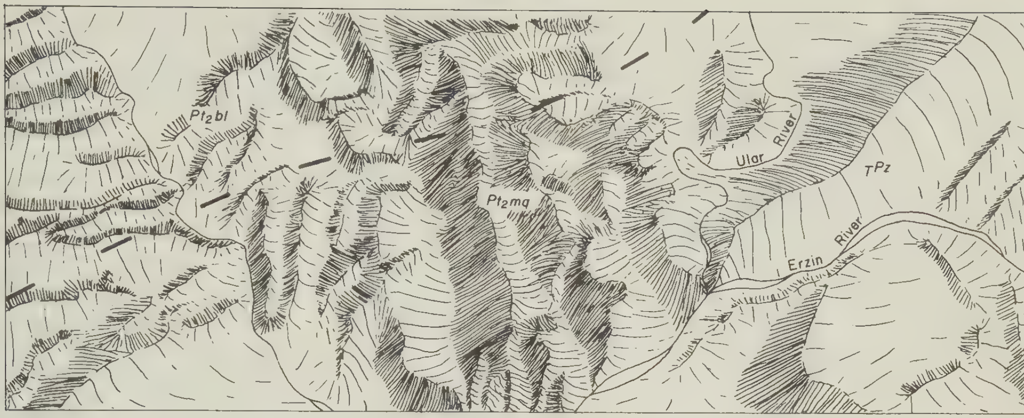


FIGURE 1. Diagram, drawn from an air photograph, of the mouth of the Ular River; scale 1:65,000. The dashed line locates the contact between two Precambrian formations: the Balyktygkhem formation, $Pt_2bl$, (marbles) in the northwestern part of the diagram, and the Mugur formation, $Pt_2mg$, (gneisses) in the center. The granite massif occurs at the mouth of the Ular River and higher along the Erzin River.

To the west, the structure rises and divides into two branches: the northern - the Changuss syncline, and the southern - the Naryn syncline (fig. 2). The Erzin anticline is situated north of the Changuss syncline, and south of the Naryn syncline lies the Kachin anticline.

phic "facies": fine-grained sericite-chlorite coaly-sericite schists, schistose sandstones and fine-gravel conglomerates, and micaceous quartzites - in the east; injected plagioclase micaceous gneisses - in the west. Tracing along the strike established the contemporaneous deposition of these differently metamorphosed rocks. The formation of gneisses resulted from the injective metamorphism associated with the upper Proterozoic granitoid intrusion.

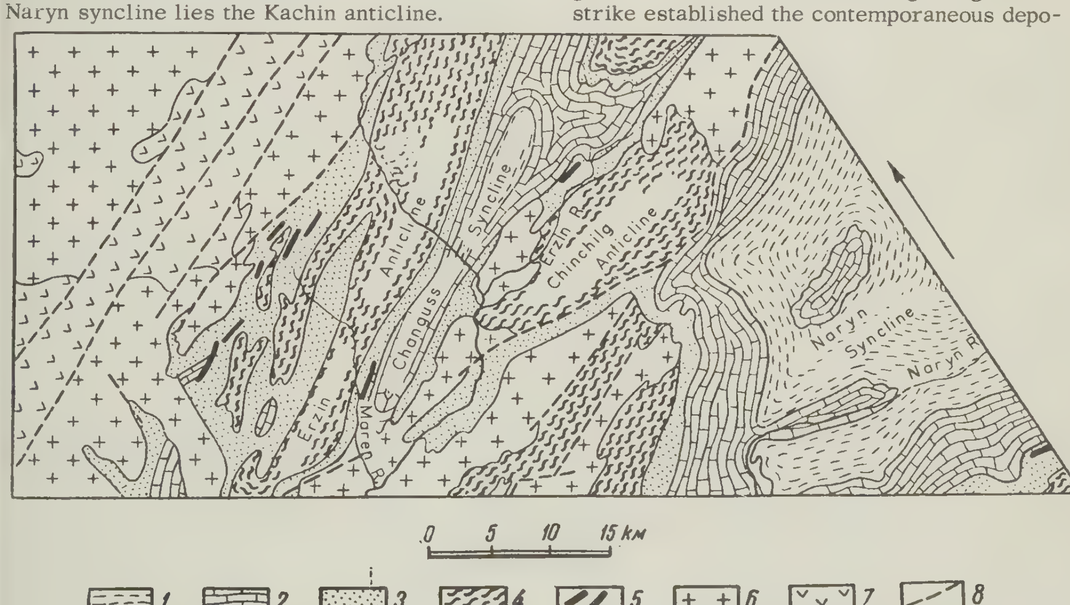


FIGURE 2. Geologic map of the western portion of the Sangilen Highland.
Proterozoic rocks: 1 - Chartyss formation; 2 - Balyktygkhem formation; 3 - Mugur formation; 4 - Teskhem formation; 5 - Beds of ferruginous quartzites; 6 - Lower Paleozoic intrusive rocks; 7 - Lower and middle Paleozoic rocks; 8 - Regional fractures.

## TESKHEM FORMATION

The Teskhem formation is the most extensive formation in the western portion of the Sangilen Highland. In the core of the Chinchilig anticline the formation is represented by two metamor-

Injected gneisses - plagioclase and cordierite

gneisses - also form the core of the Erzin anticline and the vast territory bordering the Naryn syncline from the west. Two major varieties are distinguished among the gneisses (on the lower reaches of the Naryn river):

1. Injected plagioclase and cordierite gneisses with biotite and garnet; they are medium-grained rocks with a rough banded texture. The banding is caused by numerous veins injected along parallel planes; the veins are granitic and vary in thickness from very fine up to a few centimeters. Garnet is a characteristic mineral of the gneisses, as well as of veins. In places, the material of the granite injections uniformly saturates rocks which then appear more homogeneous.

2. Micaceous gneisses lacking injections and distinguished by a finer banding and smaller grain sizes.

In the core of the Kachik anticline, the Teskhem formation consists of sericite schists formed from sandstones, siltstones and fine-gravel conglomerates. The apparent thickness of the formation is not less than 2,000 m.

## THE MUGUR FORMATION

Some differences in thicknesses and in the facies of sediments are observed in certain sections of the area. On this basis, the following sections can be distinguished: the Mugur section (northwestern flank of the Erzin anticline), the Moren-Keskelig section (Changuss syncline), and the Naryn section (Naryn syncline).

### The Mugur section

Three sequences are distinguished (from the bottom upward, fig. 3) in the cross section of the formation in the area of the Mugur deposits of ferruginous quartzites:

1. A sequence of interstratified graphitic marbles, quartzites, amphibole schists and injected biotite gneisses; thickness up to 400 m.

2. A sequence of biotite gneisses, thickness 300 m.

3. A sequence of mixed lithology, containing two layers of banded ferruginous (magnetite) quartzite and amphibolic (cummingtonite) ferruginous quartzite, each having a thickness up to 8-10 m (fig. 4 on p. 22).

The beds of ferruginous quartzites are sharply separated from the adjacent non-metalliferous beds. The thickness is up to 200 m.

The total thickness of the formation is 900 m.

In addition to the ferruginous quartzites, muscovite and graphite schists are also characteristic rocks of the third sequence. The first are distinguished by the bright reddish-brown color of their outcrops ("red" schists); the second are easily recognized due to the high graphite content.

The above profile is typical for the entire distribution of the formation - from the upper reaches of the Ular river to Lake Dus-Khol on the left bank of the Tes-Khem river. Within this 50-60 km-wide strip the ferruginous quartzites are found almost everywhere.

According to the thorough investigations of B. B. Golubev, G. N. Shaposhnikov, and A. G. Linkov, the recorded length of beds in some places is approximately 5-6 km. In comparison to other sections, the described zone is characterized by a considerable length of beds and by the predominance of quartzite over amphibolite, as well as by a higher and more uniform content of iron (39-40 percent).

### Moren-Keskelig Section

The primary rocks of the cross section of the Mugur formation, especially those of its upper portion, are very similar in both flanks of the Changuss syncline. However, the degree of metamorphism of these rocks is different: fine-grained sericite-chlorite schists of the southern flank correspond to the coarse- and medium-grained injected gneisses of the northern flank; black limestones of the southern flank correspond to marbles of the northern flank, etc.

The profile of the northern flank at the site of the Moren deposits of ferruginous quartzites situated 12-15 km across the strike from the Mugur deposits is as follows (from the bottom upward):

1. Amphibolic schists . . . . . . 20-30 m

2. The sequence of muscovite and biotite-muscovite schists with numerous large garnet crystals (1-1.5 cm). . . . . . . . . 400 m

3. Amphibolic schists. . . . . . 20-30 m

FIGURE 3. Comparison of the Precambrian geologic columns in the western part of the Sangilen Highland.
1 - gneisses and schists; 2 - gneisses with garnet; 3 - sericite schists; 4 - quartzites; 5 - coaly quartzites; 6 - amphibolic schists and amphibolites; 7 - garnet amphibolites; 8 - "red" muscovite schists; 9 - graphite schists; 10 - limestones and marbles; 11 - breccia-like marbles; 12 - calcareous-siliceous rocks; 13 - ferruginous quartzites and amphibolites with magnetite.

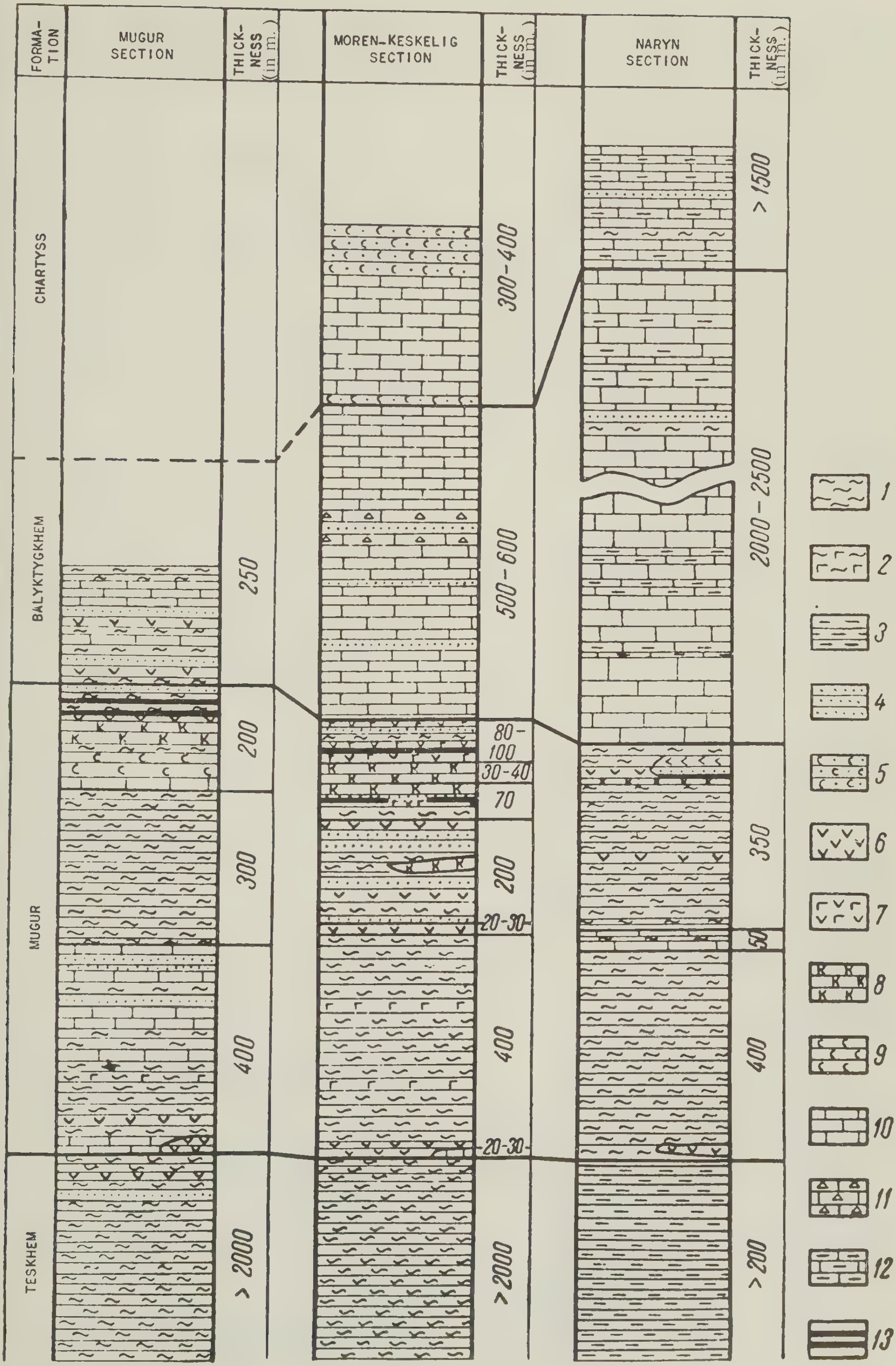
FORMATION
MUGUR SECTION
THICKNESS (in m.)
MOREN-KESKELIG SECTION
THICKNESS (in m.)
NARYN SECTION
THICKNESS (in m.)
CHARTYSS
BALYKTYGKHEM
MUGUR
TESKHEM
250
200
300
400
> 2000
300-400
500-600
80-100
30-40
70
200
20-30
400
20-30
>2000
> 1500
2000-2500
350
50
400
> 200
1
2
3
4
5
6
7
8
9
10
11
12
13

4. Interstratified quartzites, coaly garnet amphibolites, and graphite, garnet and kyanite schists . . . . . . 200 m

5. A sequence of interstratified quartzites, amphibolites, and micaceous schists; in the upper part of this sequence, amphibolic ferruginous quartzites and amphibolites are recorded, which contain magnetite; ferruginous quartzites form here one or two layers, irregular along the strike, each having a thickness not more than 2 m . . . . 70 m

6. "Red" muscovite schists, very similar to the schists of the third sequence of the Mugur profile . . . . 30-40 m

7. Muscovite schists, amphibolites, and garnet amphibolites including a layer of banded ferruginous quartzites and amphibolites with magnetite. The layer can be traced along the strike for 5 km and its thickness is 4-5 m. In some places the layer consists of laminated quartzites and amphibolites, but commonly it is completely composed of amphibolic quartzites and amphibolites with magnetite. The iron content ranges from 20 to 40 percent . . . . . . . . . . . . . . 80-100 m

The above cross section of the formation at the Moren section is complete, in spite of the fact that a small longitudinal fracture goes along the top of the upper (seventh) sequence; south of this fracture, marbles of the Balyktygkhem formation are exposed. The stratigraphic

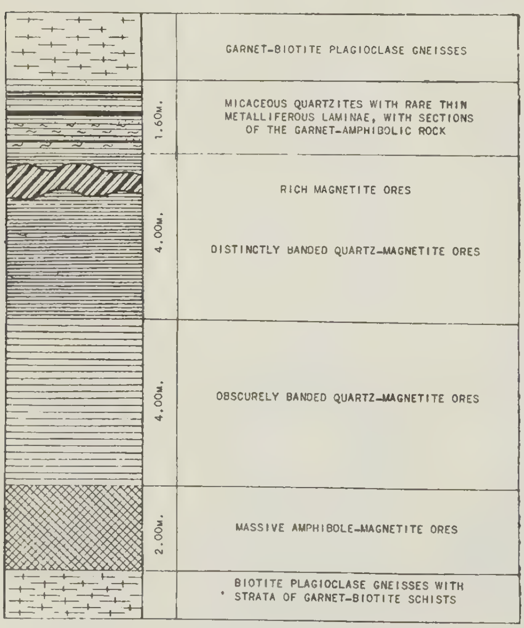


FIGURE 4. Diagram of the layer of ferruginous quartzites (according to B. B. Golubev).

thickness of the described formation is very small, as is confirmed by a comparison of the profile at the site of the Moren deposits with that at the Keskelig deposits (the southern flank of the Changuss syncline.)[1]

In the upper section of the Mugur formation, on the southern flank (the Keskelig deposits of ferruginous quartzites), the sequences 4 - 7 of the Moren profile are found; the vertical distance along the stratigraphic column from the upper layer of ferruginous quartzites to the bottom of the Balyktygkhem marbles is around 20-30 m.

The ferruginous quartzites occupy an analogous position in the profile of the southern part of the Sangilen Highland. For example, on the left bank of the Tsorigin river, thin irregular layers of ferruginous quartzites lie at the very top of the Mugur formation, 20-30 m lower than the bottom of the Balyktygkhem marbles.

Observations of the Moren profile, from the site of the Moren deposits of ferruginous quartzites along the strike in both directions, showed that the Mugur formation becomes somewhat thinner in both directions. Ferruginous quartzites almost wedge out, appearing in places as thin beds with a length not more than 500-600 m. In the valley of the Ular river, limestones appear at the bottom of the formation.

## The Naryn Section

Near the Turelchi well, the profile of the formation is as follows (from the bottom upward):

1. Biotite plagioclase gneisses, often with garnet . . . . . . . . . . . . . 400 m

2. A sequence of interstratified (8-10 m) gneisses and marbles . . . . 50 m

3. Plagioclase, or more often cordierite gneisses, with amphibolites, marbles, graphite and muscovite "red" schists in the upper section. According to data from E. L. Varand, ferruginous quartzites are found at the very top of the profile, several kilometers to the east . . . . . . 300-400 m

To the west of the Turelchi well, a uniform layer of amphibolic schists is found, having a thickness of approximately 20 m.

Generally, the profile of the Mugur formation in the Naryn section is characterized by

---

[1] A comparison of profiles of the Mugur formation in the northern and southern flanks of the Changuss syncline has already been made [1].

the following features: (a) a layer of amphibolic schists at the bottom, (b) the presence of marbles in the middle and upper sections of the profile, (c) thin and irregular beds of amphibolic ferruginous quartzites of the Moren type in the very top section.

In the comparion of the geologic columns of the Mugur formation from different localities, the top of the Teskhem gneisses, or the layer of amphibolic schists at the bottom of the Mugur formation, is taken as the lower boundary of the formation; the ferruginous quartzites and the associated complex of strata are taken as the upper boundary. The comparison shows that two types of cross sections are characteristic of the Mugur formation: the proper Mugur cross section, in the northwestern part of the Sangilen Highland, and the Naryn cross section, characteristic of the western and southwestern part of the area.

Amphibolic schists at the bottom of the cross section and ferruginous quartzites at the top are common to both cross sections.

The following features are typical for the Mugur-type cross section: (a) a considerable regularity in composition and a fairly constant thickness of the beds of ferruginous quartzites, the predominance of proper quartzite varieties, a higher and more uniform content of iron; (b) comparatively thick beds of graphitic schists; (c) the presence of calcareous rocks in the lower part of the section.

Beds of ferruginous quartzites and graphitic schists seldom occur in cross sections of the Naryn type, if found, they are irregular and of a small thickness; calcareous rocks are found in the middle and upper parts of the cross section. The thicknesses of both types of cross section are about the same (approximately 900-1,000 m).

## BALYKTYGKHEM FORMATION

In the Mugur section the Precambrian rocks end with deposits of the Balyktygkhem formation. The upper sequence of the Mugur formation containing ferruginous quartzites is replaced here by interstratified micaceous schists, quartzites and marbles with a total thickness of 250-300 m.

### Moren-Keskelig Section

In the lower reaches of the Erzin river the formation is made up of sandy laminated marbles having a thickness of approximately 300 m.

Twenty km of the east, along the Ular river, laminated gray marbles and black bituminous limestones predominate. "Breccialike" marbles are found which contain large crystals of black calcite lying in the gray fine-grained matrix. The thickness of the formation is approximately 500-600 m.

Thirty km to the east of the Ular river, the formation is clearly divided into two sections. The lower section is represented by gray marbles interstratified with micaceous and amphibolic schists, quartzites and coaly quartzites with inclusions of pyrite and pyrrhotite; calcareous rocks prevail in the upper section. The aggregate thickness of this formation is about 2,000 m. The lower boundary of the formation at both localities is drawn along the top of the Mugur gneisses; the upper boundary lies at the bottom of the coaly quartzites of the Chartyss formation.

From the southwest to the northeast in the Moren-Keskelig section the thickness of the formation gradually increases from 300 to 2,000 m. In the same direction, the number of different schists and quartzites which appear in the formation gradually increases, although calcareous rocks still prodominate.

### The Naryn Section

In the Naryn section, white graphitic coarse-grained marbles predominate; here and there they contain thin strata of gray fine-grained limestones and quartzites. The thickness of the formation attains 2,500 m. Comparison of the geologic columns of this formation from different localities shows that from northeast to southwest along the strike, and from southeast to northwest across the strike, the thickness of the formation generally decreases.

To the north of the Sangilen Highland, in the basin of the middle reaches of the Buren river, in the profile of the Precambrian deposits, the mass of marbles and quartzites, with an apparent thickness of not more than 1,500 m, overlies the bed of ferruginous quartzites. This mass is lithologically similar to the Balyktygkhem formation of the Naryn section. It seems that the thick mass of marbles and metamorphosed limestones of the western Kosogolye area, lying east of the Sangilen Highland, should be considered to be the stratigraphic equivalent of the Balyktygkhem formation.

To the west, the Sangilen Highland adjoins the spurs of the Khangay Highland which is in the Mongolian People's Republic. Folded structures of the western Sangilen, having a uniform southwestern strike, are traced, under the cover of unconsolidated deposits of the Ubsu-Nur basin, in the direction of the Khan-Khukhey range (northwestern Khangay). According to N. A. Marinov, in northwestern Khangay, the Precambrian is divided into two formations: the lower - schists-gneisses, and the upper - limestones-quartzites-schists. N. A. Marinov correlates the lower formation with the Teskhem rocks as distinghished by A. I. Levenko and corresponding to the Teskhem and Mugur

formations of our stratigraphic scheme. The upper formation can be equated with the Balyktygkhem and higher formations.

Thus, in the western part of the Sangilen Highland, as well as in a broader area including southeastern Tuva and northwestern Mongolia, two major types of the profiles of the Balyktygkhem formation are distinguished. The first type is distributed in the northwestern Sangilen (the Mugur section) and in the northwestern Khangay is characterized by marbles (limestones), schists, and quartzites. The second type occurs in the central and western part of the Sangilen Highland (Naryn section) and in the western Kosogolye area, calcareous rocks predominate in this type of profile and it seems that its thickness is greater than that of the first type. The profile of the Moren-Keskelig section, exposed between the Mugur and the Naryn sections, occupies an intermediate position in regard to thicknesses and facies of sediments of the Balyktygkhem formation.

## CHARTYSS FORMATION

### Moren-Keskelig Section

In the basin of the Ular river, this formation is made up of marbles with thin (1-2 m) strata of coaly schists, amphibolites and amphibolized limestones. At the bottom of the formation a layer of coaly schists occurs with a thickness of 20 m; in the upper part of the section there is another layer of the same rock which a thickness of 100 m. The aggregate apparent thickness of the formation is 300-400 m.

At a distance of 30 km to the east, in the basin of the Uldun river, the Balyktygkhem formation is overlain by the mass of limestones, quartzites, and coaly, amphibolic, and micaceous schists, having an aggregate thickness of 2 km. The quantity of limestones gradually decreases in this formation from the bottom upward. Amphibolic schists occur mostly in the upper part of the section, the micaceous schists in the lower part.

Apparent thicknesses of the formation are unreliable. The comparison of separate parts of two sections provides an opportunity to determine changes in true thicknesses which increase from southwest to northeast. The proportion of calcareous rocks also somewhat decreases in the same direction.

### The Naryn Section

The Chartyss formation is represented by interstratified rocks of varying composition. These strata are rather thin (1-3 m). White graphitic marbles predominate in the formation. Other strata are: marbles with biotite, phlogopite, scapolite, diopside, and other siliceous minerals ("siliceous" marbles), as well as pyroxene-amphibolic plagioclase gneisses with carbonates. The thickness of the formation is 3,000 m.

A comparison of the geologic columns of the whole area leads to the conclusion that the Chartyss formation thins from the southeast to the northwest. In general, in the same direction the calcareous rocks are replaced by calcareous-terrigenous deposits. In the eastern Sangilen the formation is almost completely made up of calcareous rocks.

## CONCLUSIONS

Consideration of the above data characterizing the stratigraphy of the Precambrian rocks in various sections of western Sangilen and in the adjacent territories leads to the following conclusions:

1. Ferruginous quartzites are associated with the very top of the rocks of the lower complex, i. e., with the principal boundary in the history of Precambrian sedimentary accumulation, marking the replacement of terrigenous sediments by calcareous. Ferruginous quartzites of great thickness, of regular distribution along the strike, and having the most uniform iron content occur in the northwestern Sangilen. The same area is characterized by the thickest and most regular beds of graphitic schists.

2. It is likely that during the period of the formation of the upper calcareous complex of the Precambrian deposits within the west Sangilen and adjacent territories, different regimes of vertical movements existed in certain sections. Steady downwarping of the greatest total extent occurred in the eastern part of western Sangilen and in the western Kosogolye area. Northwestern Sangilen, northwestern Khangay and probably the area situated north of Sangilen was at the same time relatively elevated. Characteristically, the tendency of uplift in northwestern Sangilen continued and was intensified in the Paleozoic. In the Lower Cambrian this territory was already subjected to erosion and became a source of sediments. This area was not subjected to downwarping in the Silurian time, which is attested by corresponding changes in thicknesses and in the facies of the motley rocks of the Wenlockkian-Ludlovian stages in the eastern part of the Ubsu-Nur basin.

3. The degree of metamorphism of contemporary rocks of the terrigenous and calcareous complexes generally is not steady over the area and cannot be a criterion for the establishing of stratigraphic sequences during mapping. Regional metamorphism of terrigenous deposits of the lower complex corresponds to the facies of "green schists." Of the utmost importance is the superimposed injection metamorphism associated with the Proterozoic

intrusion. Local variations in the degree of metamorphism of calcareous deposits apparently result from the instability of their original components. In particular, calcareous rocks containing a dispersed mixture of clay material usually are more fine-grained and darker than rocks lacking this admixture.

However, within some sections consisting of calcareous deposits of the upper complex, a decrease in the degree of metamorphism is clearly manifested from the bottom upward. An example can be found in the Naryn syncline where white coarse-grained graphitic marbles predominate at the bottom of the continuous thick calcareous complex, while its top section is of black fine-grained limestones with comparatively well-preserved organic remains.

REFERENCES

1. Ilin, A. V. NOVYE DANNYE PO STRATIGRAFI I METAMORFIZMU DREVNIKH TOLSHCH YUGO-VOSTOCHNOY TUVY [NEW DATA ON THE STRATIGRAPHY AND METAMORPHISM OF THE ANCIENT SERIES OF SOUTHEASTERN TUVA]: Trudy, VAGT, 1956, no. 2, Gosgeoltekhizdat.

2. Levenko, A. I. O DOKEMBRI YUGO-VOSTOCHOY TUVY (NAGORYE SANGILEN) [ON THE PRECAMBRIAN OF SOUTHEASTERN TUVA (SANGILEN HIGHLANDS)]: Akademiya Nauk SSSR, Doklady, v. 65, no. 2, 1949.

3. Marinov, N. A. DOKEMBRYSKYE OTLOZHENYA MONGOLI [PRECAMBRIAN DEPOSITS OF MONGOLIA]: Akademiya Nauk SSSR, Izvestiya, Seriya Geologicheskaya, 1956, no. 6.

4. Sokolov, B. S., and Yu. K. Dzevanovsky. O STRATIGRAFICHESKOM POLOZHENI I VOZRASTE OSADOCHNYKH TOLSHCH POZDNEGO DOKEMBRYA [ON THE STRATIGRAPHIC LOCATION AND AGE OF THE SEDIMENTARY SERIES OF THE LATE PRECAMBRIAN]: Sovetskaya Geologiya, 1957, no. 55.

# ON SEDIMENTARY FORMATIONS FROM CAPETOWN AND MORAINES OF THE ANTARCTIC[1]

*by*

*O. S. Vyalov and L. G. Tkachuk*

*• translated by Victor H. Winston •*

ABSTRACT

Cemented psammites were collected by O. S. Vyalov from Antarctic moraines and from outcrops in the vicinity of Capetown, South Africa, and were analyzed by L. G. Tkachuk. Comparison of the psammites--their chemical, mechanical, and paleontological composition--indicates the similar conditions of rock formation which prevailed in the vicinity of Capetown and in parts of Antarctica. Also, it is possible that sedimentary rocks from South Africa contributed to the drift area which supplied morainal material to parts of Antarctica. The results of this comparison are interesting in view of the assumed existence of a single Gondwana continent in the Paleozoic. --Editor.

## INTRODUCTION

O. S. Vyalov collected sedimentary-rock specimens from Antarctic moraines and also from the vicinity of Capetown [Union of South Africa] while he was a member of the 1955-56 Antarctic expedition of the Ukrainian Academy of Sciences. All samples retained by the expedition were cemented psammites. A comparison between South African and Antarctic specimens is of considerable interest in view of the assumed existence of a single Gondwana continent in the Paleozoic. L. G. Tkachuk is responsible for the petrographic study of specimens and Vyalov provided the general geological description.

## SEDIMENTARIES FROM THE VICINITY OF CAPETOWN

Capetown is situated near Table Mountain (1, 082. 75 m) and Lion's Head Mountain (670 m).* The foothills of these mountains are highly eroded granites which tend to exfoliate. A new cave discovered in the vicinity revealed the exfoliation of fresh, grayish-white, coarse-grained biotite granites. Known as "younger" Cape granites (as distinguished from ancient Cape granites), they comprise the basic foundation of Table Mountain. Their age has not yet been determined. In the vicinity of Capetown, the granites are covered by the Table series which forms the floor of the Cape system. The origin of sandstone samples collected by Vyalov is traced to this (Table mountain) series; it comprises the following five groups: (1) basal shales, represented by thinly stratified shales and argillaceous sandstones; (2) main sandstones (to be discussed below) as much as 610-m thick; (3) a horizon (as much as 305-m thick) of tillites represented by greenish, light-blue, and reddish clays with dispersed grain patterns (the glacial dislocations observed in underlying sandstones are noteworthy); (4) upper shales represented by soft, greenish clays and dark shales; and (5) upper sandstones which resemble main sandstones. No organic remains were found in this series.

Above lies the 762. 5-m thick Bokkeveld series composed of alternating sandstone and schist horizons. Some of the earliest species of ancient South African marine fauna are found in the lower part of the series (150-300 m). Representative species include brachiopods, lamellibranchs, gastropods, and trilobites which establish the Lower Devonian origin of the Bokkeveld series. Consequently, the origin of the Table series is tentatively traced to the Silurian.

The remaining component of the Cape system is the Witteberg series which comprises sandstones, quartzites, and shale; its total thickness is 750 m. Sandstones which differ from those comprising the Table series appear to predominate. Their more pronounced cleavage, greater fissility, and finer grain account for the principal distinguishing features. Among findings were remains of Sigillaria, Lepidodendron, and also traces of Toonurus (Spirophyton). Table sandstones represent a deltalike formation. The coastline advanced southward as a result of geosynclinal folding. Thus, marine environments originated during the formation of Bokkeveld series, while continental environments are identified with the subsequent epoch and the origin of Witteberg series.

The massively thick Karroo system, which lies above the previously described formations, is subdivided into the Dwyka, Ecca, Beaufort, and Stormberg stages. The Dwyka is identified with the upper Carboniferous to lower Permian, the Ecca with the middle Permian, the Beaufort with the Lower Triassic, and the Stormberg

[1] Translation of Pro osadochni porodi z Keyptauna ta z moren antarktidi: Akademiya Nauk Ukrainskoy RSR, Geologichny Zhurnal, v. 18, no. 1, p. 39-45, 1958.

* Elevations are taken from a log and maritime map.

with the Upper Triassic. Drakensberg volcanics which form the upper Stormberg series appear to have originated in the Rhaetian Lias. Tillites form the base of the Dwyka stage. Their equivalents, likewise of glacial origin, are known to exist in Australia, India, and South America. Coal beds occur in the middle of Ecca stage. Typical findings include Glossopteris flora of the type observed in Beaufort stage, which also exhibits a rich variety of vertebrate fauna (pareiassaurides, dicynodotides, lestosaurides). The Stormberg stage exhibits occurrences of Thinnfeldia flora and numerous traces of vertebrate remains. Intrusions and dolerite dikes occur throughout the Karroo system. Indubitably, the Karroo dolerites correspond to the upper layers of the Stormberg stage and should be assigned to the Jurrasic.

The Table series extends to the Cape of Good Hope where the stratification and a very gentle (up to $5^{o}$) southward dip of strata is readily visible. If one should consider the gentle southward dip of strata between Capetown and Small Lion's Head [Ed: Lion's Rump (?)], the area between Capetown and the Cape of Good Hope would appear to represent a broad, gently inclined trough with an east-trending axis. This trough comprises the quartzitic sandstones of the Table series which rest on Cape granites.

Microscopic analyses reflected the almost exclusive quartz composition of clastic material. Quartz grains range from very fine to 1.0 mm and larger. Those ranging from 0.25 and 0.3 mm or 0.4 to 0.5 mm in size appear to predominate. Also encountered are occasional grains of hornblende, muscovite leaves, and fragments of fine-grained quartzite.

Quartz appears in the form of irregular regenerated grains which exhibit a clear distinction between older clastic (mostly subrounded) and secondary quartz. Clastic grains contain angular inclusions which form small chains, streaks, or flakes, or which are distributed evenly throughout the grains. Other solid inclusions, such as apatite, zircon, biotite, iron-ore minerals, are uncommon. Fragmentary grains have normal or, less frequently, wavy extinction. Cement is secondary quartz which forms films or coatings as much as 0.10 mm wide. Devoid of inclusions and clearly visible, these films or coatings exhibit an optical orientation similar to that of disintegrated quartz. Also evident are filling-cement varieties, a thin concretion of sericite, and, less frequently, chalcedony. The cementation characteristics and compositions of the aforementioned rocks place the bulk in the category of quartzites (cement is represented by expansion quartz cement) and quartzitic sandstones (other varieties are of considerable significance). The chemical composition of quartzites and sandstones which was established by the Laboratory of Mineral Chemistry of the Ukrainian Academy of Sciences' Institute of Mineral Resources is given below:

TABLE 1. Chemical composition of quartzites and quartzitic sandstones from the vicinity of Capetown (% weight).

| Components | Quartzites | | Quartzitic sandstones |
|---|---|---|---|
| $SiO_2$ . . . . | 94.14 | 94.17 | 90.09 |
| $TiO_2$ . . . | 0.59 | 0.45 | 1.88 |
| $Al_2O_3$ . . . | 2.86 | 2.88 | 3.82 |
| $Fe_2O_3$ . . . | 0.60 | 0.50 | 1.00 |
| FeO . . . | 0.18 | 0.18 | 0.54 |
| MnO . . . | undetected | | - |
| MgO . . . | 0.31 | 0.36 | 0.55 |
| CaO . . . | 0.42 | 0.49 | 0.28 |
| $Na_2O$ . . . | 0.52 | undetected | - |
| $K_2O$ . . . | 0.20 | 0.34 | 0.17 |
| BaO . . . | 0.01 | 0.10 | 0.10 |
| S (total) . . | 0.14 | 0.10 | 0.08 |
| $SO_2$ . . . | 0.07 | 0.65 | 0.04 |
| B. p. p. . . . | 0.52 | 0.35 | 0.87 |
| $H_2O$ [Ed.: at]$105^{o}$ | undetected | 0.12 | 0.12 |
| Total | 100.56 | 100.69 | 99.54 |

The chemical composition of specimens from the vicinity of Capetown resembles that of nearly identical monogenetic quartzites. The higher $K_2O$ and MgO contents in quartzitic sandstones are traced to the influences of sericite cement.

## MORAINAL MATERIALS FROM CERTAIN AREAS OF THE ANTARCTIC

Vyalov's work in the Antarctic included a study of morainal material from several localities. An accumulation was found near the foot of Gauss Mountain, while isolated boulders were scattered on its slopes. Efforts to locate sedimentary rock in place were unsuccessful. Samples of quartzoid sandstones which came from these localities were gathered by the geologist, E. Philippi, who participated in Drygalsky's 1901-1903 expedition; a petrographic study was made by geologist R. Reinisch.

Small moraines are found in the area of Mirnyy near the sites of Mirnyy I and Mirnyy II volcanos. Boulders are scattered throughout the four volcanos which protrude from under the ice cover near the shore, and also on the islands in the vicinity of Mirnyy settlement. There are no traces of sedimentary rock among these boulders. A moraine comprising crystalline boulders occupies a narrow strip near the Union Corner [?] shore in Depot (Farr) Bay. Epfel's Glacier moraine lies in a temporary base near the outskirts of Banger Oasis. Small sandstone boulders are found among crystalline-boulder rock accumulations. These included a rather small pink quartzoid specimen and a large (1.5-m long) oblique crimson-brown boulder.

Sedimentary boulder rocks are very uncommon in the Banger Oasis area where abundant morainal material covers the slopes and reaches the summits of submerged volcanos. Vyalov noticed a few specimens of cleavable pink sandstones and one oblique schistose boulder with small (as much as 1 cm) pebbles. Also noted were conglomerates with pebbles as much as 4 cm in diameter. A boulder of variegated reddish sandstone with a mass of small pebbles, which is approximately 30 cm in diameter, was found in the northeastern section of the oasis on an island which houses an astronomical observation point called "Oasis Eastern". Scattered morainal material is found on Snyder's volcanic formations on the Knox Coast at 107°41'E. and 66°33'S. A part consists of sedimentary rock fragments; pink, crimson, and brownish-red quartz sandstones; gravel; and small pebble conglomerates.

A petrographic analysis of all sedimentary rock samples from Epfel's Glacier moraine as well as from the Banger Oasis was made by Tkachuk. The samples exhibited a marked similarity; most are unevenly grained, reddish-brown arkose sandstones or conglomerates. Of note was a bright-gray, medium-grained sample of quartziferous feldspar sandstone. Arkose sandstones usually contain from 70 to 85 percent clastic material. Clastic material is composed of quartz, feldspar, mica, and occasional fragments of fine-grained quartzites, sericitic phyllites, argillites, and chalcedony. Grains of clastic minerals and rock fragments have an angular; at times subrounded; and, unfrequently, a rounded form. Their diameter ranges in size from tiny fractions to 2 or 4 mm; diameters from 0.5 to 0.8 mm or 0.2 to 0.3 mm are most common. It is thus possible to distinguish between large-grained, medium-grained, and unevenly grained varieties of arkose sandstones; the latter variety is very common.

Quartz constitutes the bulk of clastic material. Grains have a normal and, occasionally, slightly wavy extinction. Their angular inclusions tend to form a network of small and frequently criss-crossing chains. At times, the inclusions appear as more or less widely extended stripes or flakes. They may also be scattered evenly throughout the grain. The number of inclusions varies from one grain to another. Variation limits may be so high as to place some quartz grains in over-filled and other in under-filled categories. Occasionally, one comes across a grain which contains a mass of hairlike sagenitic-type inclusions, possibly rutiles (?); needle-shaped apatites; and, quite infrequently, zircon, tourmaline, biotite, feldspar, or iron-ore.

In arkose sandstones, feldspar always constitutes 20 to 30 percent of the clastic material. Occasionally, the distribution may be uneven so that the share of feldspar may be equal to that of quartz. Represented by potassium feldspar and, at times, by highly subordinated plagioclases, the feldspar varieties appear in different stages of decomposition. Potassium feldspars tend to exhibit a grating structure which resembles the structure of microcline. Plagioclases range from almost pure albites (symmetric extinction angle, 10°) to oligoclases (symmetric extinction angle, 0°). The more basic plagioclase sandstones contain a larger share of skeleton and compact epidote. They are also more frequently wedge-shaped or in the form of polysynthetic twinning. Differential disintegration explains the proximity of new or lightly decomposed grains to species with a weakened polarization potential; the latter react to light by assuming a brownish color and exhibiting signs of turbidity. In certain localities, thin concretions of sericite assume the place of feldspar.

Mica is present in small (1 to 2 percent) or noticeable (nearly 5 percent) quantities in the form of narrow, long, or wide laminae. Considerably hydrated and greatly deformed, it is represented by hydromuscovite (hydromica) and, to a lesser extent, by hydrobiotite. Cement is composed of thin sericite concretions with quartz and iron hydroxides which form films or coatings on clastic grains. Sericite concretions serve as pore fillers and crust builders. Also noted is a small amount of secondary quartz which forms a coating around clastic quartz grains.

Microscopic examinations of a different light-gray, medium-grained variety of sandstone from Epfel's Glacier moraine reveal a composition of clastic material and cement. Clastic material, which accounts for 80 to 90 percent of the total, is represented by quartz and feldspar and also by isolated fragments of chalcedony. Grain sizes vary from 0.01 to 0.5 mm; the bulk is in the 0.25 and 0.30 mm range. Quartz appears in the form of angular and partly rounded, or elongated (length is 4 times greater than width), grains with normal or, less frequently, mildly expressed wavy extinction. Angular inclusions are distributed in streaks and chains or scatter throughout a grain. Their frequency tends to fluctuate. Hard inclusions of iron-ore minerals or, even less frequently, zircon are very uncommon.

Feldspars which constitute approximately 10 percent of the rock are represented by potassium feldspars with predominantly microcline structure. Approximating the size and shape of quartz grains, the grains of feldspar are rarely decomposed.

Cement is thin clayey sericite and siliceous, opal-chalcedony material on contacts; porous; or, occasionally, crusty.

Typical arkose sandstones from Epfel's Glacier moraine have the following composition (percent weight; based on data from the Laboratory of Mineral Chemistry of the Ukrainian Academy of Sciences' Institute of Mineral Resources):

| | | | |
|---|---|---|---|
| $SiO_2$ | 80.04 | $Na_2O$ | 0.40 |
| $TiO_2$ | 0.50 | $K_2O$ | 4.55 |
| $Al_2O_3$ | 10.43 | BaO | 0.10 |
| $Fe_2O_3$ | 1.83 | S (total) | 0.07 |
| FeO | 0.35 | $SO_2$ | 0.04 |
| MnO | 0.67 | B. p. p. | 1.08 |
| MgO | 0.56 | $H_2O$ [Ed.: at] 105°. . . | 0.22 |
| CaO | 0.40 | | |
| | | Total | 101.24 |

The composition is fully compatible with that of arkose sandstones with higher $K_2O$ and $Al_2O_3$ contents and comparatively low in $SiO_2$. A sandstone specimen received during Vyalov's trip to Adelaide from Professor D. Mawson was analyzed and compared with specimens collected by our expedition. It came from a littoral-zone moraine in King George V Land, where Mawson's expedition had worked in 1911-14.

Of light, meat-red color, the specimen exhibited a fine- and medium-grained psammitic structure.

Clastic quartz and a small quantity of secondary quartz-cemented feldspars accounted for its composition. Quartz appeared in the form of angular and half-rounded grains with secondary quartz coatings and, occasionally hairlike, angular inclusions which are distributed evenly or in a chainlike or streaklike pattern.

Feldspar, in grain sizes similar to those of quartz, was represented by gratinglike microcline, frequently in advanced degrees of decomposition, and covered by pelitic material. Cement comprised secondary quartz which forms coatings around discrete quartz grains. These show an optical orientation identical with that of secondary quartz. The prevalent coatings of iron hydroxide surround and separate the discrete quartz grains from secondary quartz coatings.

The described sandstone specimen is a quartzite-sandstone related to sedimentary quartzites; it differs from the arkose sandstones of Epfel's Glacier and Banger's Oasis, but approximates the quartzite-sandstones and quartzites from the vicinity of Capetown. This similarity, which borders on identity, is corroborated by the chemical composition of quartzite-sandstones and quartzites from the littoral zone of King George V Land. Analyzed samples of quartzite-sandstone have the following composition (percent weight; based on data from the Laboratory of Mineral Chemistry of the Ukrainian Academy of Sciences' Institute of Mineral Resources):

| | | | |
|---|---|---|---|
| $SiO_2$ | 95.00 | BaO | 0.10 |
| $TiO_2$ | 0.42 | $Na_2O$ | 0.09 |
| $Al_2O_3$ | 1.47 | $K_2O$ | 0.63 |
| $Fe_2O_3$ | 1.13 | S (total) | 0.10 |
| FeO | 0.24 | $SO_2$ | 0.05 |
| MnO | 0.03 | B. p. p. | 0.27 |
| MgO | 0.28 | $H_2O$ [Ed.: at] 105°. . | 0.13 |
| CaO | 0.35 | | |
| | | Total | 100.29 |

The chemical composition of analyzed samples approximate the composition of quartzite-sandstones from the vicinity of Capetown. This reflects the similar conditions of rock formation which prevailed in the vicinity of Capetown (South Africa) and in the distant littoral zone of King George V Land (Antarctica). Moreover, one may deduce that sedimentary rocks, which resemble African quartzites of the Table series contributed to the drift area which supplied morainal material to the littoral area of King George V Land.

Our inventory of geological knowledge of the Antarctic places the origin of our arkose sandstone, conglomerate, and quartzite-sandstone samples in Beacon sandstones. The Beacon sandstone series was discovered in South Victoria Land (1907) by Ferrar who provided its first description. It covers a large section of the high littoral ridge, which comprises the western and southwestern barrier around the sea and ice shelf of Russ and joins the ridge of Queen Maud.

Gould's data establish its thickness in the area of Queen Maud ridge of Fridtjof Nansen mountains at 2,000 m; petrographic analysis of Gould's samples was made by Stewart. The massive series comprises arkose sandstones and yellow and brown clays; the latter exhibit signs of oblique cleavage and cracks produced by drying. Also present are layers of conglomerate.

The Beacon series forms horizontal beds over a smoothed surface of an ancient crystalline foundation. Findings included remains of Devonian fish species (Smith Woodward designation). Also discovered were coal seams and wood (including Antarctoxylon) remains of Glossopteris indica Schimp (Stewart's designation), and other forms of Permian-Carboniferous origin [3]. They were identified with Glossopteris flora of Gondwana. The age of Beacon series appears within the limits of Devonian-Permian. Several scientists place the top layer in the Triassic. The series is marked by forceable intrusions of dolerite. According to Gould, the intrusions comprise one-third of the series, Fridtjof Nansen mountain. Wade [11] emphasizes the extraordinary similarity between Beacon series and other strata from certain parts of Australia and Africa. There were speculative writings on the "Gondwanic"

character of these formations.

Beyond the littoral zone of Ross Sea, the radical exfoliation of Beacon series is limited to few locations. The series accounts for the origin of our sandstone and granite specimens.

Our data indicate the considerable spread of Beacon sandstones within the limits of the Antarctic platform; the sandstones may have constituted its cover. Prolonged denudation accounted for the dissection of the platform's upper layer. Individual uplifts or depressions were traced to more recent faulting. Weathering greatly reduced the thickness of Beacon sandstone layers. The crystalline foundations of the platform's eastern section lacks a sedimentary cover. This cover is preserved in the limited inland sections of the platform's southern section. It is possible that its massive ice cover hides a greatly dissected surface rather than a flat plateau.

REFERENCES


1. Du Toit, A. L. THE GEOLOGY OF SOUTH AFRICA, 3d, ed. by S. H. Haughton: Edinburgh, 1954.
2. Ferrar, H. T. REPORT OF THE FIELD GEOLOGY OF THE REGION EXPLORED DURING THE "DISCOVERY" ANTARCTIC EXPEDITION 1901-1904: Natl. Antarctic Exped., British Mus. Nat. History, v. 1, Geology, 1907.
3. __________. THE GEOLOGICAL HISTORY OF ROSS DEPENDENCY: New Zealand Jour. Sci. & Technology, v. 7, no. 6, 1925.
4. Gould, L. M. STRUCTURE OF THE QUEEN MAUD MOUNTAINS, ANTARCTICA: Geol. Soc. America, Bull., v. 46, no. 6, 1935.
5. Mawson, D. IN THE LAND OF SNOW STORMS (A HISTORY OF THE AUSTRALASIAN ANTARCTIC EXPEDITION 1911-14): Glavsevmorput (Main Administration of the Northern Sea Route), Leningrad, 1935.
6. __________. GEOGRAPHIC NARRATIVE AND CARTOGRAPHY, AUSTRALASIAN ANTARCTIC EXPEDITION 1911-1914: Sci. Repts., ser. A, v. 1, Sydney, 1942.
7. Philippi, E. GEOLOGISCHE BESCHREIBUNG DES GAUSSBERGES, DEUTSCHE SUD-POLAR-EXPEDITION 1901-1903: Kartographie und Geologie, v. 2, no. 2, 1906.
8. Reinisch, R. PETROGRAPHISCHE BESCHREIBUNG DER GAUSSBERG GESTEINE, DEUTSCHE SUD-POLAR-EXPEDITION 1901-1903: Geographie und Geologie, v. 11, no. 1, 1906.
9. __________. ERRATISCHE GESTEINE (BESONDERS AUS EISBERGEN), DEUTSCHE SUD-POLAR-EXPEDITION 1901-1903: Geographie und Geologie, v. 2, no. 7, 1912.
10. Stewart, D. THE PETROGRAPHY OF THE BEACON SANDSTONE OF SOUTH VICTORIA LAND: Am. Mineralogist, v. 19, no. 8, 1934.
11. Wade, A. THE GEOLOGY OF ANTARCTIC CONTINENT AND ITS RELATIONSHIP TO NEIGHBOURING LAND AREAS: Royal Society, Queensland, Proc. for 1940, v. 52, pt. 1, 1941.


---

The U.S. Board of Geographic Names recommends the following forms for certain place names in this article:

| for | read |
|---|---|
| Union Corner | Junction Corner |
| Epfel Glacier | Apfel Glacier |
| Banger Oasis | Bunger Hills |
| Oasis Eastern | Windmill Islands |
| South Victoria | south Victoria Land |

-- Editor

# THE USE OF SCALE MODELS IN TECTONOPHYSICS[1]

*by*

*M. V. Gzovsky*[2]

*• translated by L. Drashevska •*

ABSTRACT

The author, using the theory of physical similarity as developed in the U. S. S. R. and equations describing the development of folds and faults in rocks, theoretically proves the possibility of using scale models in tectonophysics.

New instruments necessary for investigation of equivalent materials (which are necessary for conditions of similarity) have been created in the U. S. S. R. Some substances having properties meeting model-material requirements have been known for a long time. New materials with the required properties have also been created. As a result, scale models can be practically used to study tectonic deformation and fractures.

The fundamental principles of the optical method of investigation of stress state of elastic and plastic transparent models are described, indicating that the scale-model method may be used for the investigation of the tectonic-stress fields in the earth's crust.

Three examples demonstrate the ability of the scale-model method to help solve different geological and geophysical problems. The hypothetical physical conditions of two types of folds - longitudinal bending and longitudinal thickening - were checked.

The notions about the distribution of tectonic faults formed during the growth of transversal bending anticlines were made more precise with the aid of transparent models.

Transparent plastic models are used to study the ratio of the magnitude of tangential stresses in the region of earthquake foci to the velocity of the movement of the earth's crust. In elastic transparent models it is possible to see changes in the character of earthquake foci with time due to the development of tectonic faults. In such models, the influence of a type of tectonic deformation and fault magnitude on the value of seismic energy generating from the earthquake focus can be studied. All these data cannot be obtained by only field investigations. Therefore, even experimental information obtained from scale models facilitates the development of geological criteria of seismicity.

Tectonophysics is the study of the mechanics of tectonic deformation and fractures of the earth's crust. In stating the problems and in their solutions, the methods of tectonics (field observations) are applied, as well as the methods of physics (laboratory tests, the use of scale models, and theoretical analysis). Tectonophysics elucidates regularities in the development of the structure of the earth's crust and is of great practical importance, since locations favorable for ore concentrations are associated with tectonic deformations.

In addition, tectonic fractures affect the quality of coal and oil deposits which they cross. Tectonophysical data are also important in the solution of problems of hydrogeology and engineering geology; they are indispensable in the development of methods of earthquake prognosis. Geologic field observations are of paramount importance in tectonophysics, and laboratory experiments are also of great value.

The study of the tectonic deformations and fractures of the earth's crust by the use of scale models is an essential addition to tectonic field investigations. Although scale models have been used throughout the history of geology, the main principles still need considerable elaboration.

The results of investigation by the use of scale models can be applied to the consideration of geologic phenomena in nature only in cases where the models meet the requirements of similarity.

According to the theory of models developed in the U. S. S. R. , the conditions of similarity should be derived from equations describing fields of physical variables characteristic for the process under study, in order to avoid errors or unnecessary complications, [16, 30].

To describe tectonic deformation, a well known system of equations of equilibrium and movement advanced by Koczy may be applied, as well as Maxwell's equation:

[1] Translated from method modelirovaniya v tektonofizike: Sovetskaya Geologiya, 1958, no. 4, p. 53-72. Paper presented at the XI General Assembly of the International Geodetic and Geophysical Union in 1957.

[2] Institute of Earth Physics, Academy of Sciences, U.S.S.R.

| The rate of increase of of total deformation | | The rate of elastic deformation | | The rate of plastic deformation |
|---|---|---|---|---|

$$\frac{d\gamma_i}{dt} = \frac{1}{2G} \cdot \frac{d\tau_i}{dt} + \frac{\tau_i}{2\eta_{III}} \qquad (1)$$

A more complete equation can be employed, in which the residual elasticity (elastic reaction) is expressed independently from the conditionally momentary elastic deformation:

$$\gamma_i = \frac{\tau_i}{2G_I} + \frac{\tau_i}{2G_{II}}\left(1 - 2.7^{-t\frac{G_{II}}{\eta_{II}}}\right) + \frac{\tau_i}{2\eta_{III}}\, t \qquad (2)$$

Triaxial deformation is expressed as the amplitude of the three major extensions (elongations) $\epsilon_1$, $\epsilon_2$, $\epsilon_3$:

$$\gamma_i = \sqrt{\tfrac{1}{6}[(\epsilon_1 - \epsilon_2)^2 + (\epsilon_2 - \epsilon_3)^2 + (\epsilon_3 - \epsilon_1)^2]}.$$

The value

$$\tau_i = \sqrt{\tfrac{2}{3}(\tau_1^2 + \tau_2^2 + \tau_3^2)}$$

is a general characteristic of the summation of three principal shearing stresses; t denotes time, $G_I$ is the modulus of rigidity in the conventional momentary elastic deformation, $G_{II}$ is the modulus of equilibrial shear of the residual elasticity, $G_{III}$ is the modulus of rigidity in the total elastic deformation, $\eta_{II}$ is the viscosity of the residual elasticity, and $\eta_{III}$ is viscosity in the plastic deformation.

A number of workers established important changes in $G_I$, $G_{II}$, $\eta_{II}$, and $\eta_{III}$ for various substances, depending on the confining pressure $\sigma_m$, temperature T, and the intensity of shearing stresses $\tau_i$; [1, 2, 6, 17, 20, 21, 25, 26, 28, 53]. Principal interrelations are expressed by the following equations:

$$\eta_{III} = \eta_o\, 2.7^{\frac{u - \alpha\sigma_m}{kT}}, \qquad (3)$$

$$\eta_{III} = \eta_{III_{min}} + \left(\eta_{III_{max}} - \eta_{III_{min}}\right) \frac{\frac{\tau_i}{P_\eta}}{\operatorname{sh}\frac{\tau_i}{P_\eta}} \qquad (4)$$

where $\eta_o$, $\eta_{III_{min}}$, $\eta_{III_{max}}$, $u$, $\alpha$, $P_\eta$ are constants; k is Boltzman's constant.

The results of the experimental study of the strength of rocks [40, 41, 42] lead to the conclusion that the viscosity of rocks is a function of stresses of the type (3) and (4).

Ruptures in rock as in metals and in many other materials, are of two types: tension fractures and shear fractures. The first occur as a result of the action of normal tensional stresses, the latter as a result of shearing stresses. Correspondingly, each material is characterized by two values expressing resistance to rupture, by two strengths $P_\sigma$ and $P_\tau$. Whether a certain material will undergo failure by tension fracture, or by shear fracture depends on the interrelation between the values of two strengths of this material, as well as on the acting normal and shearing stresses [3, 12, 15, 27 and 28].

The results of experiments and the molecular theory of strength lead to the conclusion that, for the range of time from 0.0001 seconds up to tens of millions of years, the value of the stress $P_d$ inducing rupture is a linear function of the logarithm of the duration z of this stress action [3, 12, 15, 17, 28, 54]. This interrelation may be expressed by the equation:

$$P_z = P_1 - \zeta \ln \frac{z}{z} \quad \text{or}$$

$$z = \frac{\delta}{2.7^{P_z/\zeta}}, \qquad (5)$$

where $P_1$ and $\zeta$ are constants characterizing properties of the material. $P_1$ is the conventional momentary strength for the duration of the stress action of about 1 second.

The values of strength of rocks, as found experimentally, are close to the conventional momentary ones, being a little lower than the latter, because a period of time somewhat longer than 1 second was spent for the increase in stress.

Under stress action of a certain duration, the strength of rocks decreases as the temperature is increased and increases with the growth of the confining pressure [12, 17, 28, 45, 50, 57]. For the conventional shearing strength $P_{1\tau}$, this is expressed by the equation of Mohr's hypothesis:

$$P_{1\tau} = P_{0\tau} - q\sigma, \qquad (6)$$

where q is the coefficient, the value of which may be considered to be constant for a small range of values of normal stress $\sigma$. The coefficient q also determines the angle of shearing $\alpha$:

$$\tan 2\alpha = \frac{1}{q}, \qquad (7)$$

$P_{0\tau}$ denotes the conventional momentary shearing strength where $\sigma = 0$.

The values of many coefficients and moduli included in the equations (1) through (7) are already known for some rocks in the first approximation (table). A systematic determination of these values in all rocks is an important task of further laboratory investigations. They are found from the curves of continuous deformations of rocks under the action of stationary stresses (fig. 1).

for normal stresses,

$$C_\sigma = \frac{\sigma\ (\text{model})}{\sigma\ (\text{original})};$$

for strength properties,

$$C_P = \frac{P\ (\text{model})}{P\ (\text{original})};$$

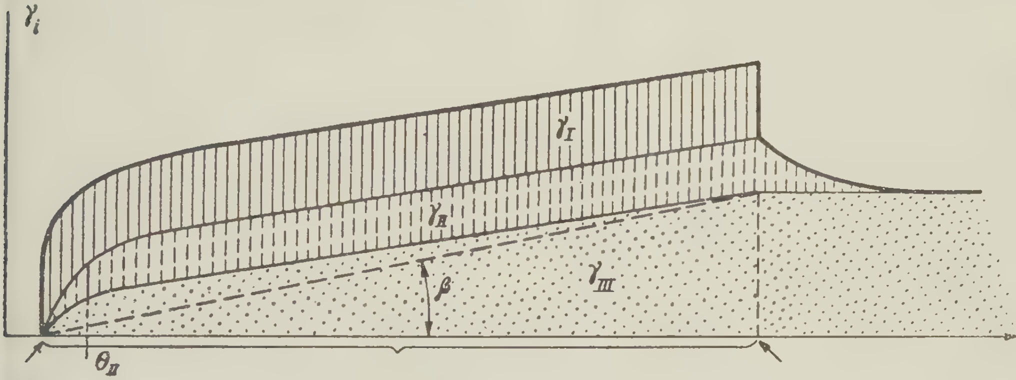


| | | | |
|---|---|---|---|
| $G_I = \dfrac{\tau_i}{2\gamma_I}$ | $G_{II} = \dfrac{\tau_i}{2\gamma_{II}}$ | $\eta_{II} = G_{II}\theta_{II}$ | $\eta_{III} = \dfrac{\tau_i}{2\,tg\,\beta}$ |

FIGURE 1. Graphical analysis of time-deformation curves obtained for rocks under the action of stationary stresses $\tau_i$; $\gamma_I$ - conventional momentary elastic deformation, $\gamma_{II}$ - residual elasticity, $\gamma_{III}$ - plastic deformation, $\theta_{II}$ - time in which 0.63 of the limit value $\gamma_{II}$ is attained, t-time.

From the equations (1) through (7), two general conditions of similarity are derived:

$$C_G = C_\rho C_g C_l \qquad (8)$$

$$C_\eta = C_\tau C_t. \qquad (9)$$

In addition, the equality

$$C_G = C_\tau = C_E = C_\sigma = C_P \qquad (10)$$

should be observed, as well as the similarity of the boundary and initial conditions [11, 16, 30].

Corresponding model ratios are as follows:

for equilibrial moduli of total elasticity: equilibrial modulus of rigidity,

$$C_G = \frac{G\ (\text{model})}{G\ (\text{original})},$$

equilibrial length modulus,

$$C_E = \frac{E\ (\text{model})}{E\ (\text{original})};$$

for shearing stresses,

$$C_\tau = \frac{\tau\ (\text{model})}{\tau\ (\text{original})}$$

for density,

$$C_\rho = \frac{\rho\ (\text{model})}{\rho\ (\text{original})};$$

for viscosity,

$$C_\eta = \frac{\eta\ (\text{model})}{\eta\ (\text{original})};$$

for time,

$$C_t = \frac{t\ (\text{model})}{t\ (\text{original})};$$

for acceleration of gravity,

$$C_g = \frac{g\ (\text{model})}{g\ (\text{original})};$$

for lengths,

$$C_l = \frac{l\ (\text{model})}{l\ (\text{original})}.$$

In studies of ruptures using models, the similarity of fields of stresses and that of values characterizing the strength properties should be observed. The similarity of fields of stress is furnished by the conditions (8), (9), and (10). When the conditions of similarity are derived from the equation (5), model ratios $C_{Pl}$ and

$C_\zeta$, referring to those strength characteristics which are of the same dimensional expressions as $\zeta$ from (5) and as momentary strengths $P_{1\sigma}$ and $P_{1\tau}$, should be equal:

$$C_p = C_\zeta = C_\rho = C_G = C_E = C_\sigma = C_\tau \qquad (11)$$

Another characteristic, $\delta$ from (5), having the dimension of time, is governed by the model ratio $C_\delta$, which equals

$$C_\delta = C_t. \qquad (12)$$

acterize the properties of models. However, approximate computations are possible and have been performed a number of times [11, 19, 29, 39, 45, 46, 51]. The results of these computations are presented in table 1.

Models should be made from such materials whose properties correspond to values which have been computed in advance according to the conditions of similarity. Special devices which make it possible to determine $G_I$, $G_{II}$, $\eta_{II}$, $\eta_{III}$, $P_\tau$, and $P_\sigma$ for materials used in models

TABLE 1 Comparison of strength properties of rocks and equivalent materials

| Strength properties of soils expressed in cgs units | Rocks | Equivalent materials: for $C_l$ from $10^{-4}$ to $10^{-5}$ and for $C_t$ from $10^{-11}$ to $10^{-13}$ — Required on the basis of theoretical considerations | Clay with a moisture content of 40-50% | Baku petrolatum | 30% solution of ethyl cellulose in benzyl alcohol | for $C_l = 10^5$ and $C_t = 10^0$ — Required on the basis of theoretical considerations | 25% gelatin |
|---|---|---|---|---|---|---|---|
| Moduli of conventional momentary elasticity $G_I$ and $E_I$ ($d/cm^2$) | $10^{11}$-$10^{12}$ | $10^6$-$10^8$ Usually $10^6$ | $10^5$-$10^6$ | $10^6$ | $10^5$ | $10^6$-$10^7$ | $10^5$-$10^6$ |
| Moduli of residual elastic $G_{II}$ and $E_{II}$ ($d/cm^2$) | $10^{11}$-$10^{12}$ | $10^6$-$10^8$ Usually $10^6$ | $10^5$-$10^6$ | $10^6$ | $10^4$-$10^5$ | $10^6$-$10^7$ | $10^5$-$10^6$ |
| The time of duration of residual elasticity relaxation $\theta_{II}$ (sec) | $10^3$-$10^4$ | $10^{-10}$-$10^{-7}$ | $10^1$-$10^2$ | $10^0$-$10^1$ | $10^0$-$10^1$ | $10^3$-$10^4$ | $10^3$-$10^4$ |
| Coefficient of viscosity $\eta_{III}$ (poise) | $10^{18}$-$10^{23}$ | $10^0$-$10^8$ Usually $10^4$-$10^6$ | $10^4$-$10^6$ | $10^3$-$10^4$ at 20°C | $10^5$-$10^6$ at 20°C | $10^{13}$-$10^{18}$ | approx. $10^{10}$? |
| The time of duration of relaxation caused by the plastic deformation $\theta_{III}$ (sec) | $10^6$-$10^{12}$ | $10^{-7}$-$10^1$ | $10^{-2}$-$10^1$ | $10^{-3}$-$10^{-2}$ | $10^0$-$10^{-1}$ | $10^1$-$10^7$ | |
| Conventional momentary shearing strength $P_{0\tau}$ ($d/cm^2$) | $10^8$-$10^9$ | $10^3$-$10^5$ Usually $10^3$ | $10^2$-$10^3$ | $10^5$ | ? | $10^3$-$10^4$ | approx. $10^7$-$10^8$? |
| Conventional momentary tensional strength $P_{1\sigma}$ ($d/cm^2$) | $10^7$-$10^8$ | $10^2$-$10^4$ Usually $10^2$-$10^3$ | $10^2$-$10^3$ | ? | ? | $10^2$-$10^3$ | $10^6$-$10^7$ |
| q | 0-2 | 0-2 | 0-0.6 | - | - | 0-2 | |

Insufficient knowledge of strength properties of rocks prohibits a high degree of precision in the computation of values which should char- should be used for this purpose. Such devices have been successfully constructed in the Soviet Union and we have used them. Figure 2 pre-

sents curves obtained from the result of experiments utilizing these devices. These curves are similar to those characterizing rocks and allow the computation of values $G_I$, $G_{II}$, $\eta_{II}$, $\eta_{III}$. The results of computations are presented in the table. They show that the values characterizing the principal strength properties of moist clays, petrolatum, and some other materials correspond in general to values which, according to the conditions of similarity (8) through (12), should characterize models with the model ratio of geometric similarity $C_l = 1.10^{-5}$ (1:100,000) and the model ratio of time similarity $C_t = 2.10^{-12}$ (when 1 minute of the experiment duration corresponds to about 1 million years in nature).

For the solution of many problems of tectonophysics, the examples of which can be found in an number of works [9, 10, 12, 13, 24, 43, 58], not only data on deformation and

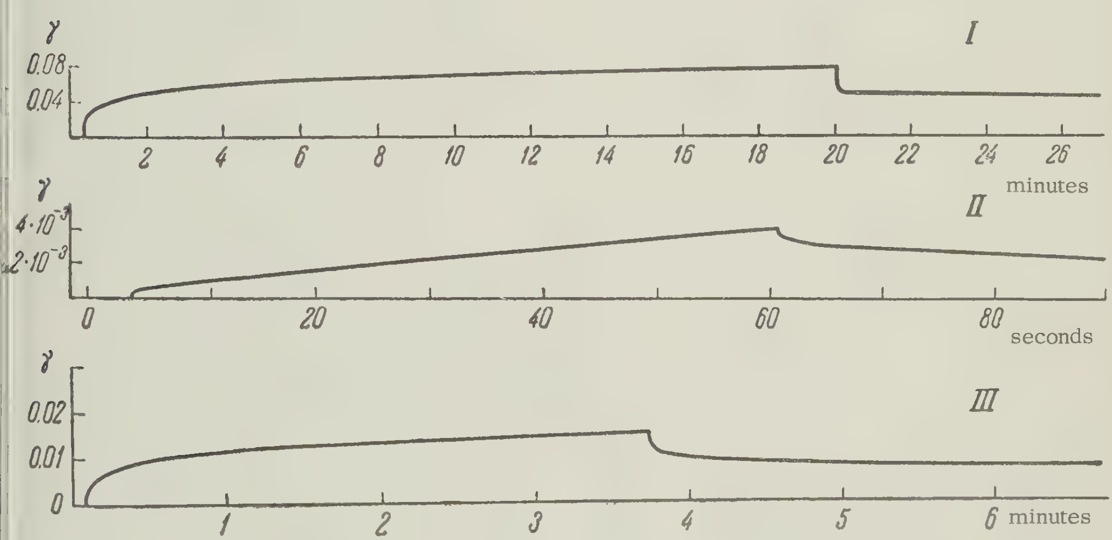


FIGURE 2. Time-strain curves of substances under the action of stationary stresses. I - clays containing 43% moisture, II - Baku petrolatum, III - 30% solution of ethyl cellulose in benzyl alcohol, γ - shear deformation. Automatic recording obtained in V.P. Pavlov's device (I and III) and in N.V. Mikhaylov's device (II).

ruptures are of great importance, but also data on stress conditions in models; the latter have not been investigated yet. The study of the stress conditions in scale models of geologic objects began with the optical method [9, 11]. The application of this method in tectonophysics was complicated by the fact that only elastic substances which were optically active and might be used for scale models were known. The required plastic materials were not known. At present, we have optically active plastic substances, as well as a special device, photoplastoviscozimeter, for the determination of strength and optical properties of these substances [14, 23].

Beginning in 1952, we tested gelatin models. They are useful only for quantitative scale-model tests in the realm of momentary stress fields, i.e., of stresses acting at a certain moment. These models satisfy only one condition of similarity (8). The deformation of such a model reproduces only the elastic part of the total deformation, since the plastic part is rendered by the initial form of the model. The strained model is viewed under polarized light by means of a device resembling a miscroscope used in petrologic studies (fig. 3). By means of an optic compensator, or directly from the color interference pattern on a screen, a relative value of maximal shearing stresses acting in the model is determined. In the work on layered models and in the investigation of some problems connected with forecasts of earthquakes, it is necessary to know the absolute value of stresses acting in each of the isochromatic curves. For this purpose, the substance should undergo a special preliminary testing.

D. N. Osokina, who worked under the guidance of this author, indicated that in gelatin the difference in the rate of movement R is associated with the elastic part of the total deformation, but not with stresses, as has been generally considered. Since the second part of the elastic deformation continues to increase in the course of more than 40 hours, the difference in the rate of movement R in the model continuously increases with time, in spite of

constancy of stresses. The value of maximal shearing stresses $\tau_{max}$ in any point of the model is determined from the equation:

$$\tau_{max} = \frac{R_t}{B_t d} \cdot 10^{-7} gr/cm^2, \quad (13)$$

where $R_t$ is the difference in the rate of movement in millimicrons between rays leaving the model at a given moment of time.

$B_t$ denotes the optical coefficient of stresses which characterizes the substance of the model and is a function of the experiment duration. The thickness of the model in cm is d.

When equation (8) is used, moduli G or E of gelatin, due to the long period of development of the second part of the elastic deformation, should be replaced by $G_t$ or $E_t$, considered as functions of time t. Our method of investigation of gelatin models differs from that applied in engineering practice in that, instead of constants G, E, B, and R, the values $G_t$, $E_t$, $B_t$, and $R_t$ are applied as dependent on time [22].

greater than that required by conditions of similarity, therefore, elastic deformation in gelatins might attain several tens of percent, but in rocks it is never higher than one percent.

The development of the optical method for the study of stresses in scale models undergoing considerable plastic deformation contributed significantly to the improvement of model testing. In this case the conditions of similarity (8) and (9) are satisfied. The joint work of physiochemist G. V. Vinogradov, physicists V. P. Pavlov and D. N. Osokina, and of this author resulted in establishing that the concentrated solution of ethyl cellulose in benzyl alcohol is one of optically active plastic substances [23]. The value of the difference in the rate of movement R observed in these solutions is directly proportional to the total value of the elastic part of deformation. Under stationary stress, after the short period of time (a few seconds), the value of the difference in the rate of movement becomes stable in regard to the time and is directly proportional to the value of the maximal shearing stress $\tau_{max}$. Hence,

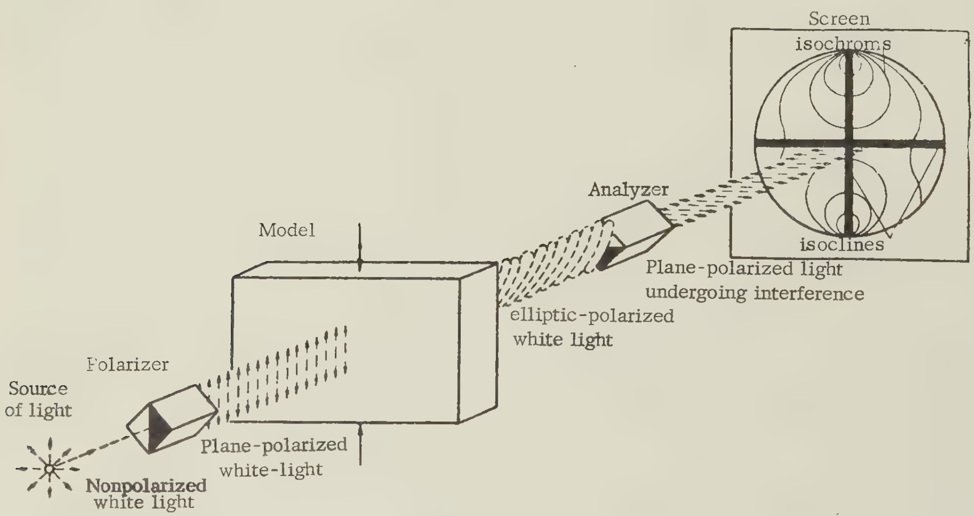


FIGURE 3. Diagram of the optical polarization device for the study of stress distribution in models.

The orientation of axes of stress can be ascertained at any point in the model since light ceases to pass through them as soon as the polarization planes of crossed nicols are parallel to the axes of stress. The term isoclines is applied to lines forming the locus of points with equal orientation of axes of stress. They form black fringes on the screen (fig. 3).

While working with gelatin models, it is necessary to keep in mind that their strength is

$$\tau_{max} = \frac{R}{Bd} \cdot 10^{-7} \text{ gr/cm}^2$$

The coefficient of optic activity B is very large, attaining 60,000 brewsters, i.e. $6 \cdot 10^{-6}$ gr/cm$^2$. The difference in the rate of movement R does not depend on the value of plastic deformation and can be correlated only with the rate of plastic deformation, which (as is the elastic part of deformation) is determined by the magnitude of stress.

Figure 4 illustrates the difference between mechanical and optical properties of ethyl cellulose solutions and those of gelatin. Diagrams show that in solutions of ethyl cellulose in benzyl alcohol, the difference in the rate of movement is well correlated with the magnitude of stress. The creation of such plastic optically active substances, in which the conditions of similarity of strength (11) and (12) are also observed, is an important task of further investigations.

similar folds, on the other hand, the thickness of beds changes considerably and the process of deformation leads to local thickening of beds; the bending is only slightly manifested. There occur also folds of intermediate or composite origin.

In addition to the consideration of changes in the external form of beds, deformations occurring inside each bed can be analyzed. In this regard, three varieties can be distinguished in similar folds. In the first variety, the deformation is nearly uniform and consists in the convergence of the adjacent limbs. The limbs are drawn somewhat closer together near the concave underside of the fold than near the convex upper part of the folds. The flatness of the limbs is retained after deformation.

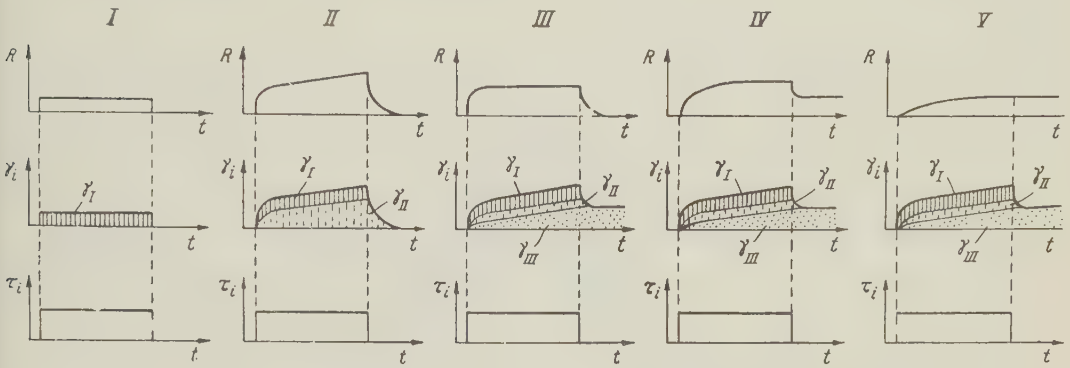


FIGURE 4. Interrelations between stresses $\tau_i$, deformations $\gamma_i$, and the difference in the rate of movement R under conditions of the laboratory experiment (under atmospheric pressure, temperature 20°C, shearing stresses less than 100 gr/cm$^2$, and the duration of the experiment t less than one hour).

Optically active materials: I - materials of the Bakelite type applied in engineering practice; II - gelatin; III - concentrated solutions of ethyl cellulose; IV - transparent soap; V - transparent lubricating grease and clay pastes. Interrelations in substances IV and V are indicated as hypotheses, according to data of G.V. Vinogradov and I.V. Popov. The difference in the rate of movement R in substances I, II, and III is directly associated only with the elastic part ( $\gamma_I + \gamma_{II}$) of the general deformation; in substance IV, the difference in the rate of movement is associated both with the elastic ( $\gamma_I + \gamma_{II}$) and the plastic ( $\gamma_{III}$) parts; in the substance V, only association with the plastic part $\gamma_{III}$ is assumed.

The method of using scale models was successfully applied in tectonophysics [4, 18, 42, 34-39, 47-49, 51, 55-56, 59]. We feel that the primary importance of this method lies in the fact that it makes it possible to ascertain physical conditions necessary for the development of the deformation and fractures under investigation. In addition, it makes it possible to establish important additional facts which cannot be determined as the result of geologic field investigations. Let us discuss three examples

## Determination of Physical Conditions Leading to the Appearance of Parallel and Similar Folds

The compression of layers in the earth's crust by a force acting parallel to the surface of the earth leads to the appearance of folds of different types. In parallel folds, the strata for the most part are of constant thickness throughout, and the process of deformation is manifested mainly by plastic bending of strata. In

The second variety is distinguished by a considerable nonuniformity and complexity of the plastic deformation of the beds. The flat limbs become intensely distorted. Usually the term "flowage fold" is applied to this variety.

Finally, folds occur whose forms are greatly influenced by numerous shearing planes accompanying the plastic deformation. Often the term shear fold is applied to this variety.

Without discussing deformation within beds in detail, we shall consider two extreme types: parallel and similar folds. Sometimes they can

be observed side by side in the same stratum (fig. 5). Each of these types of folds is accompanied by a specific complex of fractures which are often filled with ores. Therefore, it is important to know what conditions govern the appearance of a certain type.

The theoretical consideration of the plastic deformation of a separate bed lead us to the following hypothesis. At a certain duration z of compression by the force P, acting parallel to the surface of the earth, parallel folds appear only when the magnitude and the duration of acting forces are in a certain interrelation with mechanical properties of the bed; three conditions described below should be satisfied.

The First Condition

The magnitude of the horizontal force P should be larger than the value $P_k$ which depends

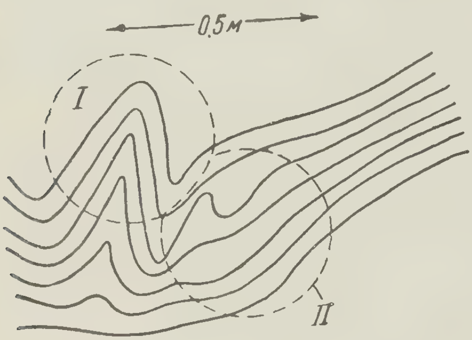


FIGURE 5. Parallel folds (I) and similar folds (II) in the Paleozoic limestones of the Karatau range (an upright outcrop).

on the viscosity of the bed $\eta_{III}$, the shearing stress at the surface of the bed f, the duration of the experiment z, the thickness of the bed m, the extent of the bed along the strike d, and on a certain numerical coefficient $k_I$.

$$P > P_k; \quad P_k = k_I \frac{f^{2/3} \eta_{III}^{1/3} md}{z^{1/3}} \tag{15}$$

If, instead of the force P, the normal stress p directed parallel to the earth's surface is considered, then the appearance of a parallel fold will be conditioned by the following expression:

$$P > P_k; \quad P_k = k_I \frac{f^{2/3} \eta_{III}^{1/3}}{z^{1/3}} \tag{16}$$

where $k_I$ is a certain numeral coefficient, the value of which might be found empirically.

The Second Condition

The compressive stress p acting parallel to the surface should be less than the double value of the continuous shearing strength of the bed $P_{Z\tau}$ corresponding to the duration z of the stress action:

$$p < 2P_Z \, . \tag{17}$$

The Third Condition

The normal stress at the surface of the bed should be less than a certain value proportional to the shearing stress f at the surface of this bed. $k_{III}$ denotes the coefficient of proportionality which should be determined empirically:

$$s < k_{III} \, f \tag{18}$$

The first problem being solved by the use of scale models comprises the verification of the correctness of the above listed conditions which are necessary for the appearance of parallel folds in an individual layer. In the simplest case, when during the same period of time a bed, which is composed of uniform material with the viscosity $\eta_{III}$, is being deformed, the minimal value of the stress $p_k$ necessary to produce a parallel fold depends only on the shearing stress f on the bottom of the layer.

From (16) it follows that:

$$p_k = k' f^{2/3} \tag{19}$$

where k' is a certain constant coefficient. The stress f depends on the weight of the layer and on the coefficient of friction $k_f$ between the layer and the underlying material. The thickness of the layer m influences the fold only because it governs the weight of the layer which determines the stress f. The first and the second conditions are also effective.

I. M. Kuznetsova and the author performed tests on a series of one-layered models in order to verify the possibility, expressed in (19), of obtaining first parallel, then similar folds by changing two factors: the normal stress p acting parallel to the surface and the shearing stress f. We based our computations of properties of models on the conditions of similarity (8), (9), and (10), in which the following model ratios were taken:

$$C_l = 10^{-4} = 1{:}10,000; \quad C_t = 10^{-12};$$

$$C_g = 1; \quad C_\rho = \frac{1}{2}; \quad C_\eta = 10^{-16}; \quad C_p = 10^{-4}.$$

It was not considered necessary that moduli of elasticity satisfy the conditions of similarity, since these moduli do not enter in (15) through (19). We considered that rocks are characterized by $\eta_{III}$ having a value of about $10^{19}$

to $10^{20}$ poises and $P_{1\tau}$ was about $10^9$ d/cm$^2$. Correspondingly, models should have $\eta_{III}$ of around $10^4$ to $10^3$ poises and $P_{1\tau}$ of about $10^5$. These properties characterize one of the varieties of petrolatum (Baku).

The results of experiments on many models confirmed that an individual layer made of an uniform plastic substance, depending on the values f or p may form either a similar or a parallel fold (fig. 6). The most significant result of the experiments lies in the fact that the location of points on the diagram (fig. 7) does not contradict the equation (19).

Of greatest importance is the determination of physical conditions of the formation of parallel and similar folds not in one layer, but in a many-layered system. It is very difficult to determine these conditions theoretically.

The second task which can be solved by the use of scale models is the determination of the degree to which conditions derived for the deformation of a single layer may be extended to the deformation of a layered system. The thicknesses of separate layers m and the coefficient of friction $k_f$ between the layers are the most important mechanical properties of the system.

It follows from (15) that if a constant force P

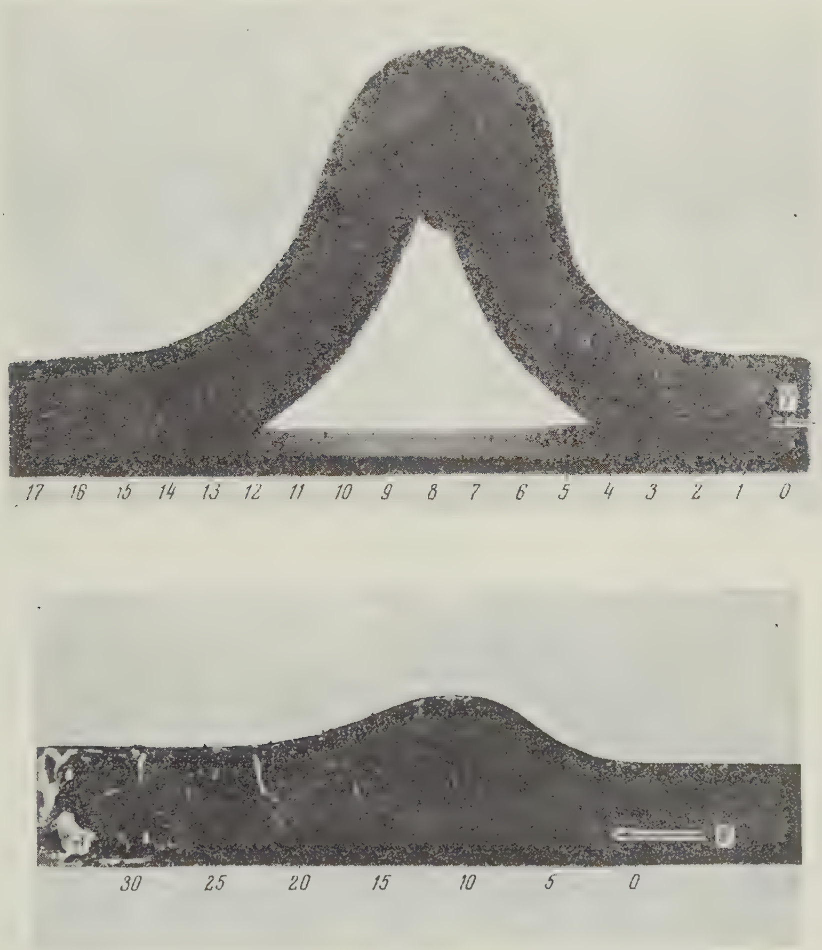


FIGURE 6. Parallel folds (above) and similar folds (below) in the homogeneous models made of petrolatum, P - the compressive force acting parallel to the surface of the bed. Linear dimensions in cm.

acts on a single layer, then, depending on the interrelation between its thickness m and the coefficient of friction $k_f$, folds of various types may appear at the top and the bottom of this layer. A parallel fold appears when:

$$m < \frac{k''}{k^{2/3} f}, \qquad (20)$$

where k" is the coefficient dependent on the viscosity of substance, the duration of the experiment and the selected value of the force P.

distributed in such a way that they do not contradict the dependence (20).

Corresponding to (15), we obtained in many-layered models different types of folds depending on the viscosity of the material.

Thus, the method of scale models contributed to the understanding that the equation (15) may be used in considering physical conditions governing the formation of parallel and similar

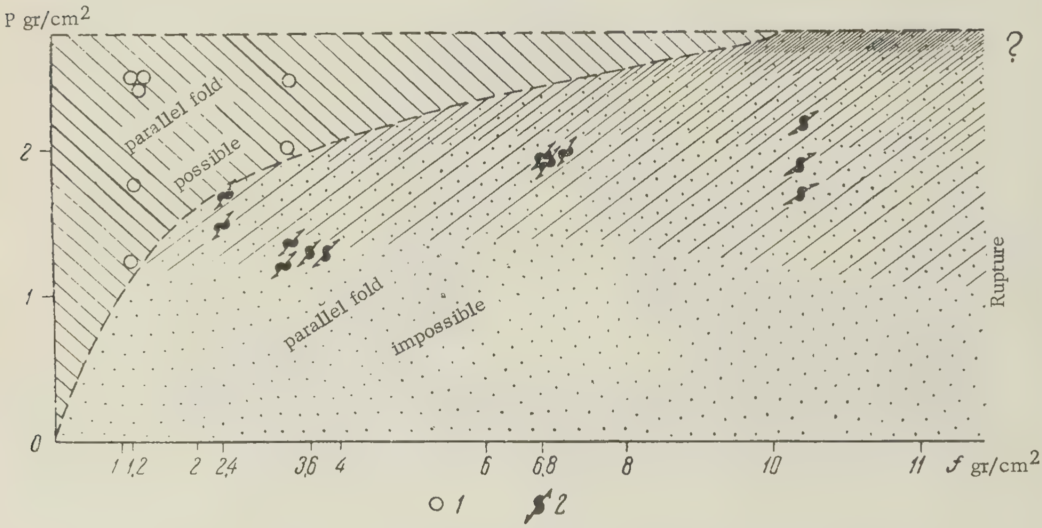


FIGURE 7. Diagram of physical conditions governing the formation of different folds in a homogeneous layer (after M.V. Gzovsky and I.M. Kuznetsova). $P_{\text{пт}}$ - conventional momentary shearing strength, P - the active normal stress at the cross section of the bed (plotted along the ordinate axis), f - reactive shearing stress at the surface of the bed, 1 - recorded parallel folds, 2 - recorded similar folds complicated by shear fractures.

In order to verify the applicability of (20) to layered systems, I. M. Kuznetsova and the author performed tests on many-layered scale models. Model ratios were the same as those taken for one-layered models. Models were made of petrolatum. The value of friction between the layers $k_f$ was governed by properties of the lubricator which covered separate layers.

The experiments established that folds of both types under discussion may be obtained by changing only thicknesses of layers m or the coefficient of friction between them, $k_f$. All other factors (a total thickness of the system, the compressing force along the layer P and others) were constant in the course of the described series of experiments (fig. 8). It is worthwhile to note that points on the diagram plotted for many-layered models (fig. 9) are

folds in layered rocks.

## Investigations of Regularities in the Distribution of Fractures in Space and Time.

Model tests carried out under controlled conditions make possible the understanding of the distribution of tectonic fractures in space and time, as well as the understanding of the succession in time of their development under the condition of a certain deformation of the earth's crust. In a certain ore-bearing area, we studied anticlinal folds which are dissected at their crests by longitudinal faults and in limbs by longitudinal reverse faults which flatten upward. In order to solve the question of the possibility of the simultaneous development of both types of

fractures, as well as to clarify the origin of folds, we reproduced the field to stresses [10]. A similar field of stresses can be observed in plastic models of folds which appear due to the transverse bending under the action of vertical forces (fig. 10). Therefore, we associate the origin of investigated natural anticlines with the action of vertical forces.

In all cases, the fields of stresses appearing in transparent models attested to the opinion that, in general, faults and reverse faults appear simultaneously, but develop in opposite directions. Faults develop from the earth's surface downward, but the reverse faults develop from below upward. Just such a development of fractures can be observed in plastic models made of moist clay [11]. It is clear that this conclusion has a practical importance in planning prospecting for hydrothermal ore deposits and and oil fields. This conclusion is also of interest in connection with the study of earthquake distribution. Small faults which come to the surface in crests and extinguish with depth (having appeared under the action of small stresses) should be less dangerous in respect to earthquakes than larger reverse

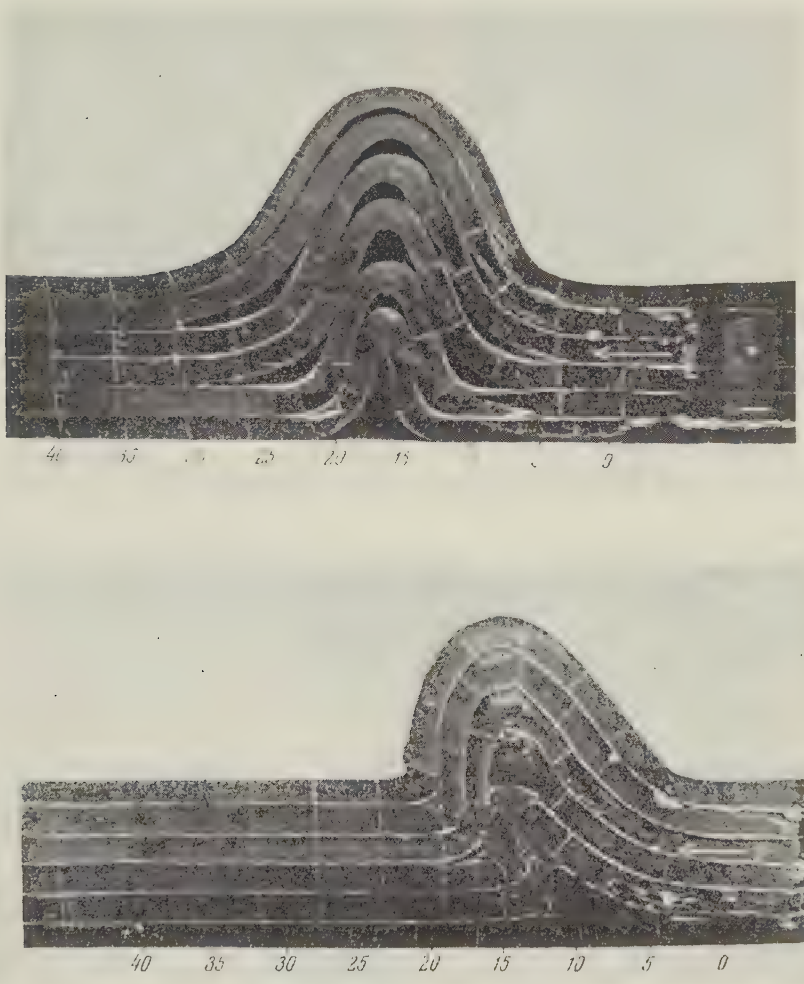


FIGURE 8. Parallel folds (above) and similar folds (below) in many-layered models made of petrolatum. P - compressive force acting along the layers. Linear scale in cm.

faults which develop at greater depths [13]. It is very important to note that the more dangerous fractures may not appear at the surface.

Three-dimensional models of brachyanticlines made of moist clay clearly show that after the above described longitudinal faults and reverse faults are formed, later transverse fractures appear. Their appearance is caused by the existence of longitudinal disturbances which change the initial field of stresses, excluding the possibility of considerable tensional stresses across the axis of the fold [11]. As shown by geologic field investigations and seismic data on the character of foci of earthquakes in Central Asia and the Caucasus, the

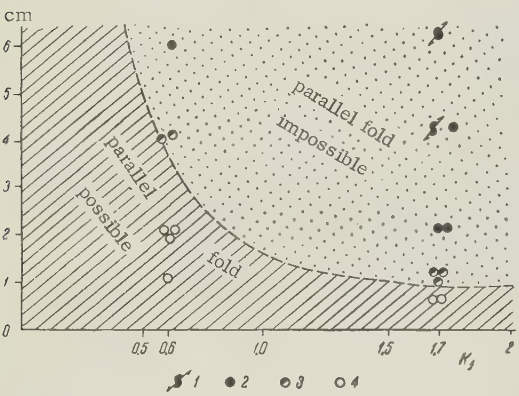


FIGURE 9. Diagram of physical conditions governing the formation of different folds in multi-ayered models (after M.V. Gzovsky and I.M. Kuznetsova). M - the initial thickness of each layer of the model $k_f$ - the coefficient of friction between layers; 1 - recorded similar folds complicated by shear fractures, 2 - recorded similar folds, 3 - recorded folds of the composite type, 4 - recorded parallel folds.

transverse fractures often occur on fold crests and generally appear after the formation of longitudinal fractures. Probably this is the reason why transverse fractures are often loci of secondary ore deposits.

## The Development of Hypotheses on Earthquake Foci

Beginning in 1955, we applied scale models to the consideration of seismo-geologic questions. The association of earthquakes with tectonic fractures is now positively established. Proceeding from the dependence of strength on time, which is expressed in the first approximation by (5), it is possible to consider that tectonic fractures and earthquakes may appear as a result of the action of different stresses $\tau_i$ acting in the earth's crust or below it. The intensity of earthquakes in the epicenter depends on the depth of the hypocenter, on the structure of the earth's crust around this center, and on the aggregate kinetic energy of seismic waves $U_s$, $\lambda$ which constitutes a certain part of the total energy of the focus, $\Delta U_I$. In the further development of theories by H. Benioff [31], G. A. Gamburtsev [7, 8], and K. E. Bullen [33], $\Delta U$ should be considered equal to that decrease in the potential energy of the conventional momentary elastic change in form which is caused by the appearance of a tectonic fracture.

It is possible to correlate the energy of an earthquake with the length l of the tectonic fracture along the strike and with the intensity of stresses $\tau_i$:

$$U_s = \frac{\omega n \lambda}{2} \frac{\tau_i}{G_I} . l^3, \qquad (21)$$

where $G_I$ is the conventional momentary rigidity modulus; $\omega$, n, and $\lambda$ represent the following: $\omega^- \lambda$, that part of the total energy $U_I$ which is released with the appearance of the fracture, and which represents $\Delta U_I$, n - $\lambda$ that part of the released energy $\Delta U_I$ which is transformed into $U_s$, $\lambda$ - the proportionality between the volume of the earthquake focus and $l^3$.

Since it follows from (1) that the value $\tau_i$ can be juxtaposed with the rate of the continuous deformation of the earth's crust $\frac{d\gamma_i}{dt}$ and, in addition, that this rate is approximately proportional to the rate gradient of tectonic movements of the earth's surface $\frac{d\gamma_i}{dt} \approx \Phi [\text{grad } V]$, it becomes possible to derive from (21) the following approximate equation [13]:

$$U_s \approx \psi \frac{\eta^2_{III}}{G_I} l^3 [\text{grad } V]^2 , \qquad (22)$$

$$\psi = 2 \omega \Phi^2 \lambda n. \qquad (23)$$

Thus it is possible to associate the aggregate energy of seismic waves $U_s$ with the following values: a) the coefficient $\psi$, which is determined by the type of tectonic fracture and depends on the appearance of the fracture which changes the initial field of stresses, the part of $\Delta$ u which is constituted by $U_s$, and the interrelation between the volume of the earthquake focus and $l^3$; b) the square of the coefficient of viscosity $\eta$ III; c) the conventional momentary modulus of rigidity $G_I$; d) the cube of the length l of the tectonic fracture; e) the square of the value of the rate gradient of the tectonic movements of the earth's surface [grad V].

Assuming that the equation (5) in the first approximation is valid both for ruptures and shears, we should apply it to the solution of questions relating to the time of the appearance of earthquakes. This equation can be transformed into the following expression:

$$z_S \approx \frac{\delta}{2\,\Phi\;\;2.7\,\dfrac{\eta_{III}}{\zeta}\cdot[\mathrm{grad}\;V]}, \qquad (24)$$

where $z_S$ is the duration of the period from the moment of the beginning of tectonic movements having a steady gradient of rate grad V, up to the appearance of the fracture and the earthquake. All other symbols were explained before.

Equations (21) through (24) express a hypothesis which generalizes our idea concerning geological criteria of seismicity. Correspondingly, it is not the surface of the fracture which was obtained approximately equal to 2-3.5.

Elastic gelatin models were used for the investigation of short processes of changes in stress at the moment of the rupture formation. These models give a chance to see how the type of tectonic deformation and the size of the rupture affect the form and the volume of the earthquake focus and the quantity of energy originated from this focus. The coefficient $\lambda$ in the models shown on figures 10 and 11 had a value in the range 0.1-2, the value of the coefficient $\omega$ was in the range -.01-0.3.

The scale models give a change to observe changes with time in the character of the earth-

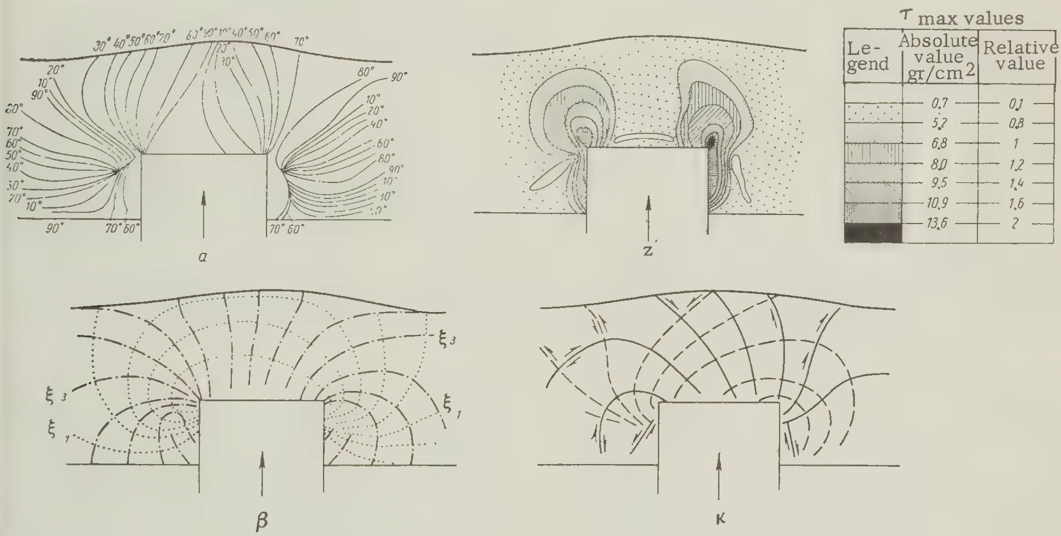


FIGURE 10. Stress distribution in the plastically deformable model of the anticline formed as a result of transverse bending. The model was made of 30% solution of ethyl cellulose in benzyl alcohol; model ratios: $C_l$ from $10^{-6}$ to $10^{-5}$, $C_t$ - $10^{-13}$, $C_G$ from $10^{-6}$ to $10^{-5}$, $C_\rho$, from $10^{-19}$ to $10^{-18}$, $C_p$ were not observed. a - isoclines, z - the value of maximal shearing stresses; $\beta$ - trajectories of principal normal stresses; $\kappa$ - trajectories of maximal shearing stresses. (After M.V. Gzovsky, I.M. Kuznetsova, and D.N. Osokina).

is considered to be a focus of the earthquake, but that volume of rocks in which a conventional momentary change in stresses occurs due to the appearance of a new fracture, or due to the rejuvenation of an ancient one.

The plastic models were used in our experiments in which the optical method was applied to the study of the interrelation between the rate gradient of the movement of the upper surface of the deformed part of the earth's crust, the intensity of shearing stresses and the rate of deformation within the earth's crust in the area of the appearance of foci of earthquakes. In plastic models representing the transverse bending of the type shown in figure 10, the coefficient $\Phi$ quake foci, depending on the development of tectonic fractures (fig. 11). At present, all these data cannot be obtained just by the observation of natural geologic objects in the field. Therefore, even approximate data obtained in the results of model tests present a valuable addition to the results of seismic and geologic field investigations and contribute to the development of criteria of seismicity.

## CONCLUSIONS

In conclusion let us list the principal theses presented in this paper:

1. On the basis of the theory of physical

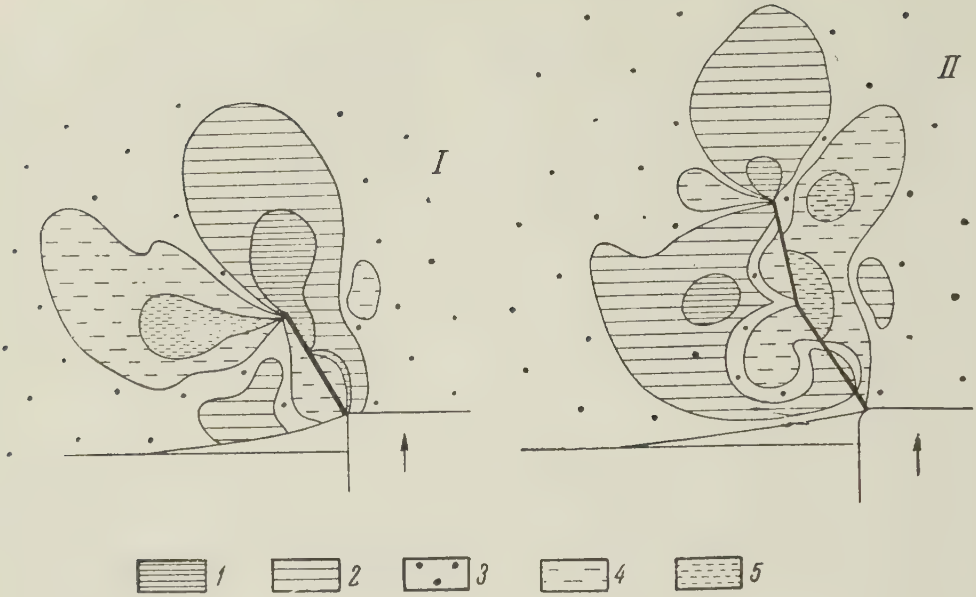


FIGURE 11. The models of earthquake foci associated with anticlines of transverse bending (after M.V. Gzovsky and T.A. Tikhomirova). The models are made of gelatin
Model ratios: $C_l = 10^{-6}$.
I - the first stage (the formation of a small reverse fault), II - the second stage (the further development of the fracture). Changes in the stresses $\tau_{max}$, after the appearance of separate parts of the fracture: 1 - a large increase (averaging 1.7 times) changes; 2 - a slight increase (averaging 1.3 times) - no changes; 4 - a slight decrease (averaging 0.8); 5 - a large decrease (averaging 0.6).

similarity and the available data on strength properties of rocks, it is possible to establish what properties should characterize models similar to natural geologic objects. Thus, the investigation of tectonic deformations and fractures in the earth's crust by the method of scale models is based on sound theoretical considerations.

2. There are certain devices which make it possible to measure the values of strength properties of models which enter conditions of similarity. Some substances having properties meeting requirements for model materials have been known for a long time. Also new substances were created having properties which had been planned beforehand. It means that it is practically possible to apply the model tests to the study of tectonic deformation and fractures.

3. As a result of model tests, the regularities and additional facts have been established, the understanding of which just by the study of geologic objects in the field either takes too much effort, or is impossible. This refers to the investigation of details of the earth's crust structure up to the large depth, to the understanding of the history of development of deformations and fractures in the course of a very long period, to the study of stress conditions in the earth's crust, and to the determination of physical conditions of the appearance of deformation and fractures of certain types. Hence, the method of scale models may contribute to the solution of various geologic and geophysical problems.

## REFERENCES

1. Abduragimova, L. A., P. A. Rebinder, and N. N. Serb-Serbina. UPRUGO-VYAZKO-STNYYE SVOYSTVA TIKSOTROPNYKH STRUKTUR V VODNYKH SUSPENZIYAKH BENTONITOVYKH GLIN [ELASTIC-VISCOUS PROPERTIES AND STRUCTURES OF WATER-SUSPENDED BENTONITIC CLAY]: Kolloidnyi Zhurnal, v. 17, no. 3, 1955.

2. Aleksandrov, A. P. MOROZOSTOYKOST VYSOKOPOLIMERNYKH SOYEDINENY [COLD-RESISTANCE PROPERTIES OF HIGH POLYMERIC COMPOUNDS]: Akademiya Nauk SSSR, Izvestiya, Trudy 1-2, Conference on High Polymeric Com-

pounds, 1945.

3. Bartenev, G. M. OVREMENNOY I TEMPERATURNOY ZAVISIMOSTI PROCHNOSTI TVERDYKH TEL [ON TEMPORARY TEMPERATURE AND VARIABLE STRENGTH OF HARD SOLIDS]: Akademiya Nauk SSSR, Izvestiya, Otdelenie Tekhnicheskikh Nauk, 1955, no. 9.

4. Beloussov V. V. OSHOVNYYE VOPRODSY GEOTETEONIKI [THE PRINCIPAL PROBLEMS OF GEOTECTONICS]: Gosgeoltekhizdat, 1954.

5. Vinogradov, G. V. STROYENIYE OPTICHESKIYE I MEKHANICHESKIYE SVOYSTVA PSEUDOGELEY MYL (SMAZOK) [STRUCTURAL, OPTICAL AND MECHANICAL PROPERTIES OF PSEUDOGEL FATS (OIL)]: Akademiya Nauk USSR, Izvestiya, Trudy, All-Union Conference on Collodial Chemistry, p. 249, Kiev, 1952.

6. Volarovich, M. P., and D. B. Balashov. ISSLEDOVANIYE SKOROSTEY UPRUGIKH VOLN V OBRAZTSAKH GORNYKH POROD PRI DAVLENII DO 500 KG/CM$^2$ [RAPID INVESTIGATION OF ELASTIC WAVES IN MODEL ROCK STRATA AT 500 kg/cm$^2$ PRESSURE]: Akademiya Nauk SSSR, Izvestiya, Seriya Geofizicheskaya, 1957, no. 3.

7. Gamburtsev, G. A. SOSTOYANIYE I PERSPEKTIVY RABOT V OBLASTI PROGNOZA ZEMLETRYASENY [STATUS AND PERSPECTIVE OF WORK IN THE FIELD OF EARTHQUAKE PROGNOSIS]: Byulleten Soveta po Syesmologii, 1955, no. 1.

8. __________. KRATKOYE SODERZHANIYE DOKLALA 'O PROGNOZE ZEMLETRASENII" V KHRONIKE [SUMMARY OF THE CONTENTS OF THE PAPER "ON THE PROGNOSIS OF EARTHQUAKES" IN CURRENT LITERATURE]: Akademiya Nauk SSSR, Izvestiya, Seriya Geofizicheskaya, 1955, no. 3.

9. Gzovsky, M. V. O ZADACHAKH I SODERZHANII TEKTONOFIZIKI [ON THE FORM AND PROBLEMS OF TECTONOPHYSICS]: Akademiya Nauk SSSR, Izvestiya, Seriya Geofizicheskaya, 1954, no. 5.

10. __________. TEKTONICHESKIYE POLYA NAPRAZHENIY [TECTONIC EARTH STRAIN]: Akademiya Nauk SSSR, Izvestiya, Seriya Geofizicheskaya, 1954, no. 5.

11. __________. MODELIROVANIYE TEKTONICHESKIKA POLEY NAPRYAZHENY I RAZRYVOV [TECTONIC SCALE MODELS IN EARTH STRAIN AND DEFORMATION]: Akademiya Nauk SSSR, Izvestiya, Seriya Geofizicheskaya, 1954, no. 6.

12. Gzovsky, M. V. SOOTHOSHENIYA MEZHDU TEKTONICHESKIMI RAZRYVAMI I NAPRYAZHENIYAMI V ZEMNOY KORE [CORRELATION BETWEEN TECTONIC DEFORMATION AND STRAINS IN THE EARTH'S CRUST]: Razvedka i Okhrana Nehr, 1956, no. 11.

13. __________. TEKTONOFIZICHESKOYE OBOSNOVANIYE GEOLOGICHESKIKH KRITERIYEV SEYSMICHNOSTI [TECTONOPHYSICAL BASES FOR GEOLOGICAL SEISMIC CRITERIA]: Akademiya Nauk SSSR, Izvestiya, Seriya Geofizicheskaya, 1957, nos. 2-3.

14. __________. SOVESHCHANIYE PO TEKTONOFIZIKE. KHRONIKA [CONFERENCE ON TECTONOPHYSICS. CURRENT LITERATURE]: Akademiya Nauk, SSSR, Izvestiya, Seriya Geofizicheskaya, 1957, no. 7.

15. Zhurkov, C. N., and B. N. Narzullayev. VREMENNAYA ZAVISIMOST PROCHNOSTI TVERDYKH TEL [TEMPORARY VARIABLE STRENGTH OF HARD SOLIDS]: Zhurnal Teknicheskoi Fiziki, v. 23, no. 10, 1953.

16. Kirpichev, M. V. TEORIYA PODOBIYA [THEORY OF SIMILARITY]: Akademiya Nauk SSSR, Izvestiva, 1953.

17. Kuznetzov, G. N. MEKHANICHESKIYE SVOYSTRA GORNYKH POROD [MECHANICAL PROPERTIES OF ROCK STRATA]: Ugletekhizdat, 1947.

18. Lebedeva, N. B. MODELIROVANIYE PROTSESSA OBRAZOVANIYA DIAPIROVYKH KUPOLOV [SCALE-MODEL PROCESSES FOR MODEL DIAPIRIC FOLDS]: Sovetskaya Geologiya, 1956, no. 54.

19. Lustikh, E. N. USLOVIYA PODOBIYA PRI MODELIROVANII TEKTONICHESKIKH PROTSESSOV [SIMILARITY CONDITIONS FOR TECTONIC SCALE-MODEL PROCESSES]: Akademiya Nauk SSSR, Doklady, v. 14, no. 5, 1949.

20. Mikhaylov, N. V. UPRUGO-PLASTICHESKIYE SVOYSTRA NEFTYANYKH BITUMOV [ELASTIC-PLASTIC PROPERTIES OF PETROLEUM ASPHALT]: Kolloidnyi Zhurnal, v. 17, no. 3, 1955.

21. Mikhaylov, N. V., and A. M. Likhtgeym. ISSLEDOVANIYE POLNYKH GEOLOGICHESKIKH KRIVYKH I FORMULY DLYARASCHETA EFFEKTIVHOY VYAEKOSTI

STRUKTURIROVANNYKH ZHIDKOSTEY S MOLEKULYARNO KINETICHESKOY INTERPRETATSIEY VKHODYASHCHIKH V NIKH CHLENOV [INVESTIGATION OF GEOLOGIC CURVES AND FORMULAE FOR EFFECTIVE CALCULATIONS OF VISCOSITY IN STRUCTURE LIQUID WITH MOLECULAR-KINETIC INTERPRETATION IN ITS INCOMING MEMBER]: Kolloidnyi Zhurnal, v. 17, no. 5, 1955.

22. Osokina, D. N. ZHELATINO-GLITSERINO-VYYE STUDIN KAK MATERIAL DLYA OPTICHESKOGO METOD ISSLEDOVANIYA NAPRYAZHENY [STUDY OF GELATIN-GLYCERIN AS MATERIAL FOR INVESTIGATION OF STRAIN BY THE OPTICAL METHOD]: Kolloidnyi Zhurnal, v. 19, no. 6, 1957.

23. Osokina, D. N., V. P. Pavlov, G. V. Vinogradov, and M. V. Gzovsky. GEOLOGICHESKOYE I POLYARIZATZIONNO-OPTICHESKOYE ISSLEDOVANIYE RASTVOROV I GELEY ETILTSELLYULOZY [GEOLOGIC AND POLARIZATION-OPTIC INVESTIGATION OF DEFORMATION AND ETHYL-CELLULOSE GEL]: Akademiya Nauk SSSR, Izvestiya, Tezisy Dokladov IX Konfer. Po Obshchim Voprosam Khimii i Fiziki Vysokomolekul. Soedineny [Thesis Papers, IX Conference on General Questions of High Molecule Bond Chemistry and Physics]: Akamediya Nauk SSSR, Izvestiya, p. 124, 1955.

24. Riznichenko, Yu. V. SEYSMOAKUSTICHESKIE METODY IZUCHENIYA NAPRYAZHENNOGO SOSTOYANIYA GORNYKH POROD [SEISMO-ACOUSTIC METHOD OF INVESTIGATING COMPETITIVE STRAIN IN ROCK STRATA]: Akademiya Nauk SSSR, Izvestiya, Seriya Geofizicheskaya, 1955, no. 6.

25. Cinitzyn, V. V., and G. V. Vinogradov. VYAZKOSTNYE SVOYSTVA UGLEBODORODNYKH SMAZOK [VISCOUS PROPERTIES OF HYDROCARBONS]: Kolloidnyi Zhurnal, v. 17, no. 3, 1955.

26. Frenkel, Ya. I. KINETICHESKAYA TEORIYA ZHIDKOSTEY [KINETIC THEORY OF LIQUIDS]: Akademiya Nauk SSSR, Izvestiya, 1945.

27. Fridman, Ya. B. EDINAYA TEORIYA PROCHNOSTI MATERIALOV [UNIT THEORY OF MATERIAL RESISTANCE]: Oborongiz, 1943.

28. ______. MEKHANICHESKIYE SVOYSTVA METALLOV [MECHANICAL PROPERTIES OF METALS]: Akademiya Nauk SSSR, Izvestiya, 2-e, 1958.

29. Shneerson, B. L. O PRIMENENII TEORII PODOBIYA PRI TEKTONICHESKOM MODELIROVANII [ON THE ADAPTABLE SIMILARITY THEORY FOR TECTONIC SCALE MODELS]: Akademiya Nauk SSSR, Trudy, In-ta Teoretichesky Geofizika, v. 3, 1947.

30. Eygenson, L. S. MODELIROVANIE [SCALE MODELS]: Soveta Nauka, Gos. Izvestiyavo, 1952.

31. Benioff, H. EARTHQUAKES AND ROCK CREEP: Seismol. Soc. America, Bull., v. 41, no. 1, 1951.

32. Bucher, W. ROLE OF GRAVITY IN OROGENESIS: Geol. Soc. America, Bull., v. 67, p. 1295-1318, Oct. 1956.

33. Bullen, K. E. ON THE SIZE OF THE STRAINED REGION PRIOR TO AN EXTREME EARTHQUAKE: Seismol. Soc. America, Bull., v. 45, no. 1, 1955.

34. Chang, W. G. ADAPTATION AS A MODE OF DEVELOPMENT OF FRACTURES AND ITS RELATION TO GEOLOGICAL PHENOMENA: Academia Sinica, Nat. Res. Inst., Contr. no. 8, 1948.

35. Cloos, E. EXPERIMENTAL ANALYSIS OF FRACTURE PATTERNS: Geol. Soc. America, Bull., v. 66, no. 3, 1954.

36. Cloos, H. EXPERIMENTE ZUR INNEREN TEKTONIK [EXPERIMENTS ON TECTONICS]: Zentralbl. fur Mineralogie, v. 12, p. 609-21, 1928.

37. ______. ZUR EXPERIMENTELLEN TEKTONIK, BRUCHE UND FALTEN [ON EXPERIMENTAL TECTONICS, FOLDS AND FAULTS]: Naturwissenschaften Jahrbuch 19, no. 11, p. 242-47, 1931.

38. Daubree, A. ETUDES SYNTHETIQUES DE GEOLOGIE EXPERIMENTALE [SYNTHETIC STUDIES ON EXPERIMENTAL GEOLOGY]: Paris, 1879.

39. Dobrin, M. B. SOME QUANTITATIVE EXPERIMENTS ON A FLUID SALT-DOME MODEL AND THEIR GEOLOGICAL IMPLICATIONS: Am. Geophys. Union, Trans., II, 1941.

40. Griggs, D. T. DEFORMATION OF ROCKS UNDER HIGH CONFINING PRESSURES: Jour. Geology, v. 44, no. 5, 1936.

41. ______. CREEP OF ROCKS: Jour. Geology, v. 47, no. 3, 1939.

42. ______. EXPERIMENTAL FLOW OF

ROCKS UNDER CONDITIONS FAVORING RECRYSTALLIZAION: Geol. Soc. America, Bull., v. 51, no. 7, 1940.

43. Hafner, W. STRESS DISTRIBUTIONS AND FAULTING: Geol. Soc. America, Bull., v. 62, no. 4, 1951.

44. Hubbert, M. K. THEORY OF SCALE MODELS AS APPLIED TO THE STUDY OF GEOLOGICAL STRUCTURES: Geol. Soc. America, Bull., v. 48, p. 1459-1520, 1937.

45. Karman, T. FESTIGKEITVERSUCHE UNTER ALLSEITGEM DRUCK. [STRENGTH TESTS UNDER VARIABLE PRESSURE]: Zeitschrift de Ver. Deutsch. Ingeniur, v. 5, p. 1749-57, 1911.

46. Koenigsberger, G., and O. Morath. THEORETISCHE GRUNDLAGEN DER EXPERIMENTELLEN TEKTONIK [THEORETICAL FOUNDATIONS OF EXPERIMENTAL TECTONICS]: Zeitschrift der Deutsch. Geologisch. Gesellschaft, v. 65, p. 65-86, 1913.

47. Lee, I. S., C. H. Chen, and M. T. Lee. EXPERIMENTS WITH CLAY ON SHEAR FRACTURES: Geol. Soc. China, Bull., v. 28, nos. 1-2, 1948.

48. Li, Szu-Kuang. VORTEX STRUCTURE AND OTHER PROBLEMS RELATING TO THE COMPOUNDING OF GEOTECTONIC SYSTEMS OF NORTHWESTERN CHINA: Academia Sinica, 1955.

49. Link, T. A. THE ORIGIN AND SIGNIFICANCE OF "EPIANTICLINAL" FAULTS AS REVEALED BY EXPERIMENTS: Am. Assoc. Petroleum Geologists, Bull., v. 11, no. 8, 1927.

50. Mohr, O. UEBER DIE DARSTELLUNG DES SPANNUNGSZUSTANDES UND DES DEFORMATIONSZUSTANDES EINES KORPERSELEMENTS UND UBER DIE ANWENDUNG DERSELBEN IN DER FESTIGKEITALEHRE: Der Civilingeniur, v. 2, no. 3, 1882.

51. Nettleton, L. L. RECENT EXPERIMENTAL AND GEOPHYSICAL EVIDENCE OF MECHANICS OF SALT-DOME FORMATION: Am. Assoc. Petroleum Geologists, Bull., v. 27, no. 1, 1943.

52. Parker, T. J., and A. N. McDowell. MODEL STUDIES OF SALT-DOME TECTONICS : Am. Assoc. Petroleum Geologists, Bull., v. 39, no. 12, 1955.

53. Philippoff, W. ZUR THEORIEN DER STRUCTURVISKOUSITAT [ON THE THEORY OF STRUCTURE VISCOSITY]: Kolloid-Zeitschrift Band, no. 71, 1935.

54. Phillips D. S. TECTONICS OF MINING: Colliery Engineering, June-Oct. 1948.

55. Ramberg, H. NATURAL AND EXPERIMENTAL BOUDINAGE AND PINCH AND SWELL STRUCTURES: Jour. Geology, v. 63, no. 6, 1955.

56. Reier, E. GEOLOGISCHE UND GEOGRAPHISCHE EXPERIMENTE .I FALTEN. II VULKANISCHE UND MASSEN ERUPTIONEN. III RUPTUREN. IV METHODEN UND APPARATE [GEOLOGIC AND GEOGRAPHIC EXPERIMENTS. I FAULTS. II VOLCANISM AND MASS ERUPTIONS. III RUPTURES. IV METHODS AND APPARATUS]: Leipzig, 1892-94.

57. Robertson, E. C. EXPERIMENTAL STUDY OF THE STRENGTH OF ROCKS: Geol. Soc. America, Bull., v. 66, no. 2, 1951.

58. Wallace, R. GEOMETRY OF SHEARING STRESS AND RELATION TO FAULTING: Jour. Geology, v. 59, no. 2, 1951.

59. Willis, B. THE MECHANICS OF APPALACHIAN STRUCTURE: U. S. Geol. Survey, Ann. Rept., pt. 2, p. 211-81, 1893.

# MINERALOGICAL AND CHEMICAL COMPOSITION OF THE SILT FRACTION OF SOME SOILS, SOIL-BUILDING ROCKS, AND DISPERSED MATERIAL OF RIVERS IN THE KURA-ARAXES LOWLAND[1]

*by*

*N. I. Gorbunov*

*• translated by Sahil Faizi •*

ABSTRACT

The physical, mineralogical, and chemical properties of soils, soil-building rocks, and dispersed materials of rivers in the Kura-Araxes lowland, U. S. S. R., are dependent upon the quantity and quality of organic substances contained, distribution and characteristics of silt and colloidal fractions, and amount and composition of bases and salts absorbed in the soils. These characteristics affect swelling, maximum hygroscopic capacity, and hardness.

Iron-oxide films on the surfaces of micro-aggregates increase soil stability, essentially maintained by capillary forces and by swelling of hydrophilic colloids. During irrigation, soils increase in volume; nonstructured soils become packed when dry. Crust building involves soil swelling, soil-lump soaking and destruction by enclosed or adsorbed air, soil packing, and hardening with simultaneous shrinkage and cracking.

Slow irrigation along furrows, subsoil irrigation, and rain-making are recommended for the prevention of crust building, as are other general agrotechnical measures. --Editor.

## INTRODUCTION

The physico-chemical properties of soils depend on various factors. The most important are (1) quantity and quality of organic substances; (2) distribution of physical composition of soils; (3) mineralogical and chemical composition of soils, especially of the highly dispersed silt and colloidal fractions; and (4) amount and composition of the bases and salts absorbed in soils. The above factors alter the properties of soils in different ways, depending on the physico-geographical conditions both at the time of soil building and now.

The mineral composition of the silt fraction of the soils and river sediments in the Kura-Araxes lowland [Kura-Araksinskaya Nizmennost, U. S. S. R.; 42°N. 48°30'E.] has not been previously studied. Mineralogical and chemical data concerning the silt and colloidal fractions of gray soils in Central Asia can be found in the publications of A. N. Rozanov [15] and A. N. Rozanov in collaboration with I. E. Sedletsky [16]. These gray soils have certain similarities to those occurring in the semideserts of Azerbaidzhan, but they also have great differences. A study of the soils of the Kura-Araxes lowland permitted A. N. Rozanov to define a special type of gray-brown soil [15].

Although his definition is controversial, it must be noted that the higher clay content in the gray-brown soil than in the gray soil of Central Asia (as noted by A. N. Rozanov) coincides with our conclusion that the silt fraction of the former contains greater amounts of beidellite and beidellized mica, the most dispersed clay mineral. This coincidence of opinion demonstrates the importance of mineralogical investigation in studies of the origin of soils. Another example of the same effect is seen in the nature of crust building in the soils, as in Shirvan. The investigation of this phenomenon undertaken by the author in cooperation with N. E. Bekarevich [6, 7] permitted him to disclose the causes of crust building and to select practical means to prevent it in the irrigated area of Shirvan.

Although the study of dispersion in soils, soil-building rocks, and river sediments is closely related to the study of the mineralogical and chemical composition of the silt fraction of these unconsolidated materials, we will review these two aspects of the studies independently in order to make the subject more understandable.

## PHYSICAL COMPOSITION OF SOILS, SOIL-BUILDING ROCKS, AND THE DISPERSED MATERIAL OF RIVERS IN THE KURA-ARAXES LOWLAND

We studied the physical composition of areas

---

[1]In: Mineralogichesky sostav pochv i ikh fiziko khimi cheskie svoystav: Akademiya Nauk SSSR, Trudy, Pochvennogo Instituta im. V.V. Dokuchaeva, v. 53, p.3038, Moscow, 1958. This work was carried out by the Kura-Araxes expedition. The following persons took part in the expedition: V. A. Kovda, corresponding member of the Academy of Sciences, U.S.S.R., and scientific leader; Prof. A.N. Rozanov, in change of the expedition; Prof. N.E. Gorbunov, scientific leader of the physico-chemical team; I. G. Tsyurupa, E.A. Shurygina, G.B. Basova, and M. G. Melnikova, laboratory technicians; N.E. Bekarevich, in charge of field studies of the soil crusts of the Shirvan steppe.

most typical of the regions of the Kura-Araxes lowland which are, from the practical point of view, most suitable for cultivation. We also studied certain regions beyond the Kura-Araxes lowland that affect the soil building in this region, in order to evaluate the results of the investigation more accurately, particularly the extent of the sediments beyond the limits of the lowland along the rivers that cross the principal area of our studies (table 1).

In contrast to the usual method of determining the physical composition of soils--in which the soils are first treated chemically, as suggested by N. A. Kachinsky[10]--we prepared the soils for physical analysis by repeatedly mashing all fractions and separating them in water until they were completely dispersed[4]. Mashing of samples as a treatment preliminary to physical analysis was first used by G. V. Nefedov in 1901[12]. He also established the duration of mashing and the size of samples for the separation of particles under 0.001 mm. Later, in 1925, A. N. Puri[21] made similar experiments.

In 1939-1940, A. I. Tsurinov[19] and a group of his associates used mashing for the preparation of clay solutions, and in 1947 R. Kh. Aidinyan [1] made a number of experiments for comparative evaluation of methods of preliminary treatment of soils--the method suggested by Kachinsky and the mashing method--prior to physical analysis. The method of separating silt and colloidal fractions was slightly altered by us; we mashed twice and in some cases sampled three times instead of once, in order to provide a complete separation of clay minerals without boiling them. The separation of the fraction under 0.001 mm was undertaken after the dissolving of carbonates and other salts in weak solutions of hydrochloric acid and water.

The salts must be extracted prior to X-ray analysis, for otherwise it would be impossible to interpret the X-ray diagrams of the silt fraction. As far as the decomposition of minerals in hydrochloric acid is concerned, our experiments and those undertaken by Zalmanson and Shishova [9], Kalashnikova and Labenets, Zhernov and Kislitsina [11] indicate that it is not significant.

Washing in water improves the peptization of colloids. Red-earth soils are difficult to peptize because of the presence of mobile and hydrophobic aluminum and iron minerals, but, after they have been washed in water and the coagulators extracted, a relatively good peptization and a complete separation of silt and colloid fractions can be achieved. Soil colloids can also be peptized by adding organic substances such as humic acid, but this method can be used only in specific cases.

The percent of particles under 0.001 mm separated after mashing was, in a number of cases, equal to that recovered by the Kachinsky method, but in samples containing large amounts of montmorillonite we recovered 15 to 25 percent more of these particles than by using the Kachinsky method. Therefore, mashing of samples twice is especially important where soils contain large amounts of montmorillonite and humus [4].

The results of the physical composition of the analyzed soils and river-bottom sediments are briefly compiled in tables 2 and 3.

As can be seen in the tables, all the samples analyzed are heavily loamy sediments and clays. The quantity of particles under 0.01 mm exceeds 60 percent and in many cases reaches 70 to 80, or even 90 percent.

The fraction under 0.01 mm contains large quantities of particles under 0.001 mm. The content of these fine-grained substances varies from 40 to 70 percent and drops only in a few cases to 35 percent. Particles over 0.25 mm are present in small amounts, usually less than 2.5 percent, reaching 6.5 percent in only one case (section 805/19). The quantity of particles from 0.25 to 0.1 mm is also small, although in some cases it reaches 9.7 to 14.3 percent (sections 936, 948, and 805/19).

The soils and rocks showed great variation in the content of particles from 0.1 to 0.01 mm (from 1.2 to 42.2 percent), although in the majority of cases they were within 15 and 25 percent.

Thus, the finest-grained particles are most common in the soils. The fraction from 0.005 to 0.001 mm comprises the second largest portion of the soils, reaching 45 percent and dropping to 10 or 15 percent in only a few cases. The other fractions are present, but their quantity is in inverse ratio to their grain-size. Studies of the physical composition have revealed that clays and soils developed upon them are much heavier than soils and sediments of the Kura river.

The physical properties of clays and soils of the Araxes area, despite their heavy physical composition, are more permeable and have better developed structures than soils developed upon the sediments of the Kura river.

The physical composition of dry remnants of river suspensions is also very important in understanding the physical composition and origin of soils and and rocks of the Kura-Araxes lowland. These remnants are heavy (table 4). The amount of the fraction under 0.001 mm is from 45 to 57 percent and is about the same in all rivers during transitional periods. The quantity of particles under 0.01 mm varies

TABLE 1. List of the soils studied*

| Section Number | Soil Type | Location of Section | Author of the Section |
|---|---|---|---|
| MUGAN STEPPE | | | |
| | Red clay of Araxes<br>Altered clay of Araxes | Dzhafarkhan<br>Dzhafarkhan | N. I. Gorbunov |
| 624 | Light-gray soil of a meadow salt marsh overlying the sediments of Araxes | Central Mugan, right bank of Araxes river at the village of Karayevka 2d | V. V. Yegerov |
| 631 | Light-gray soil of a meadow salt marsh on the young sediments of Araxes | Middle Mugan, alluvial plain of Araxes, 3 km south of the head constructions of a canal | V. V. Yegerov |
| 100K | Soils of a meadow salt marsh on the Bolgarchay delta | Southern Mugan, north of the village of Novograzhdanovka | S. I. Dolgov,<br>L. I. Yegerov,<br>A. A. Zhitkova |
| MILSK STEPPE | | | |
| 936 | Soil of a meadow salt marsh passing into a steppe | Milsk steppe, central part of the present Araxes delta, 1 km south of the burial mound of Nazraly-Tan | V. V. Yegerov |
| 948 | Gray-brown soil, irrigated, secondarily salted | Milsk steppe, irrigated part of an inclined plain 1 km from the canal of Ordzhonikidze | V. V. Yegerov |
| 805/19 | Gray-brown soil, strongly salted, remnant of a meadow on a diluvial mantle* | Milsk steppe, southern part of a diluvial-proluvial plain, 6 km north-northeast of Zhdanovsk | V. V. Yegerov |
| 776 | Gray-brown meadow soil, slightly salty | Milsk steppe, an alluvial plain at the Kura river, its old delta, 6 km northeast of Agdzhabeda | V. V. Yegerov |
| SHIRVAN, SALYAN, AND KIROVABAD STEPPES | | | |
| 180 | Soils on the irrigated sediments of the Kura river overlying those of Araxes | Shirvan, 3 km north of Kovler | Yu. P. Lebedev |
| 70 | Old diluvial hill sediments | Shirvan | Yu. P. Lebedev |
| 174 | Meadow soils on the present Kura sediments | Shirvan, 3.5 km south of Zangene | Yu. P. Lebedev |
| 22 | Gray-brown heavy loamy soil, slightly crusted (1-2 grade) | Kirovabad | N. I. Gorbunov,<br>N. E. Bekarevich |
| 18 | Tertiary clay soil | The region of Geokchaisk | N. I. Gorbunov,<br>N. E. Bekarevich |
| 14 | Soil of a meadow salt marsh on alluvial-proluvial sediments, slightly crusted (3-4 grade) | The region of Zardob | N. I. Gorbunov,<br>N. E. Bekarevich |
| 11 | Soil of an irrigated meadow on heavy alluvial-proluvial sediments, medium crusted (5-6 grade) | Shirvan, experimental station | N. I. Gorbunov,<br>N. E. Bekarevich |
| 10 | Soil of an irrigated meadow on heavy alluvial-proluvial sediments, heavily crusted (9-10 grade) | Shirvan, experimental station | N. I. Gorbunov,<br>N. E. Bekarevich |
| SALYAN STEPPE | | | |
| 528 | Soils of a meadow salt marsh, weakly developed on delta-marine (Caspian) sediments | Salyan steppe, the first Caspian terrace | V. V. Yegerov |
| 514 | Slightly salty soil of a meadow salt marsh on delta-marine sediments of the Caspian Sea | Central part of the Salyan steppe, formerly a sea bay, 6 km south-southwest of Karamanly | V. V. Yegerov |

* Diluvium (diluvial) and alluvium (alluvial) in Russian do not refer to the two subdivisions of the Quaternary period, but are rather applied to certain kinds of unconsolidated sediments: diluvium--to superficial accumulations on slopes (clay, sand, gravel) slightly transported by gravity, raindrops, or glacial action; alluvium--to all detrital deposits resulting from the operation of rivers, including those laid down in river beds, flood plains, deltas, terraces, etc. The term "ancient alluvium" may also occur in Russian publications and mean pre-Quaternary deposits of similar origin.--Translator. Proluvium is a complex friable formation accumulated at the foot of a slope as a result of occasional torrential washing of fragmental material derived from weathered shale. --Editor.

TABLE 2. Physical composition of soils and soil-building rocks in the Kura-Araxes lowland (in percent after extracting carbonates)

| Section Number | Soil Type | Depth of Samples (cm) | Loss of Carbonates and Soluble Salts (%) | Grain Size (mm) <0.001 | <0.01 |
|---|---|---|---|---|---|
| | Red clay of Araxes (Dzhafarkhan) | 60-100 | 17.5 | 69.2 | 95.4 |
| | Altered clay of Araxes (Dzhafarkhan) | 320-350 | 11.4 | 63.9 | 96.1 |
| 624 | Light-gray soil of a meadow salt marsh on young sediments of Araxes | 9-26 | 26.0 | 58.5 | 97.3 |
| | Young sediments of Araxes | 26-52 | 26.7 | 63.0 | 93.3 |
| | Soils of recent sediments of Araxes and buried in the 1920's | 52-90 | 21.0 | 65.0 | 90.4 |
| | Old well-packed sediments of Araxes | 220-260 | 22.9 | 61.4 | 87.8 |
| 631 | Light-gray soil of a meadow salt marsh on young sediments of Araxes | 11-22 | 20.1 | 69.0 | 93.3 |
| | | 55-80 | 23.0 | 35.5 | 87.0 |
| | | 155-250 | 20.5 | 53.2 | 82.9 |
| 100K | Soils of a meadow salt marsh on the Bolgarchay delta | 0-16 | 7.5 | 58.2 | 77.0 |
| | | 39-47 | 17.1 | 63.3 | 88.2 |
| | | 90-100 | 12.8 | 65.2 | 90.7 |
| 936 | Soil of a meadow salt marsh passing into a steppe | 0-7 | 14.8 | 40.8 | 59.7 |
| | | 16-32 | 25.4 | 43.7 | 80.6 |
| | | 77-125 | 24.5 | 36.5 | 88.8 |
| 948 | Gray-brown soil, irrigated, secondarily salty | 0-18 | 13.8 | 49.7 | 68.7 |
| | | 54-74 | 20.8 | 59.5 | 80.7 |
| | | 74-106 | 20.7 | 62.5 | 83.8 |
| | | 146-180 | 23.2 | 50.6 | 75.1 |
| 805/19 | Gray-brown soil, strongly salty, remnant of a meadow on a diluvial mantle | 0-5 | 12.6 | 37.1 | 77.1 |
| | | 5-20 | 18.8 | 49.7 | 69.0 |
| | | 110-132 | 21.4 | 34.4 | 74.6 |
| | | 132-159 | 23.8 | 38.8 | 66.8 |
| 180 | Soils on the irrigated present sediments of the Kura river overlying those of Araxes | 0-12 | 28.8 | 35.6 | 57.0 |
| | | 33-53 | 25.6 | 42.0 | 67.0 |
| | | 120-140 | 21.0 | 62.0 | 92.0 |
| | | 140-160 | 20.1 | 58.3 | 87.3 |
| 70 | Old diluvial hill sediments | 20-36 | undetermined | 70.2 | 93.0 |
| | | 614-660 | | 73.3 | 91.9 |
| 174 | Soil of an alluvial meadow on the present Kura sediments | 15-25 | 24.0 | 39.1 | 67.7 |
| | | 210-252 | 31.8 | 41.4 | 68.7 |
| | | 294-336 | 13.9 | 53.8 | 80.6 |
| | | 336-378 | 19.1 | 51.1 | 82.7 |
| 22 | Gray-brown heavily loamy soil, slightly crusted (1-2 grade) | 0-16 | 18.1 | 48.4 | 70.9 |
| 18 | Tertiary clay | 0-20 | 34.6 | 63.6 | 88.2 |
| 14 | Soil of a meadow salt marsh on alluvial-proluvial sediments, medium crusted (3-4 grade) | 0-15 | 31.9 | 41.0 | 65.9 |
| 11 | Soil of an irrigated meadow on heavy alluvial-proluvial sediments, heavily crusted (9-10 grade) | 0-15 | 33.2 | 46.1 | 70.8 |
| 10 | Soils of irrigated meadow on alluvial-proluvial sediments; crust very salty (9-10 grade) | 0-16 | 29.3 | 57.7 | 85.6 |
| 528 | Soil of a meadow salt marsh, weakly developed on delta-marine (Caspian) sediments | 0-23 | 23.6 | 46.5 | 75.8 |
| | | 60-111 | 25.8 | 60.0 | 91.1 |
| | | 135-210 | 24.4 | 37.6 | 58.1 |
| 514 | Slightly salty soil of a meadow salt marsh on delta-marine sediments of the Caspian Sea | 0-12 | 12.6 | 43.3 | 77.1 |
| | | 88-120 | 26.5 | 53.3 | 90.4 |
| | | 160-300 | 2.0 | 26.0 | 84.8 |

TABLE 3. Physical composition of river-bottom sediments (in percent after extracting carbonates; samples of June 1950)

| Location of Water Sample | Carbonates (%) | Other Losses (%) | Grain size | |
|---|---|---|---|---|
| | | | <0.001 | <0.01 |
| Kura (Samukh) . . . . . . . . . . . . . . | 10.32 | 8.3 | 26.0 | 45.7 |
| Iori (Samukh) . . . . . . . . . . . . . . | 17.84 | 7.8 | 30.8 | 48.5 |
| Alazani (Samukh) . . . . . . . . . . . . . | 13.00 | 6.0 | 27.2 | 56.3 |
| Kura (Yevlakh) . . . . . . . . . . . . . . | 10.20 | 11.0 | 23.4 | 45.6 |
| Kura (Zardob) . . . . . . . . . . . . . . | 11.74 | 7.4 | 36.2 | 59.8 |
| Kura (Ali-Bayramly) . . . . . . . . . . . | 19.54 | 7.4 | 40.0 | 57.6 |
| Araxes (Zhdanovsk) . . . . . . . . . . . | 12.45 | 12.2 | 24.9 | 49.8 |
| Araxes (Imishli) . . . . . . . . . . . . . | 11.06 | 5.8 | 28.0 | 41.2 |
| Araxes (Saatly) . . . . . . . . . . . . . | 13.61 | 8.4 | 29.4 | 49.2 |
| Araxes (Sabirabad) . . . . . . . . . . . . | 13.03 | 8.3 | 27.3 | 47.8 |
| Kura (Salyan) . . . . . . . . . . . . . . | 11.34 | 8.0 | 26.1 | 42.3 |
| Terek (Dzaudzhikau) . . . . . . . . . . . | 1.98 | 2.7 | 3.2 | 13.6 |

TABLE 4. Weight of the dry remnants of river suspension

| Location of Samples | Dry Remnant gram/liter | Location of Samples | Dry Remnant gram/liter |
|---|---|---|---|
| Kura (Samukh) . . . . . . . . | 0.23 | Kura (Salyan) . . . . . . . . | 1.77 |
| Kura (Yevlakh) . . . . . . . . | 0.90 | Araxes (Zhdanovsk) . . . . . | 0.25 |
| Kura (Zardob) . . . . . . . . | 2.40 | Araxes (Imishli) . . . . . . . | 0.56 |
| Kura (Mollakend) . . . . . . . | 3.92 | Araxes (Saatly) . . . . . . . | 0.53 |
| Kura (Sabirabad) . . . . . . . | 4.76 | Iori (Samukh) . . . . . . | 3.30 |
| Kura (Ali-Bayramly) . . . . . | 1.98 | Alazani (Samukh) . . . . . . | 3.57 |

from 70.5 percent to 90.3 percent. Particles over 0.1 mm are absent, and this is a very significant difference between the physical composition of river suspensions and that of soils and bottom sediments. Particles from 0.1 to 0.001 mm are present in substantial amounts, ranging from 9.9 percent in Alazan river suspensions to 29.5 percent in the Araxes river suspensions in the Saatly region.

If we take the physical composition of soils, river suspensions, and soil-building rocks as data that gives us some idea of their origin, we may conclude that soils and rocks differ substantially from the present river sediments. If we assume that soils are formed by materials similar to that of present river suspensions, then the question arises of why the particles over 0.1 mm are present in soils, sometimes in large amounts, while they are absent in suspensions. It is likely that the soil-building rocks were coarser-grained than the suspensions. Despite the fact that soils contain coarse-grained particles, they have the silt fraction under 0.001 mm in the same or larger quantities than do suspensions. This means that either the destruction of coarse-grained particles took place when the soil-building process was still in progress or that other rocks took part in the formation of soils. Large particles, occurring in the soil as a result of river floods or diluvial streams, became decomposed and made the physical composition of the soils heavier. It is interesting to note that the particles from 0.1 to 0.01 mm occur frequently in soils in smaller quantities than in suspensions. This means that the river suspensions upon which the soils were formed had also been decomposed. The above facts indicate intensive weathering of soil-building rocks and the minerals that produce soils are of heavy physical composition. It is possible that the evolution of soils in irrigated areas leads to accumulation of fine dispersed particles produced by the decomposition of large particles, for water and high temperature contribute greatly to this effect.

Data on the physical composition alone is not adequate to explain the physical properties of soils. A little later we will try to explain these properties from the viewpoint of mineralogical and chemical pecularities of soils.

The difference between soils and river sediments can also be noted in respect to their mineral composition.

## MINERAL COMPOSITION OF SOILS, SOIL-BUILDING ROCKS, AND RIVER SEDIMENTS

Soils, coastal and bottom sediments, and river suspensions in the Kura-Araxes lowland contain minerals of the montmorillonite group, micas, hydromicas, minerals of the kaolinite group, quartz, and hydroxides of trivalent elements. This was established during 1948-50 by thermal and X-ray studies of the fractions under 0.001 mm extracted from the above soils and sediments. The minerals of the montmoril-

lonite group, as determined by the thermal studies, consist principally of beidellite and beidellized hydromica. They were discovered by comparing the thermograms of the studied subjects with those of pure minerals. Beidellite can hardly be distinguished from montmorillonite by the X-ray method, but the thermograms of these two minerals have peculiarities that permit us to establish easily which of the minerals predominates in the sample. The thermogram of montmorillonite has the first endothermic stop at about 100°C in the form of a broad peak. In the case of beidellite, the first stop is much narrower. The second endothermic stop in the case of beidellite is about 500° to 575°C, and, for montmorillonite, it is over 600°C. The thermogram of beidellized hydromica is close to that of beidellite. However, the thermal effects of hydromica are longer along the time axis.

Interpretations of the thermograms are given below for fractions under 0.001 mm extracted from soils, rocks, and river suspensions of the Kura-Araxes lowland.

Mugan Steppe (fig. 1)

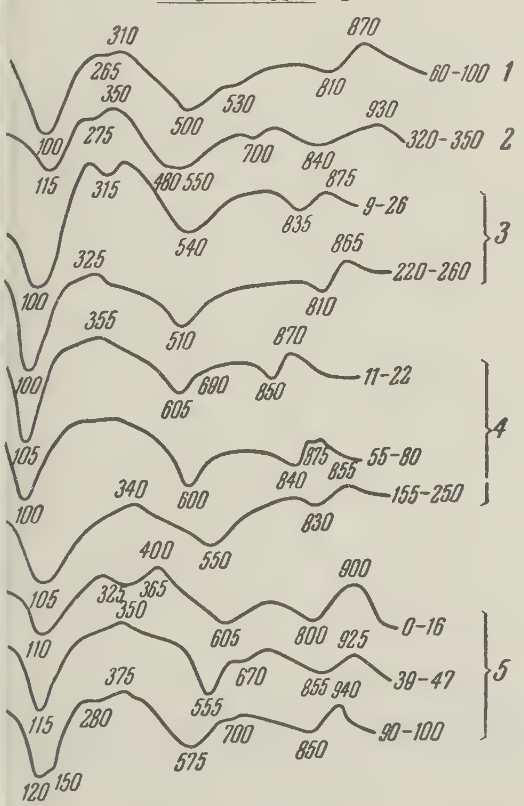


FIGURE 1. Thermogram of the fraction under 0.001 mm (Mugan steppe).
1--red clay of Araxes, 2--altered clay of Araxes, 3--section 624, 4--section 631, 5--section 100K.

The red clay of the Araxes area (Dzhafarkhan) at a depth of 60 to 100 cm and 320 to 350 cm consists largely of beidellite mixed with lesser amounts of montmorillonite and trivalent oxides.

In the altered clay of the Araxes area (section 624), beidellite dominates in light-gray soils of a meadow salt marsh on the young sediments of the Araxes river, and trivalent oxides are present in smaller amounts; organic substances also occur in small quantities at a depth of 9 to 25 cm.

In section 631, beidellite predominates in light-gray soils of a meadow salt marsh on young sediments of the Araxes.

In section 100K, beidellite predominates in the soils of a meadow salt marsh on the delta of the Bolgarchay, and trivalent oxides are present, while montmorillonite is admixed in small amounts. All samples contain small amounts of amorphous substances.

Milsk Steppe (fig. 2)

In section 877, beidellite predominates in red clays of Araxes at depths of 245 to 260 cm.

In section 822, beidellite predominates in red clays of Araxes at depths of 265 to 330 cm, and montmorillonite is present in small amounts.

In section 928, beidellite predominates in the brown-gray clay of Araxes at depths of 10 to 20 cm and from 180 to 200 cm, and montmorillonite, trivalent oxides, and organic substances are present in small amounts.

In section 936, beidellite predominates from the surface to depths of 7 cm in soils of a meadow salt marsh passing into steppe and is contaminated with hydromicas at depths of 16 to 32 cm; beidellite predominates at depths of 77 to 125 cm, and montmorillonite and trivalent oxides are present in small amounts.

In section 948, in gray-brown soils on an irrigated secondarily salty field, beidellite predominates at depths of 0 to 18, 54 to 74, 74 to 106, and 146 to 180 cm, and mica, hydromica, and trivalent oxides are present in small amounts in all four samples.

In section 805/19, in gray-brown soils on a heavily salty remnant of a meadow covering a diluvial mantle, beidellite predominates at depths of 0 to 5, 5 to 20, 110 to 132, and 132 to 150 cm, and muscovite or beidellized hydromica occur as contaminations; at depth of 132 to 150 cm, trivalent oxides are also present.

In section 776, in gray-brown, slightly salty soils of a meadow, beidellite dominates at depths of 3 to 16, 52 to 72, and 135 to 160 cm and is contaminated by mica or hydromica; at a depth of 3 to 16 and 135 to 150 cm, amorphous trivalent oxides are also present in small

amounts. Other amorphous substances are present everywhere.

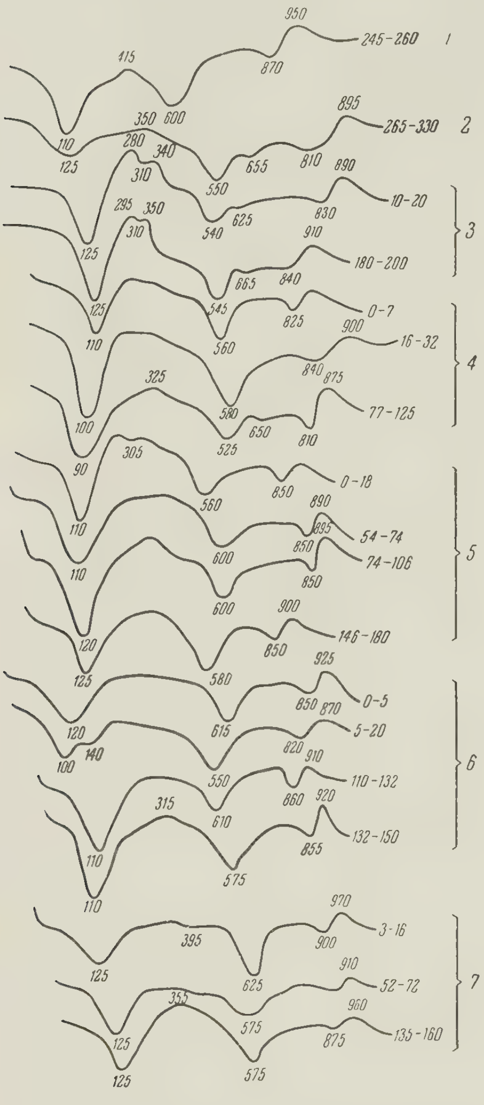

FIGURE 2. Thermogram of the fraction under 0.001 mm (Milsk steppe),
1--section 877, 2--section 822, 3--section 928, 4--section 936, 5--section 948, 6--section 805/19, 7--section 776.

Shirvan Steppe (fig. 3)

In section 174, in alluvial meadow soils on alluvial sediments of the Kura river, beidellized mica predominates at depths of 15 to 25, 210 to 252, and 294 to 336 cm and is contaminated by beidellite, hydrophilic colloids, and crystalline hydroxides of trivalent elements.

In section 180,. in irrigated soils of recent sediments of the Kura river overlying recent sediments of the Araxes river, beidellized hydromica predominates at a depth of 140 to 160 cm and is contaminated by beidellite and hydroxides of trivalent elements.

In section 70, in old diluvial hill sediments, beidellized mica predominates at depths of 20 to 36 and 614 to 660 cm and is contaminated by hydrophilic amorphous colloids.

In section 18, consisting of Tertiary clays, beidellized hydromica predominates at a depth of 0 to 20 cm and is contaminated by trivalent oxides.

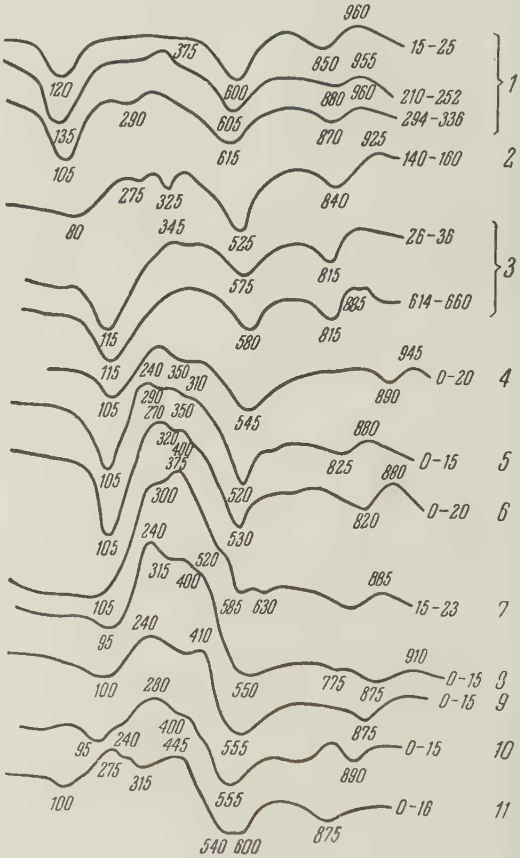

FIGURE 3. Thermogram of the fraction under 0.001 mm (Shirvan steppe).
1--section 174, 2--section 180, 3--section 70, 4--section 18, 5--section 22a, 6--section 22b, 7--section 14, 8--section 11, 9--section 11a, 10--section 11b, 11-section 10.

In section 22a, in gray-brown heavily loamy and slightly crusted soils, beidellite dominates at a depth of 0 to 15 cm and is contaminated by hydromica and amorphous colloids.

In section 22b, in a weakly developed crust at a depth of 0 to 18 cm, beidellite is present along with small amounts of hydromica, organic colloids, and trivalent oxides.

In section 14, in soils of a meadow salt marsh

on alluvial-proluvial sediments, and on a weakly developed crust (3 to 4 grade), beidellized hydromica predominates and is contaminated by trivalent hydroxides.

In section 11, in soils of an irrigated meadow on heavy alluvial-proluvial sediments and a medium-developed crust (5 to 6 grade), beidellized hydromica predominates at a depth of 0 to 15 cm and is contaminated by organic substances and trivalent oxides.

In section 11a, in a medium-developed crust at a depth of 0 to 15 cm, beidellized hydromica predominates and is contaminated by organic substances.

In section 11b, in a strongly developed crust at a depth of 0 to 15 cm, beidellized hydromica predominates and is contaminated by organic substances and small amounts of trivalent oxides and possibly mica.

In section 10, in soils of an irrigated meadow on alluvial-proluvial sediments and a hard crust (9 to 10 grade) at a depth of 0 to 16 cm, beidellized hydromica predominates and is contaminated by trivalent oxides and organic substances.

The curves of heating of the crust-building soils and clays of the Kura-Araxes lowland indicate the prevalence of hydromicas in the fraction under 0.001 mm, and a mixture of beidellite and hydromica predominates only in two sections: 22a (0 to 15 cm) and 22b (0 to 18 cm). Amorphous substances are present everywhere.

## Salyan Steppe (fig. 4)

In section 528, in weakly developed soils of a meadow salt marsh on delta-marine (Caspian) sediments, beidellite predominates at depths of 0 to 23, 62 to 111, and 135 to 210 cm and contains substantial amounts of hydrophilic amorphous colloids, possibly small amounts of mica or hydromica, and trivalent oxides at depths of 60 to 111 and 135 to 210 cm.

In section 514, in slightly salty soils of a meadow salt marsh on delta-marine sediments, beidellite predominates at depths of 0 to 12, 88 to 120, and 160 to 300 cm and is possibly contaminated by mica or hydromica.

In the sediments of the former Caspian Sea bottom beidellite predominates at a depth of 50 cm and is contaminated by trivalent oxides and hydrophilic colloids.

## Conclusions

In accordance with the predominating minerals in the fraction under 0.001 mm, the soils of the Kura-Araxes lowland can be divided into two groups. The first group consists of soils of the Mugan, Milsk, and Salyan steppes, in

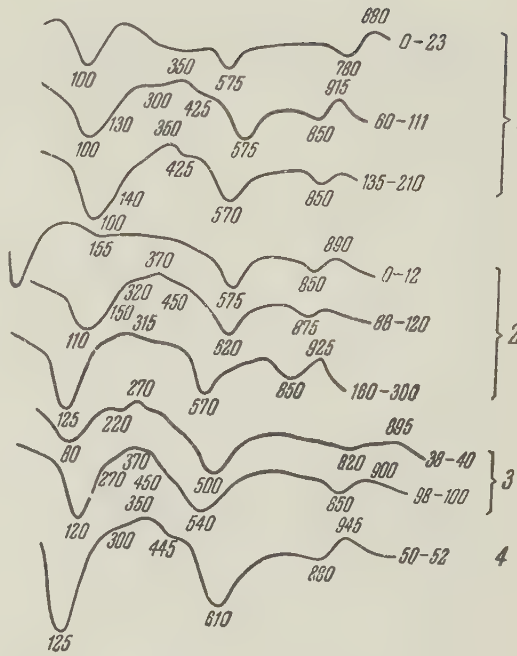


FIGURE 4. Thermogram of the fraction under 0.001 mm (Salyan steppe).
1--section 528, 2--section 514, 3-- bayat, 4--former bottom of the Caspian Sea.

which, in the silt fraction, beidellite predominates. The second group consists of the soils of the Shirvan steppe, in which, in the silt fraction, beidellized mica frequently predominates in the Tertiary clays and diluvial hill sediments.

## The River-bottom Sediments in the Kura-Araxes Lowland (fig. 5)

The curves of heating disclose that beidellite or beidellized mica, depending on the location of the samples concerned, are the principal minerals in the silt fraction of the bottom sediments in the Kura-Araxes lowland. For instance, in the sediments of the Kura river in the region of Ali-Bayramly and in those of the Araxes river in the region of Zhdanovsk, a higher content of beidellite is evident. Besides, there is an admixture of thermically indifferent and amorphous substances.

The prevalence of beidellite or beidellized hydromica depends on the intensity of the weathering of primary minerals and the speed of the river's flow, on which turbulence and transportation of minerals depend. Both minerals are apparently formed of primary minerals, but, because of the greater dispersion of the hydrophilic beidellite, it predominates in the fraction under 0.001 mm. Beidellized hydromica changes its dispersity according to the intensity of the weathering of micas or other primary minerals. Hydromica may be deposited at the bottom earlier than beidellite,

provided the streams are not rapid. In the case of river floods, beidellite becomes deposited farther from the river beds in basins, while micas and hydromicas remain near the river beds, since they sink to the bottom sooner than beidellite or montmorillonite.

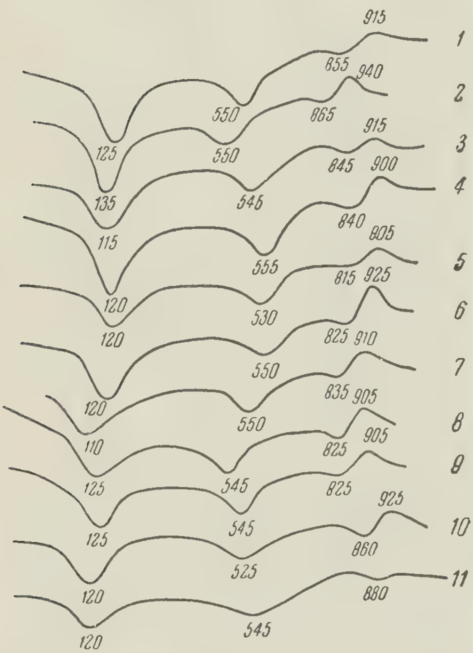


FIGURE 5. Thermogram of the fraction under 0.001 mm extracted from the bottom sediments of the Kura river and its tributaries.

1--the upper Kura river; 2,3,4--middle Kura river; 5--the lower Kura river; 6--the middle Araxes; 7,8,9--the lower Araxes; 10--the lower Iori; 11--the lower Alazan.

## River Suspensions in Azerbaidzhan and in the Terek River (fig. 6)

In the suspension of the Iori river (Samukh), beidellite predominates; trivalent oxides and hydrophilic colloids are also present.

In the suspension of the Alazani river (Samukh), beidellite predominates; hydrophilic colloids are admixed.

In the suspension of the Kura river (Samukh), hydromica and hydrophilic amorphous substances predominate.

In the suspension of the Kura river (Yevlakh), beidellized hydromica predominates; hydrophilic colloids are admixed.

In the suspension of the Kura river, beidellite is present; hydromicas, amorphous substances, and hydrargillite are admixed.

In the suspension of the Kura river (Ali-Bayramly), beidellite contaminated by hydromica predominates; hydrophilic colloids and goethite are admixed.

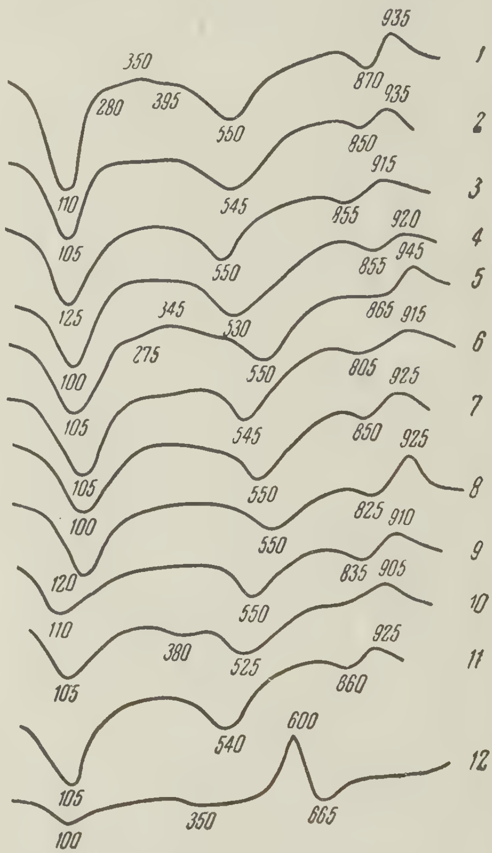


FIGURE 6. Thermogram of the fraction under 0.001 mm extracted from suspensions of the Kura river and its tributaries.

1--Iori, 2--Alazan, 3--Kura (Zardob), 4--Kura (yevlakh), 5--Kura (Zardob), 6--Kura (Ali-Bayramly), 7--Kura (Salyan), 8--Araxes (Zhdanovsk), 9--Araxes (Imishli), 10--Araxes (Saatly), 11--Kura (Sabirabad), 12--Terek.

In the suspension of the Kura river (Salyan), beidellite predominates.

In the suspension of the Araxes (Zhdanovsk), beidellite predominates.

In the suspension of Araxes (Imishli), beidellite predominates.

In the suspension of Araxes (Saatly), a transitional mineral between beidellite and hydromica predominates, trivalent oxides (endothermic peak at $380^{\circ}$ C) and amorphous hydrophilic colloids are admixed.

In the suspension of the Kura river (Sabirabad), beidellite predominates; amorphous hydrophilic substances are admixed.

In the suspension of the Terek river, beidellized hydromica predominates; small amounts of goethite (endothermic stop at 350°C) and organic substances are present.

The study of the curves of heating of river suspensions in Azerbaidzhan and the Terek river permits us to establish the prevalence of the following minerals: beidellite; a mixture of beidellite, hydromica, and amorphous substances; and in some cases trivalent oxides.

Now let us review the results of X-ray studies of the silt fraction of soils, sediments, and river suspensions. In tables 5, 6, and 7 the interpretation of the X-ray diagrams is given. The data shows that all the samples consist principally of minerals of the montmorillonite group. This group includes beidellite and, partially, beidellized mica. Thus the X-ray data confirm the results of the thermal studies. The other clay minerals are present in small amounts. The content of the highly dispersed quartz does not exceed 7 percent. If we take into account the fact that quartz is a very stable mineral and its amount is substantial, we have to assume an intensive destruction of coarse quartz grains under the conditions existing in the Kura-Araxes lowland. The presence of transitional minerals, such as hydromica and illite indicates weathering of the primary minerals (micas and feldspars) from which they can be derived. Substantial amounts of amorphous substances which could not be determined by X-ray studies indicate weathering of secondary and primary minerals to such an extent that they became highly dispersed. The amorphous substances must inevitably be assumed because the sum of the determined minerals is less than 100 percent. The amorphous substances occur in especially great amounts in river suspensions in which decomposition of the crystalline clay minerals is more intensive because of the constant influence of water.

TABLE 5. Mineral composition of the silt fraction of soils in the Kura-Araxes lowland (according to X-ray data)

| Section Number | Soil Type | Depth of Samples (cm) | Fraction under 0.001 mm(%) | Mineral Content (%) | | |
|---|---|---|---|---|---|---|
| | | | | Montmorillonite group (beidellite) | Micas and Hydromicas | Quartz |
| MUGAN STEPPE | | | | | | |
| | Red clay of Araxes (Dzhafarkhan) | 60-100 | 69.2 | 50 | 15 | 2 |
| | Altered clay of Araxes | 320-350 | 63.9 | 50 | 15 | 2 |
| 624 | Light-gray soil of a meadow salt marsh on the sediments of Araxes: | 9-26 | 58.5 | 40 | 15 | 3 |
| | Young sediments of Araxes | 26-52 | 63.0 | 50 | 15 | 5 |
| | Soils on recent sediments of Araxes and buried in the 1920's | 52-90 | 65.0 | 40 | 15 | 3 |
| | Old well-packed sediments of Araxes | 220-260 | 61.4 | 50 | 15 | 5 |
| 631 | Light-gray soils of a meadow salt marsh on young sediments of Araxes | 11-22 | 69.0 | 40 | 15 | 2 |
| | | 55-80 | 35.5 | 40 | 15 | 2 |
| | | 155-200 | 53.2 | 40 | 15 | 2 |
| 100K | Soils of a meadow salt marsh on the Bolgar-chay delta | 0-16 | 58.2 | 40 | 10 | 2 |
| | | 39-47 | 63.3 | 40 | 15 | 2 |
| | | 90-100 | 65.2 | 40 | 15 | 2 |
| MILSK STEPPE | | | | | | |
| 928 | Brown-gray clay of Araxes | 180-200 | 54.8 | 50 | 25 | 3 |
| 936 | Soil of a meadow salt marsh passing into a steppe | 0-7 | 40.8 | 40 | 15 | 3 |
| | | 16-32 | 43.7 | 50 | 15 | 2 |
| | | 77-125 | 36.5 | 40 | 15 | 2 |
| 948 | Gray-brown soil, irrigated, secondarily salty | 0-18 | 49.7 | 50 | 15 | 3 |
| | | 54-74 | 59.5 | 40 | 15 | 2 |
| | | 74-106 | 62.5 | 40 | 15 | 2 |
| | | 146-180 | 50.6 | 40 | 15 | 2 |
| 805/19 | Gray-brown soil, strongly salty, remnant of a meadow on a diluvial mantle | 0-5 | 37.1 | 40 | 15 | 2 |
| | | 5-20 | 49.7 | 40 | 15 | 3 |
| | | 110-132 | 34.4 | 40 | 15 | 5 |
| | | 132-159 | 38.8 | 40 | 15 | 3 |

TABLE 5. Mineral composition of the silt fraction of soils in the Kura-Araxes lowland (Concluded)

| Section Number | Soil Type | Depth of Samples (cm) | Fraction under 0.001 mm(%) | Mineral Content (%) | | |
|---|---|---|---|---|---|---|
| | | | | Montmorillonite group (beidellite) | Micas and Hydromicas | Quartz |
| SHIRVAN STEPPE | | | | | | |
| 180 | Soils on the irrigated present sediments of the Kura river overlying those of Araxes | 0-12<br>33-53<br>120-140<br>140-160 | 35.6<br>42.0<br>62.0<br>58.3 | 40<br>40<br>50<br>50 | 15<br>15<br>15<br>15 | 5<br>5<br>5<br>6 |
| 70 | Old diluvial hill sediments | 20-36 | 70.2 | 50 | 15 | 5 |
| 174 | Alluvial meadow soils on the present Kura sediments | 15-25<br>40-252<br>294-336<br>336-378 | 39.1<br>41.4<br>53.8<br>51.1 | 40<br>40<br>40<br>40 | 15<br>15<br>15<br>15 | 6<br>6<br>6<br>6 |
| 22 | Gray-brown heavily loamy soil, slightly crusted (1-2 grade) | 0-16 | 48.4 | 65 | 15 | 3 |
| 18 | Tertiary clay | 0-20 | 63.6 | 35 | 40 | 2 |
| 14 | Soil of a meadow salt marsh on alluvial-proluvial sediments slightly crusted (3-4 grade) | 0-15 | 41.0 | 45 | 15 | 3 |
| 11 | Soil of an irrigated meadow on heavy alluvial-proluvial sediments, medium crusted (5-6 grade) | 0-15 | 38.4 | 40 | 20 | 5 |
| 10 | Soil of an irrigated meadow on alluvial-proluvial sediments, strongly crusted (9-10 grade) | 0-16 | 57.7 | 40 | 20 | 5 |
| SALYAN STEPPE | | | | | | |
| 528 | Soil of a meadow salt marsh weakly developed on delta-marine (Caspian) sediments | 0-23<br>60-111<br>135-212 | 46.5<br>60.0<br>37.6 | 40<br>40<br>40 | 20<br>20<br>20 | 3<br>3<br>3 |
| 514 | Slightly salty soil of a meadow salt marsh on delta-marine sediments of the Caspian Sea | 0-12<br>88-120<br>160-300 | 37.1<br>53.3<br>26.0 | 40<br>50<br>40 | 20<br>20<br>20 | 5<br>5<br>5 |

TABLE 6. Mineral composition of the silt fraction of river suspensions in the Kura-Araxes lowland (according to X-ray data)

| Location of Samples | Fraction under 0.001 mm(%) | Mineral Content (%) | | |
|---|---|---|---|---|
| | | Montmorillonite group (beidellite) | Hydromicas and Micas | Quartz |
| Samples of June 1950 | | | | |
| Iori (Samukh) | 57.9 | 25 | 15 | 6 |
| Alazani (Samukh) | 55.6 | 25 | 15 | 6 |
| Kura (Samukh) | 51.5 | 30 | 15 | 6 |
| Kura (Sabirabad) | 47.8 | 20 | 10 | 2 |
| Kura (Yevlakh) | 45.5 | 25 | 10 | 6 |
| Kura (Zardob) | 48.6 | 20 | 10 | 2 |
| Kura (Mollakend) | 52.3 | 20 | 10 | 2 |
| Kura (Ali-Bayramly) | 49.7 | 20 | 10 | 3 |
| Araxes (Zhdanovsk) | 51.1 | 20 | 10 | 2 |
| Araxes (Imishli) | 67.4 | 20 | 10 | 2 |
| Araxes (Saatly) | 52.6 | 20 | 12 | 2 |

TABLE 7. Mineral composition of the silt fraction of river sediments in the Kura-Araxes lowland and the Terek river (according to X-ray data)

| Location of Samples | Fraction under 0.001 mm(%) | Mineral Content (%) | | |
|---|---|---|---|---|
| | | Montmorillonite group (beidellite) | Hydromicas and Micas | Quartz |
| Kura (Samukh) | 26.0 | 20 | trace | 2 |
| Kura (Yevlakh) | 23.4 | 20 | trace | 2 |
| Kura (Zardob) | 36.2 | 25 | trace | 3 |
| Kura (Ali-Bayramly) | 40.0 | 20 | trace | 2 |
| Kura (Salyan) | 26.1 | 20 | trace | 2 |
| Araxes (Zhdanovsk) | 24.9 | 20 | trace | 2 |
| Araxes (Sabirabad) | 27.3 | 25 | trace | 2 |
| Terek (Kazbek) | 3.2 | 20 | trace | 5 |

## Electron Microscope Studies

We took electron microscope pictures, enlarged 5,000 times, of the fraction under 0.001 mm in order to study the red clay of Araxes and gray sediments of the Kura river more thoroughly.

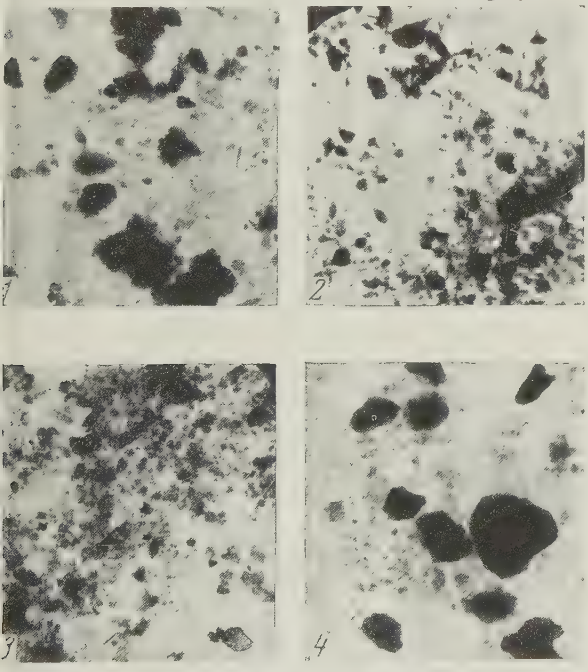

FIGURE 7. Electron microscopic films of river sediments and rocks (enlargement 5,000).
1--the clay of Araxes (Dzhafarkhan), depth 60 to 100 cm; 2--the present sediments of Araxes (section 180, depth 120 to 140 cm); 3--the present sediments of the Kura river (section 180, depth 140 to 160 cm; 4--Tertiary clay.

Figure 7 shows these pictures. In figures 7-1 (altered clay of Araxes), we see a number of coarse-grained aggregates and a small amount of fine colloidal particles. The large particles in the picture are not fragments of minerals but aggregates, since they have various forms, fractures, and corroded and sometimes costal edges. The aggregate structures of these particles are formed, we believe, by partially crystallized minerals of iron and aluminum. These minerals apparently have a partially crystalline structure and are partially a hardened gel of trivalent oxides. The films of crystallized and hardened oxides of trivalent elements protect the soil aggregates from being disintegrated in water.

The present sediments of the Araxes and Kura rivers (figs. 7-2 and 7-3) contain less amounts of large aggregates and substantially greater amounts of fine colloidal and pre-colloidal substances. Obviously, during the redeposition of silt particles from water, the aggregates become corroded and mixed with the Kura sediments, which do not have films of iron and aluminum oxide. A comparison of the sediments of the Araxes and Kura rivers shows that the clay of Araxes (fig. 7-1) has a greater number of micro-aggregates than the present sediments of the Kura and Araxes rivers (figs. 7-2 and 7-3). The latter sediments are very close to each other with respect to their physical composition, the first sample contains 62 percent of the fraction under 0.001 mm, the second 58.3 percent. The samples have equal maximum hygroscopic capacities because of their high dispersity and the predominating amounts of beidellite and beidellized hydromica; the hygroscopic capacity of the Araxes sediments is 21.7 percent and that of the Kura river 20.8 percent.

As can be seen in the electron microscope photograph (fig. 7-4), the Tertiary clay contains a large number of coarse-grained particles and essential amounts of colloidal substances. Coarse particles are fragments of mica, not aggregates, as can be assumed because of the sharp edges and the absence of fractures.

The X-ray studies also disclosed great amounts of mica in Tertiary clays. According to the thermal studies, beidellized mica predominates in these clays. The low maximum of hygroscopic capacity (5.5 percent), despite the high content of particles under 0.001 mm, indicates that hydrophobic minerals such as mica or hydromica, not yet altered to beidellite, predominate.

TABLE 8. Total analysis of particles under 0.001 millimeter extracted from soils and sediments of the Kura-Araxes lowland (% dry-sample weight)

| Section Number | Soil | Depth of Samples | Fraction under 0.001 mm(%) | Hygroscopic water | Humus | Loss by annealing | $SiO_2$ | $R_2O_3$ | $Fe_2O_3$ | $Al_2O_3$ | CaO | MgO | MnO | $\frac{SiO_2}{R_2O_3}$ |
|---|---|---|---|---|---|---|---|---|---|---|---|---|---|---|
| | MUGAN STEPPE | | | | | | | | | | | | | |
| | Red clay of Araxes (Dzhafarkhan) | 60-100 | 69.2 | 6.02 | 3.88 | 11.67 | 44.21 | 32.97 | 12.98 | 19.99 | 0.79 | 1.41 | - | 2.70 |
| | Altered clay of Araxes (Dzhafarkhan) | 320-350 | 63.9 | 2.13 | 4.35 | 11.57 | 41.87 | 41.91 | 14.05 | 27.86 | 0.65 | 1.03 | - | 1.94 |
| 624 | Light-gray soil of a meadow salt marsh on the sediments of Araxes: | | | | | | | | | | | | | |
| | Young sediments of Araxes | 9-26 | 58.5 | 5.91 | 1.89 | 10.95 | 49.77 | 29.61 | 12.64 | 16.97 | 0.26 | 3.23 | - | 3.37 |
| | | 26-52 | 63.0 | 5.89 | 1.77 | 10.76 | 49.66 | 29.21 | 11.70 | 17.51 | 0.79 | 4.63 | - | 3.40 |
| | Soils on recent sediments of Araxes, buried in the 1920's | 52-90 | 65.0 | 6.15 | 1.47 | 10.83 | 51.06 | 25.91 | 9.25 | 16.66 | 1.01 | 4.0 | - | 3.86 |
| | Old well-packed sediments of Araxes | 220-260 | 61.4 | 6.42 | 1.00 | 10.19 | 49.22 | 30.76 | 9.74 | 21.02 | 0.69 | 2.76 | - | 3.15 |
| 631 | Light-gray soils of a meadow salt marsh on young sediments of Araxes | 11-22 | 69.0 | 12.20 | 0.91 | 8.30 | 49.55 | 31.16 | 12.01 | 19.15 | 0.94 | 0.73 | None | 3.16 |
| | | 155-250 | 53.2 | 8.90 | 2.40 | 9.84 | 47.20 | 32.44 | 11.36 | 21.08 | 1.05 | 2.18 | None | 2.84 |
| 100K | Soils of a meadow salt marsh on the Bolgarchay delta | 0-16 | 58.2 | 6.07 | 1.69 | 8.63 | 46.33 | 34.94 | 14.15 | 20.79 | 1.05 | 2.50 | 0.1 | 2.65 |
| | | 90-100 | 65.2 | 8.77 | 0.25 | 7.11 | 49.04 | 34.00 | 10.85 | 23.15 | 0.82 | 2.54 | 0.1 | 2.77 |
| | MILSK STEPPE | | | | | | | | | | | | | |
| 936 | Soil of a meadow salt marsh passing into a steppe | 0-7 | 40.79 | 8.60 | 2.44 | 9.11 | 49.71 | 27.91 | 10.24 | 17.07 | 0.66 | 3.95 | 0.006 | 3.64 |
| | | 77-124 | 36.47 | 11.15 | 0.98 | 7.24 | 50.70 | 30.00 | 10.66 | 19.34 | 0.86 | 1.82 | 0.005 | 3.33 |
| 948 | Gray-brown soil, irrigated, secondarily salty | 0-18 | 49.7 | 10.15 | 2.00 | 8.24 | 51.42 | 28.00 | 11.59 | 16.41 | 0.50 | 3.83 | 0.003 | 3.79 |
| | | 146-180 | 50.6 | 9.27 | 1.09 | 11.32 | 50.18 | 30.20 | 10.55 | 19.65 | 0.57 | 2.20 | 0.003 | 3.20 |
| 805/19 | Gray-brown soil, strongly salty, remnant of a meadow on a diluvial mantle | 0-5 | 37.1 | 8.82 | 2.60 | 10.09 | 50.22 | 30.98 | 11.01 | 19.97 | 0.86 | 4.10 | 0.005 | 3.08 |
| | | 132-159 | 38.8 | 7.50 | 0.73 | 9.14 | 46.33 | 34.84 | 11.44 | 23.40 | 0.80 | 3.44 | 0.006 | 2.66 |
| 928 | Brown-gray clay of Araxes | 180-200 | 38.4 | 3.73 | 2.96 | 11.60 | 48.47 | 26.94 | 12.44 | 14.50 | 2.50 | 3.05 | None | 3.66 |

| | | | | | | | | | | | | | |
|---|---|---|---|---|---|---|---|---|---|---|---|---|---|
| **SHIRVAN STEPPE** | | | | | | | | | | | | | |
| 180 | Soils on the irrigated present sediments of the Kura river overlying those of Araxes | 0-12 | 35.6 | 5.51 | 3.56 | 12.95 | 45.50 | 32.34 | 10.61 | 21.73 | 0.83 | 3.84 | None | 2.73 |
| | | 33-53 | 42.0 | 3.09 | 2.70 | 18.71 | 45.94 | 28.40 | 10.86 | 17.54 | 0.50 | 2.65 | None | 3.20 |
| | | 120-140 | 62.0 | 4.50 | 0.93 | 12.23 | 48.10 | 31.30 | 11.31 | 19.99 | 0.41 | 4.45 | 0.08 | 3.0 |
| | | 140-160 | 58.3 | 5.04 | 1.70 | 11.20 | 48.26 | 31.72 | 7.68 | 24.04 | 0.45 | 3.72 | 0.03 | 3.0 |
| 70 | Old diluvial hill sediments | 20-36 | 70.24 | 8.68 | None | 7.78 | 50.89 | 30.53 | 7.22 | 23.31 | 1.55 | 1.54 | 0.04 | 3.10 |
| 174 | Soils of an alluvial meadow on the present Kura sediments | 336-378 | 51.13 | 8.32 | 3.48 | 7.71 | 47.14 | 34.05 | 7.61 | 26.44 | 1.86 | 2.18 | None | 2.56 |
| 22 | Gray-brown heavily loamy soil, slightly crusted (1-2 grade) | 0-16 | 48.4 | 7.68 | 2.30 | 9.65 | 43.38 | 34.06 | 10.47 | 23.59 | 0.62 | 3.98 | 0.07 | 2.44 |
| 18 | Tertiary clay | 0-20 | 63.6 | 3.01 | 0.48 | 4.97 | 51.04 | 38.03 | 7.50 | 30.53 | 0.34 | 3.62 | 0.03 | 2.53 |
| 14 | Soil of a meadow salt marsh on alluvial-proluvial sediments, slightly crusted (3-4 grade) | 0-15 | 41.0 | 3.30 | 11.55 | 9.89 | 44.58 | 30.52 | 9.16 | 20.36 | 0.51 | 3.88 | 0.07 | 2.90 |
| 11 | Soil of an irrigated meadow on heavy alluvial-proluvial sediments, medium crusted (5-6 grade) | 0-15 | 46.0 | 2.97 | 5.02 | 8.59 | 47.16 | 31.84 | 8.27 | 23.57 | 0.28 | 3.11 | 0.04 | 2.78 |
| 10 | Soil of an irrigated meadow on alluvial-proluvial sediments, strongly crusted (9-10 grade) | 0-16 | 57.7 | 2.57 | 4.08 | 9.13 | 47.09 | 30.21 | 7.78 | 22.43 | 0.66 | 3.50 | 0.03 | 2.94 |
| **SALYAN STEPPE** | | | | | | | | | | | | | |
| 528 | Soil of a meadow salt marsh, weakly developed on delta-marine (Caspian) sediments | 0-23 | 46.5 | 9.03 | 1.04 | 10.52 | 50.40 | 32.66 | 8.35 | 24.31 | 1.27 | 2.41 | None | 2.89 |
| | | 135-210 | 37.6 | 8.53 | None | 8.91 | 50.94 | 33.64 | 12.23 | 21.41 | 1.28 | 2.79 | Trace | 2.96 |
| 514 | Slightly salty soil of a meadow salt marsh on delta-marine sediments of the Caspian Sea | 0-12 | 43.27 | 8.32 | 2.88 | 9.82 | 50.55 | 31.30 | 10.00 | 21.30 | 0.66 | 2.24 | 0.005 | 3.12 |
| | | 160-300 | 26.01 | 7.76 | 2.00 | 8.71 | 47.28 | 32.80 | 13.32 | 19.48 | 0.71 | 1.95 | 0.003 | 2.90 |

Remarks: The samples of the sections 624, 180, 528, 514, and those of the clays of Araxes were assayed by I. G. Tsyurupa; and those from sections 631, 100K, 936, 948, 805/19, and 928 by Z. I. Gerasimovich; and the remainder by A. A. Budakova.

## The Regularities in the Mineral Composition of the Silt Fraction of Soils And Sediments in the Kura-Araxes Lowland

The thermal studies and X-ray data permit us to make the following conclusions:

1. The silt fraction of soils and river sediments in the Kura-Araxes lowland consist principally of crystalline clay minerals. The river suspensions contain amorphous substances and highly dispersed minerals along with the above crystalline minerals.

2. The silt fraction of soils and sediments in the Kura-Araxes lowland contains beidellite, hydromica (beidellized hydromica), mica, and quartz, in that order. Hydromica predominates in some samples (soils of Shirvan, Tertiary clay, etc.). In some samples, trivalent oxides (apparently goethite, hydrogoethite, hydrargillite) were found.

Each of these minerals, in one way or another, affects the properties of soils and to a certain degree indicates the type of weathering of primary minerals. Since quartz occurs in small amounts, it does not affect the properties of soils substantially. However, its presence in the silt fraction indicates intensive destruction of large quartz grains due to cracking.

The high hydromica (beidellized hydromica) content also indicates weathering of primary minerals, including micas. As a general rule, micas and hydromicas contain potassium, and the soils consequently become rich in potassium and in highly dispersed particles.

Beidellite--as the most dispersed mineral, along with amorphous colloids and hydromicas, makes the soils hydrophilic, viscous, capable of swelling, and contributes to the soils' capacity to adsorb great amounts of water. Beidellite, amorphous substances, and hydromicas also make the soils cohesive and relatively impermeable.

The combination of beidellite, hydromicas, amorphous colloids, and coarse-grained minerals such as quartz, mica, feldspar, and carbonates makes the soils very hard after becoming dry.

Organic substances, if they occur along with beidellite, are retained strongly by the latter, for they penetrate its crystal structure, filling the spaces between its sheets.

3. The red clays of Araxes have aggregates and micro-aggregates enveloped in films of crystalline iron oxides (goethite). These films produce the structure of the soils and sediments on which the former develop and prevent the disintegration of aggregates and the formation of hard crusts in dry soils.

4. Unlike the clays of Araxes, the Tertiary clays and the soils formed upon them and intermixed with them do not have films of crystalline iron oxides and consequently do not have any structure. Therefore, when irrigated, they become mud. These soils form the thickest hard crusts.

The silt fraction extracted from Tertiary clays differs sharply from that of soils and river suspensions because of its high mica content, which causes the maximum hygroscopic capacity to drop (5.52 percent).

### CHEMICAL COMPOSITION OF THE SILT FRACTION OF SOILS, SEDIMENTS, AND RIVER SUSPENSIONS IN THE KURA-ARAXES LOWLAND

The chemical composition of the silt fraction permits us to clarify the latter's mineral composition determined by thermal and X-ray methods.

First we studied the chemical composition of the silt fraction of soils and river suspensions on three samples after their dispersity, mineral composition, and other properties had been examined.

The ratio $SiO_2$:$R_2O_3$ is one of the most important chemical indicators that help us to clarify the mineral composition. In the case of montmorillonite, this ratio is 4:1, in beidellite about 3:1, and in the minerals of the kaolinite group 2:1. The data compiled in tables 8 and 9 show that this ratio in many cases is close to 3:1. This indicates the prevalence of beidellite in the fraction under 0.001 mm. The decrease of this ratio may be explained by the presence of admixed kaolinite and hydromicas, and its increase by admixed montmorillonite or amorphous colloids rich in silica. This assumption is most likely true in the case of river suspensions which, according to X-ray studies, contain large amounts of noncrystalline substances.

The amount of trivalent oxides in the fractions extracted from soils is 30 percent or less, and in those extracted from river suspensions it is a little higher.

The amount of aluminum is about 20 percent in the majority of samples. However, it ranges from 16.41 percent (gray-brown irrigated soils of section 948) to 27.86 percent (altered clay of Araxes). The clays and soils of Araxes formed upon the sediments brought in from the Little Caucasian Mountains usually contain lesser amounts of aluminum than do soils formed upon the sediments brought in from the spurs of the Great Caucasian Mountains.

The iron content decreases with increasing

TABLE 9. Total analysis of the fraction under 0.001 millimeter extracted from river suspensions of the Kura-Araxes lowland (% of dry-sample weight)

| Location of Samples | Fraction under 0.001 mm(%) | Hygroscopic water | Loss by Annealing | $SiO_2$ | $R_2O_3$ | $Fe_2O_3$ | $Al_2O_3$ | CaO | MgO | MnO | $\frac{SiO_2}{R_2O_3}$ |
|---|---|---|---|---|---|---|---|---|---|---|---|
| Samples of June 1950 | | | | | | | | | | | |
| Iori (Samukh) | 57.9 | 8.04 | 8.30 | 51.20 | 28.40 | 8.58 | 19.82 | 0.40 | 0.23 | trace | 3.45 |
| Alazani (Samukh) | 55.6 | 7.80 | 7.22 | 53.10 | 28.40 | 7.93 | 20.47 | 0.50 | 0.63 | trace | 3.54 |
| Kura (Samukh) | 51.5 | 10.79 | 11.70 | 50.52 | 27.50 | 9.04 | 18.46 | 0.69 | 0.55 | trace | 3.50 |
| Kura (Sabirabad) | 47.8 | 8.88 | 9.00 | 51.32 | 27.60 | 8.58 | 19.02 | 0.40 | 0.28 | trace | 3.57 |
| Kura (Yevlakh) | 45.9 | 7.65 | 10.70 | 51.72 | 28.00 | 8.94 | 19.06 | 0.41 | 0.28 | trace | 3.54 |
| Kura (Zardob) | 48.6 | 8.27 | 9.36 | 51.68 | 28.40 | 8.58 | 19.82 | 0.64 | 1.49 | trace | 3.50 |
| Kura (Ali-Bayramly) | 47.9 | 8.52 | 9.54 | 49.98 | 31.49 | 8.96 | 22.53 | 0.64 | 0.20 | trace | 3.0 |
| Kura (Salyan) | 49.3 | 8.66 | 9.03 | 50.94 | 30.00 | 9.02 | 20.98 | 0.48 | 0.89 | trace | 4.02 |
| Araxes (Saatly) | 52.6 | 6.28 | 8.7 | 53.44 | 27.30 | 9.00 | 18.30 | 1.57 | 2.40 | trace | 3.77 |
| Araxes (Zhdanovsk) | 51.1 | 9.15 | 11.70 | 49.34 | 28.00 | 9.21 | 18.79 | 0.82 | 0.41 | trace | 3.36 |

amounts of aluminum. In river suspensions, the fraction under 0.001 mm contains smaller amounts of aluminum than do soils.

A slight increase of silica and a decrease of trivalent oxides in the fraction under 0.001 mm of river suspensions leads to a decrease in the ration $SiO_2$:$R_2O_3$ [sic. "increase of ratio"?] compared with that of soils. This indicates a prevalence of beidellite or amorphous colloids rich in silica in river suspensions. The silt fraction of the altered clays of Araxes contain higher amounts of iron, sometimes reaching 14 percent. This permits us to assume the presence of such minerals as ferribeidellite, hydrogoethite, goethite, and hematite. These minerals occur principally on surfaces of soil colloids and micro-aggregates and cause red or brown coloring in the soil-building sediments.

Soils formed upon clays brought in from the spurs of the Great Caucasian Mountains usually contain smaller amounts of iron in the silt fraction than do soils formed upon clays from the Little Caucasian Mountains. For example, the soils of the Shirvan steppe (also the suspensions of the Kura river) contain less than 10 percent iron in the silt fraction. The soil-building sediments and soils in this region of the Kura-Araxes lowland are gray. This indicates that iron occurs within the crystal structure and that iron on surfaces of colloidal substances and micro-aggregates exists in reducing conditions. The clays of Araxes become gray only in reducing conditions.

The altered clay of Araxes at a depth of 320 to 350 cm is a good illustration of this case. The fraction under 0.001 mm extracted from these clays contains 14.05 percent iron oxides, i.e., more than the other samples. The gray color of these clays indicate, therefore, the presence of ferrous iron on the surface of the particles of the silt fraction. It is interesting to note that aluminum oxide occurs in larger amounts in this sample than in the layer below, at a depth of 60 to 100 cm. This fact permits us to conclude that the alteration of this sample is related not only to reduction of iron from the ferric to the ferrous form, but also to migration of aluminum from higher horizons into lower ones. Consequently, the surfaces of colloids become covered by a film of ferrous iron and aluminum as a result of alteration of soils.

The presence of films of ferric iron alters the properties of the silt fraction and those of the soil as a whole. The micro-aggregates covered by film peptize hardly at all in water and the soils containing them have a structure that cannot be destroyed by water. These soils do not turn into mud or form hard crusts, unlike the soils of the Shirvan steppe, parts of Salyan, and certain regions of Mugan. The films of iron and aluminum hydroxides crystallize by getting dry and wet alternately. This prevents disintegration of micro-aggregates by irrigation.

As far as the calcium and magnesium contents in the silt fraction of soils and river suspensions are concerned, the following peculiarities must be noted. The amount of magnesium sharply predominates over that of calcium in all soils, but in river suspensions the two occur in about equal amounts.

Thus it can be assumed that calcium silicate occurs in minerals that are more easily decomposed and taken out during the soil-building than is magnesium. Both elements become washed out of river suspensions, and consequently their content remains about equal. The amount of manganese is insignificant in all samples.

## THE DEPENDENCE OF SOIL PROPERTIES ON THE MINERAL COMPOSITION IN THE KURA-ARAXES LOWLAND

### The Relationship between the Mineral Composition and Maximum Hygroscopic Capacity

The mineral composition greatly affects the physico-chemical properties of soils. Let us review the most important of these properties in relation to the mineral composition of the fraction under 0. 001 mm extracted from soils and sediments upon which the soils are formed. One of these properties is the capacity to adsorb water. The amount of adsorbed water can be estaimated in accordance with the effects of low temperature on the heating curves (thermograms) of samples. The broader the intervals of temperature under 115°C, the greater the amount of hygroscopic water extracted. The samples with predominating beidellite and amorphous colloids have a greater hygroscopic capacity than those in which beidellized hydromica predominates. The examples illustrating the maximum hygroscopic capacity of the fractions under 0. 001 mm are compiled in table 10.

It is usually believed that the amount of water that cannot be absorbed up by plants is about one and one-half times greater than that of the maximum hygroscopic capacity. Taking this figure as the water-extraction capacity of plants, we can understand that the soils investigated by us contain large amounts of water which cannot be absorbed by plants. It is clear that we have to take this figure into account in estimating the water balance and determining the duration of irrigation.

The high content of beidellite, hydromicas, and highly dispersed colloids, including organic substances, increases the maximum hygroscopic capacity. According to our estimates, the maximum hygroscopic capacity of the fraction under 0. 001 mm in soils of the Kura-Araxes lowland is 20 to 25 percent (table 10). The high content of these minerals therefore indicates large amounts of water not available for plants.

Water, adsorbed or bound to beidellite, is more difficult to evaporate by heating soils than water adsorbed by hydromicas and micas. In the former, the substantial part of the water is within crystals, and its evaporation is prevented by internal walls of the crystals. In hydromicas, and especially in micas, the substantial part of the water occurs on the surface of silt and colloidal particles. This water can more easily be extracted by heating than can water occurring within minerals. The amount of water bound to the surface of minerals also depends on the dispersity of soils, especially of their silt and colloidal particles. Consequently, we have to conclude that both the mineral composition and the dispersity of minerals determine the hydrophilic nature of soils and their capacity to give the adsorbed water to plants.

TABLE 10. Maximum hygroscopic capacity of some soils in the Kura-Araxes lowland

| Section Number | Soil Type | Depth of Samples (cm) | Maximum hygroscopic capacity of the fraction under 0. 001 mm (%) |
|---|---|---|---|
| 624 | Light-gray soil of a meadow salt marsh on the sediments of Araxes: | | |
| | Soils on recent sediments of Araxes and buried in the 1920's | 52-90 | 24. 86 |
| | Old well-packed sediments of Araxes | 220-260 | 24. 80 |
| 180 | Soils on the irrigated recent sediments of the Kura river overlying those of Araxes | 0-12 | 22. 56 |
| | | 120-140 | 21. 74 |
| | | 140-160 | 20. 89 |
| | | 320-350 | 16. 33 |
| 528 | Soil of a meadow salt marsh, weakly developed on delta-marine (Caspian) sediments | 0-23 | 22. 13 |
| 776 | Gray-brown soil of a meadow, slightly salty | 3-16 | 21. 16 |
| 948 | Gray-brown soil, irrigated, secondarily salty | 11-22 | 25. 98 |
| | | 155-250 | 26. 09 |
| 10 | Soil of an irrigated meadow on alluvial-proluvial sediments, heavily crusted (9-10 grade) | 0-16 | 15. 47 |

## The Structure of Soils and the Significance of the Film of Trivalent Oxides

We have previously mentioned films of crystallized minerals of trivalent oxides, particularly iron hydroxides in red sediments of Araxes and in soils formed upon them, and the significance of these films in the formation of structures that cannot be destroyed by water. Our assumption concerning the presence of iron in the ferric form does not arouse any doubt, because of the red-brown color of the

sediments of Araxes. It was necessary, however, to find out experimentally how great the speed of crystallization of trivalent oxides is, particularly that of iron hydroxides.

Z. Ya. Berestneva and V. A. Kargin [2] discovered that the crystallization of sols and $Al(OH)_3$ and other oxides begins within a few days after preparation. Our experiments were dedicated to the study of this process in swollen gels. For this purpose, our laboratory prepared hydrated oxides of aluminum and iron and let them crystallize spontaneously, leaving them untouched for various periods of time. After a certain time they were treated by heating and X-ray methods.

The data of the X-ray studies of these samples and minerals of trivalent oxides is compiled in tables 11 and 12.

The newly prepared hydrated oxide of aluminum did not show rings of interference on the X-ray film, and, therefore, we may consider it as an amorphous substance. The same gel showed several lines of interference (table 11) after one year. This indicated the formation of boehmite and hydrargillite. The examination of the same sample by the thermal method according to E. A. Shurygina confirmed the conclusion based on the X-ray studies.

The crystallization of iron hydroxide takes place even more rapidly (table 12). The newly prepared gel of iron hydroxide showed the lines of interference on the X-ray diagram, and after six months the lines of hematite and goethite were clearly expressed.

Thus, we may conclude that the trivalent oxides crystallize relatively quickly and spontaneously. It is possible, therefore, to assume that the crystallization of iron hydroxide in soils begins as soon as iron gets out of the crystal

TABLE 11. X-ray data on aluminum hydroxide during its crystallization

| Duration of Crystallization | | | | | | | | Temperature of Heating | | | | Standards of Comparison | | | |
|---|---|---|---|---|---|---|---|---|---|---|---|---|---|---|---|
| 1 year | | 2 years | | 3 years | | 4 years | | 60-70°C | | 800°C | | Boehmite | | Hydrargillite | |
| d Å | I | d Å | I | d Å | I | d Å | I | d Å | I | d Å | I | d Å | I | d Å | I |
| 3.17 | 3 | 3.18 | 6 | 3.18 | 5 | 3.18 | 6 | 3.14 | 7 | 3.02 | 2 | 5.79 | 10 | 4.75 | 10 |
| 2.45 | 3 | 2.40 | 10 | 2.35 | 10 | 2.32 | 6 | 2.32 | 8 | 2.78 | 2 | 3.04 | 10 | 4.34 | 9 |
| 1.89 | 5 | 1.88 | 10 | 1.88 | 8 | 1.86 | 8 | 1.86 | 10 | 2.42 | 4 | 2.30 | 10 | 3.34 | 5 |
| - | - | - | - | 1.60 | 1 | 1.61 | 3 | 1.60 | 3 | 2.30 | 3 | 2.04 | 8 | 3.21 | 5 |
| 1.45 | 7 | 1.45 | 7 | 1.45 | 9 | 1.45 | 6 | 1.45 | 10 | 2.19 | 3 | 1.82 | 10 | 2.47 | 8 |
| | | | | | | | | | | 2.01 | 9 | 1.63 | 10 | 2.40 | 8 |
| | | | | | | | | | | 1.55 | 8 | 1.50 | 10 | 1.71 | 9 |
| | | | | | | | | | | 1.41 | 10 | 1.43 | 8 | 1.47 | 9 |

Remark: The X-ray diagram has a great background of darkness. Nearly all the interference lines are broad and diffuse.

TABLE 12. X-ray data on iron hydroxide during crystallization

| Duration of Crystallization | | | | | | Temperature of Heating | | | | | | Standards of Comparison | |
|---|---|---|---|---|---|---|---|---|---|---|---|---|---|
| 2 years | | 4 years | | 10 years | | 40°C | | 350°C | | 1030°C | | Hydrogoethite, Hydrohematite, Goethite | |
| d Å | I | d Å | I | d Å | I | d Å | I | d Å | I | d Å | I | d Å | I |
| 3.30 | 8 | 3.30 | 8 | 3.03 | 5 | 3.31 | 7 | 3.06 | 5 | 2.94 | 5 | 2.92 | 4 |
| 2.87 | 2 | 2.87 | 2 | 2.75 | 10 | 2.84 | 3 | 2.79 | 10 | 2.68 | 10 | 2.69 | 10 |
| 2.55 | 10 | 2.55 | 10 | 2.57 | 10 | 2.58 | 10 | 2.58 | 10 | 2.51 | 10 | 2.45 | 10 |
| 2.32 | 5 | 2.32 | 9 | 2.25 | 8 | 2.31 | 6 | 2.27 | 8 | 2.21 | 7 | 2.19 | 9 |
| 1.98 | 4 | 1.98 | 9 | 1.88 | 9 | 1.97 | 7 | 1.90 | 9 | 1.84 | 10 | 1.82 | 8 |
| 1.79 | 2 | 1.79 | 2 | 1.73 | 10 | 1.77 | 3 | 1.75 | 10 | 1.70 | 10 | 1.72 | 8 |
| 1.65 | 6 | 1.65 | 6 | 1.63 | 8 | 1.67 | 8 | 1.65 | 4 | 1.61 | 5 | 1.61 | 5 |
| - | - | - | - | 1.51 | 9 | 1.53 | 5 | 1.54 | 10 | 1.49 | 10 | 1.49 | 8 |
| 1.54 | 4 | 1.54 | 5 | 1.48 | 10 | 1.50 | 2 | 1.49 | 10 | 1.46 | 10 | 1.46 | 7 |

Remarks: In the table we can see that the distance between the sheets (d Å) decreases with the increasing age of iron hydroxide, and the intensity of the lines of interference thereby increases. Heating speeds up the crystallization and at the same time lessens the water content, and the distance between the sheets (d Å). The crystallization of iron hydroxide leads to the formation of such minerals as hydrogoethite, hydrohematite, and goethite.

structure of primary minerals. It must be assumed that alternate drying and wetting speeds up crystallization [5].

The X-ray diagrams of boehmite and hydrargillite show sharp and narrow lines. The number in the latter is greater than that used in calculations. X-ray diagrams of aluminum hydroxide dehydrated at a temperature of 60°C and kept for various periods of time have a great background of darkness and a few diffuse lines.

The X-ray diagrams of aluminum oxide annealed at a temperature of 800°C has intensive and less diffuse lines than those of aluminum oxide dehydrated and kept for a time. However, there are fewer lines than in the case of boehmite and hydrargillite. It appears that aluminum hydroxide becomes crystallized during storage, dehydration, and annealing, but the crystallization does not reach the same completeness as in the case of boehmite and hydrargillite. Iron hydroxide apparently becomes better crystallized than aluminum hydroxide.

Heating affects oxides of trivalent elements in a similar way. It is known that the curves of heating of trivalent oxides give lines on the X-ray film which indicate the crystallization of the oxides concerned.

Trivalent oxides lose a part of their water during crystallization and become more hydrophobic, and their solubility even in acids decreases sharply.

I. G. Tsyurupa [20] examined the solubility of aluminum and iron hydroxides in acids at different stages of crystallization. In doing so, she established that the solubility changes sharply. Our studies on red soils and red-colored sediments disclosed that only 25 to 30 mgr of iron of a 100-gram soil sample containing 15 g of iron dissolves in 0. 2 normal hydrochloric acid.

It is known that newly prepared iron hydroxide had a substantial solubility in acid. The decrease of solubility may be explained by its structure and crystallization. Consequently, the oxides of trivalent elements not bound to silicates crystallize rapidly and envelope the soil aggregates and microaggregates, which therefore become resistant to disintegration by water and produce the soil structure.

## Swelling of Soils in the Kura-Araxes Lowland and Its Causes

It is known that water becomes adsorbed by soil colloids during irrigation, and the soil becomes swollen and ancreases in volume. Drying out of swollen soil leads to cracking and consequently, the water become irregularly distributed during the next irrigation.

Soil with a great swelling capacity is usually viscous if wet and very hard if dry.

The swelling capacity can be determined by measuring the linear increase of the subject under test, according to the volume of mercury displaced by it or by special apparatus. The type of apparatus we used [3] for our experiments is shown in figure 8. It is used in the following

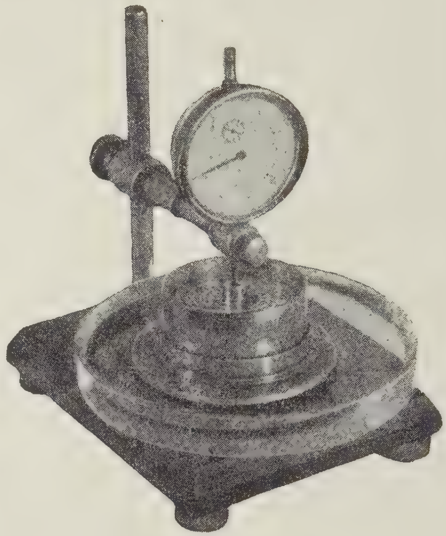

FIGURE 8. A.M. Vasilyev's apparatus for determining the swelling of soils and clays.

way: the soil sample, powdered or in its natural form, must be installed in a metallic ring; the bottom of the ring must be closed by a porous plate (pumice) through which water penetrates to the sample under test; the top of the ring must be covered by a metallic plate with holes through which air from sample can escape; the plate on the top touches the deformation indicator, which, having a dial plate, automatically records the swelling of the sample when the top plate rises. If 1-cm of soil is in the ring, one division of the dial plate means a 0.1 percent volume increase. For our experiments we used soil crushed and strained through a sieve with 1-mm holes.

The swelling of soils or slays is usually not identical with the increase in their volume when they are wet. The volume increase of wet soil depends on several factors, of which the most important are: the dispersity of the soil, the mineral composition of their highly dispersed parts, the composition and amount of the adsorbed bases, the composition and amount of humus, the composition and amount of salts, and finally, the stability of the soil aggregates.

The more colloids, adsorbed monovalent cations, and minerals of the montmorillonite group of soils contain, the more intensively the soils swell. If the soil contains great amounts of salts, they may cause coagulation or even salt

out, which decrease swelling. The stability of aggregates in water, which is related to the quantity and quality of humus and the chemical and mineral composition of soils, substantially affects the volume increase of soils. If the soil aggregates remain stable when wet, the apparatus shows an increase of the volume for two reasons. First, because a real swelling takes place, that is, the distance between the sheets of the crystal structure of clay minerals increase, and water adheres to the surface of hard particles. Second, the volume of the pores increases, for the more the aggregates swell and the more stable they are, the greater the spaces that develop between them. Besides the volume increase is caused by the air, part of which remains in the samples after they are wet.

It is quite different if the soil aggregates are unstable in water. Such aggregates disintegrate and reduce the interaggregate spaces after being made wet. The volume increase in soils is less in this case than in soils with stable aggregates. It is clear that the agricultural significance of the volume increase in structural and nonstructural soils will differ.

The soils in the Kura-Araxes lowland have a complicated combination of the above factors of swelling. The majority of these soils contain large amounts of silt particles (under 0.001 mm) which consist principally of beidellite, a mineral with a very strong capacity to swell. At the same time, soils contain substantial amounts of nonswelling minerals (mica, quartz, carbonates) which affect volume very slightly. The water stability of aggregates in the soils of the Kura-Araxes lowland is generally low, but differs in different soils, depending on the humus content and the presence of crystalline films of trivalent oxides, as we mentioned above, on adsorbed bases, salt content, and so forth.

Soils with the greatest capacity to form crusts have the most unstable structures, as can be seen by the large cracks that form in them as they dry. Data on the swelling of soils with a strong or weak capacity to form crusts in the Kura Araxes lowland is compiled in table 13. The data permits us to draw the following conclusions.

1. The volume increase of soils in this area varies from 3 to 25 percent.

2. The volume increase of wet soils does not always conform with the amount of highly dispersed particles (under 0.001 mm), and this is because of the disintegration of aggregates and the filling in of spaces between those remaining, i.e., because of diffusion of soils.

3. Soils formed upon the red sediments of Araxes contain water-stable aggregates (cultivated soils) and show a greater volume increase than do soils tending greatly to form crusts and those formed upon the Kura sediments.

Along with the total extent of swelling, the speed of swelling has a great significance in the diffusion of soils.

## Causes of Crust Building in Soils

The nature of crust building in soils has already been discussed in the literature [6]. Consequently, we will mention here only some conclusions and the significance of the mineral composition of the colloidal and silt particles of soils in crust building and the means of preventing it.

Crust building is very frequent in irrigated soils, especially in the Shirvan steppe of the Azerbaidzhan SSR. Crust building means packing of soils within plowed sections and directly underneath them, which reduces the permeability of soils greatly. Plants suffer from this, especially when they have just sprouted, and they sometimes even die because of the soil crust. Packing of soils is preceded by diffusion during irrigation. Not only the aggregates disintegrate but also the structure, and the artificial composition of soils becomes destroyed. The diffused soil cracks when dry, forming large blocks which break the roots of plants and damages sprouting plants, especially cotton plants. It is difficult to loosen such soils. The spaces between the cracked blocks cause an irregular distribution of water during the next irrigation, for water hardly dampens the well-packed blocks but easily penetrates the deeper layers along the cracks. The exposed surfaces of the blocks become destroyed during the next irrigation and the broken pieces of soil fill in the cracks and cause further packing and hardening of the soil.

Crust building is especially harmful in the spring when the cotton plants come up, but the damage continues during the further growth of the plants, first of all with respect to biochemical processes.

N. E. Bekarevich explains the death of cotton plants and the survival of grass in the following way. Cotton plants sprout at a temperature of about 14°C, at which soils readily dry and form crusts, while grass sprouts at lower temperatures, prior to the drying out and formation of the crust.

Hard crusts suppress the development of micro-organisms and, consequently, the lower parts of the soil become very poor in them, and this in turn has a harmful effect on the decomposition of fertilizing organic substances and the accumulation of humus.

There are several causes of crust building in soils. The most important are a high content of silt and colloidal particles, the specific mineral and chemical composition of the silt fraction, the low humus content, climatic

TABLE 13. Swelling of soils in the Kura-Araxes lowland

| Section Number | Soil Type | Depth of Samples (cm) | Content of fraction under 0.001 mm (%) after extraction of carbonates | Percent of swelling | | Wetness after Complete Swelling |
|---|---|---|---|---|---|---|
| | | | | After 1 hour | Total | |
| 14 | Soil of a meadow salt marsh on alluvial-proluvial sediments, weakly crusted (3-4 grade) | 0-15<br>15-28 | 41.0<br>40.0 | 3.0<br>9.3 | 3.2<br>9.6 | 52.1<br>48.1 |
| 10 | Soil of an irrigated meadow on alluvial-proluvial sediments, strongly crusted (9-10 grade) | 0-16<br>16-20 | 57.7<br>- | 4.0<br>5.5 | 4.2<br>5.6 | 62.3<br>Undetermined |
| 180 | Irrigated soil on recent sediments of the Kura river overlying those of Araxes | 0-12<br>33-53<br>120-140<br>140-160 | 35.6<br>42.0<br>62.0<br>58.3 | 1.8<br>9.6<br>9.0<br>6.0 | 1.8<br>9.7<br>9.8<br>6.3 | 46.6<br>57.3<br>59.0<br>55.4 |
| 624 | Light-gray soil of a meadow salt marsh on the sediments of Araxes: | | | | | |
| | Young sediments of Araxes | 9-26<br>26-52 | 58.5<br>63.0 | 10.2<br>14.2 | 10.7<br>14.7 | 38.7<br>57.3 |
| | Soils of present sediments of Araxes buried in the 1920's | 52-90 | 65.0 | 17.3 | 18.3 | 70.0 |
| | Old sediments of Araxes | 220-260 | 51.4 | 13.6 | 16.3 | 58.4 |
| 100K | Soil of a meadow slightly salty, on the Bolgarchay delta | 0-16<br>39-50<br>90-100 | 58.3<br>63.3<br>65.2 | 15.8<br>18.0<br>22.0 | 17.5<br>21.2<br>25.1 | 52.5<br>40.1<br>Undet. |
| 805/19 | Gray-brown soil, strongly salty, a meadow remnant of a diluvial mantle | 0-5<br>5-20<br>110-135<br>132-159 | 37.1<br>49.7<br>34.4<br>38.8 | 6.3<br>7.6<br>4.9<br>6.3 | 7.2<br>7.8<br>5.4<br>6.6 | 34.3<br>33.2<br>22.8<br>24.1 |
| 631 | Light-gray soil of a meadow salt marsh on young sediments of Araxes | 55-80<br>155-250 | 35.5<br>53.2 | 9.2<br>10.6 | 10.5<br>13.1 | 32.1<br>37.8 |
| 948 | Gray-brown soil, irrigated, secondarily salty | 0-18<br>54-74<br>74-106<br>146-180 | 49.7<br>59.5<br>62.5<br>50.6 | 10.0<br>14.3<br>11.0<br>6.2 | 10.3<br>15.8<br>12.8<br>6.6 | 34.7<br>Undet.<br>34.9<br>30.4 |
| 18 | Tertiary clay | 0-20 | 63.3 | 4.9 | 5.4 | 46.7 |

conditions, and incorrectly regulated irrigation.

Let us review these causes of crust building separately, keeping in mind, however, that they work simultaneously and are interrelated.

The physical composition or dispersity of soils substantially affects their physical and physico-chemical properties, including the capacity to form crusts, viscosity, and permeability. Because our samples contained 15 to 30 percent carbonates, the dispersity of the soils was determined after the extraction of the carbonates with hydrochloric acid, followed by removal of the remaining acid and calcite by washing and separation of particles of different sizes. From the physical composition compiled in table 2, we can see that the soils with great inclination to form crusts have heavy physical compositions (sections 10 and 11).

It is interesting to note that soils in the sections with greater crust-building tendencies contain silt fractions slightly more than does the clay of Araxes and the gray-brown soils of section 221, the crust-building capacity of which is weak. However, the properties of the former, including the thickness of the crusts, differ sharply from those of the latter. Therefore, dispersity of soil does not adequately explain the crust-building capacity. The structure of soil micro-aggregates therefore has great significance. The structure of micro-aggregates depends in turn on the humus content, the presence or absence of films of crystallized iron hydroxides, and the mineral composition, especially that of the highly dispersed parts of soils.

We used the following method for evaluating microstructures of soils. After the carbonates had been extracted, the soil sample was shaken with water 10 times the volume of the sample, and the content of particles under 0.001 mm

was determined above the sedimented soil; then the wet sediment was mashed with a rubber pestle and shaken with water and the content of the particles under 0.001 mm was again determined. After the silt fraction completely settled and the water was again clear, the mashing was repeated a second time. In the process, the micro-aggregates became peptized and turned into suspension. The more stable the aggregates, the less they became disintegrated. The results of these experiments have been compiled in table 14.

lonite group (beidellite), and beidellized hydromicas.

Beidellite has a crystal structure in which the distance between the sheets depends on wetness. The volume decrease in soils because of dehydration and the formation of cracks is substantially related to the presence of beidellite and partially to that of beidellized hydromicas. Beidellite cements other minerals because of its high dispersity and makes the soils viscous and almost impermeable. The combination of

TABLE 14. The amount of particles under 0.001 millimeter extracted after repeated mashing (% of fraction under 0.001 mm)

| Section Number | Soil Type | Depth of Samples (cm) | Before mashing | After 1st mashing | After 2nd mashing | After 3rd mashing | Total particles under 0.001 mm |
|---|---|---|---|---|---|---|---|
| 22 | Gray-brown, heavily loamy soil, slightly crusted (1-2 grade) | 0-15 | 48.00 | 35.60 | 11.02 | 5.98 | 48.4 |
| 22a | | 0-18 | 37.14 | 52.72 | 6.15 | 3.99 | 38.3 |
| 14 | Soil of a meadow salt marsh on alluvial-proluvial sediments, slightly crusted (3-4 grade) | 0-15<br>15-23 | 22.47<br>15.25 | 54.96<br>60.25 | 21.51<br>24.50 | 1.06<br>None | 41.0<br>41.3 |
| 11 | Soil of an irrigated meadow on heavy alluvial-proluvial sediments, medium crusted (5-6 grade) | 0-15 | 75.72 | 8.23 | 12.22 | 3.83 | 38.4 |
| 11a | | 0-15 | 85.56 | 9.36 | 5.18 | None | 46.1 |
| 11b | | 0-15 | 82.65 | 13.11 | 4.24 | None | 59.4 |
| 10 | Soil of an irrigated meadow on alluvial-proluvial sediments, heavily crusted (9-10 grade) | 0-16 | 70.21 | 23.72 | 3.50 | 2.57 | 57.7 |
| 18 | Tertiary clay | 0-20 | 90.39 | 4.57 | 4.14 | 0.90 | 63.6 |
| 180 | Soils on the irrigated recent sediments of the Kura river overlying those of Araxes | 0-12<br>33-53<br>140-160 | 51.6<br>53.8<br>85.8 | 32.8<br>29.5<br>10.5 | 15.6<br>16.7<br>3.7 | -<br>-<br>- | 35.64<br>42.0<br>58.3 |

The consecutively extracted amounts of particles under 0.001 mm after the first, second, and third mashing appear to indicate the structural strength of the micro-aggregates. The table reveals that crust-building soils and Tertiary clays which take part in the formation of the crust-building soils become intensively peptized even prior to mashing; this means that the structure of their micro-aggregates is very weak. In the soils with the greatest crust-building capacity, 70 to 80 percent of the particles under 0.001 mm can be extracted before mashing, while in those with only a slight capacity to form crusts this percentage is 37 to 48.

Soil disintegration depends on the properties of colloids, particularly on their swelling capacity and their dispersion in water. The significance of swelling and diffusion of soils has already been mentioned; we can only add here the significance of the speed of swelling in the disintegration of soil aggregates. Let us remember that the silt fraction of the majority of soils in the Kura-Araxes lowland consists of amorphous colloids, minerals of the montmoril-

beidellite, micas, carbonates, quartz, and other minerals produces hard soils when dry. Beidellite, amorphous colloids, and hydromicas are highly dispersed swelling minerals. During irrigation they swell first at the edges of lumps, which remain dry and unswollen inside. The edges of the lumps then break off from the internal dry cores, and the lumps gradually become decomposed, turning the soil into mud which forms a crust on drying. The disintegration of lumps may be prevented if humus and films of trivalent oxides are present, for they keep the soil particles cemented together.

The cracking of soils is also related to the montmorillonite content. Nearly 80 percent of the montmorillonite is under 0.001 mm. This mineral has a mobile crystal structure and, therefore, absorbs a great deal of water. Dehydration of montmorillonite causes large cracks. Very wet kaolinite shrinks very little in drying and does not form cracks. Figure 9 shows the formation of cracks in dry samples of various minerals.

Air, which is replaceable by water during

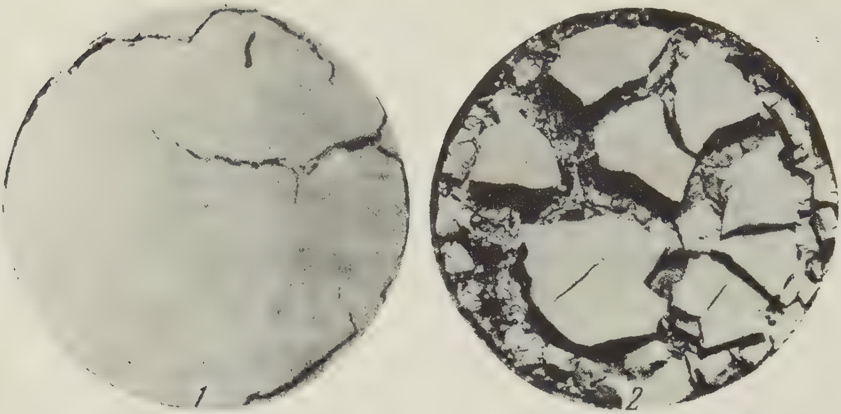

FIGURE 9. Dry samples of minerals. 1 -- crust formed in kaolinite 2 -- crust formed in montmorillonite

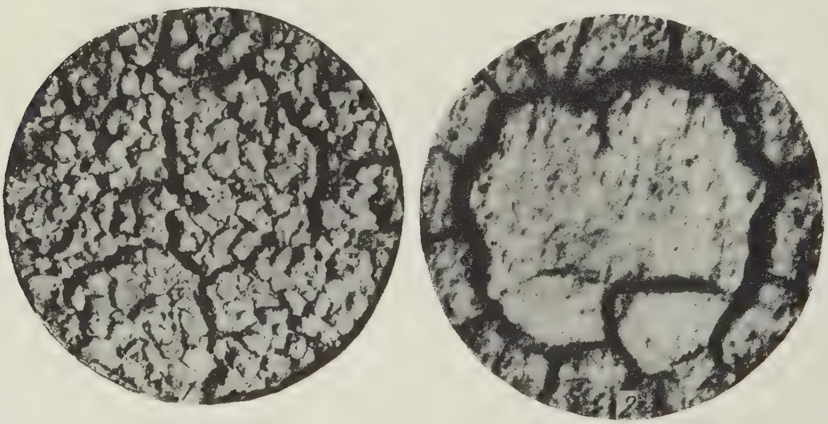

FIGURE 10. Effect of the irrigation method in soils: a crust formed in the soil as a result of a rapid overflow. 1 -- red clay of Araxes 2 -- soil of a meadow (section 10)

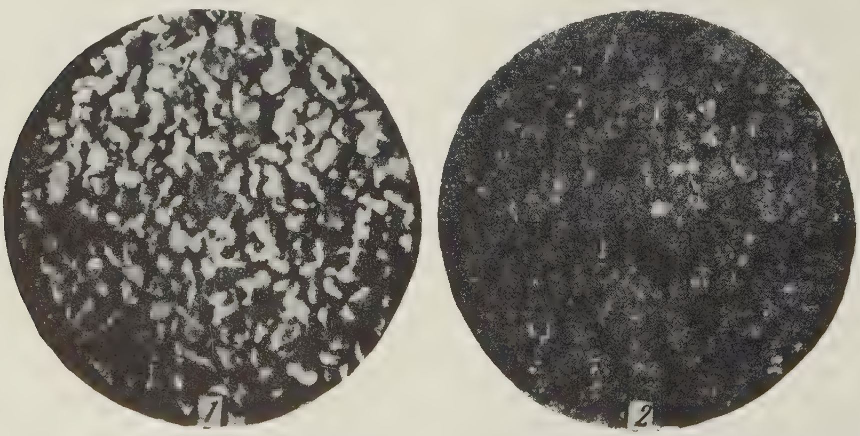

FIGURE 11. Effect of the irrigation method in soils: a crust formed in the soil as a result of slow wetting through capillaries from below. 1 -- red clay of Araxes 2 -- soil of a meadow (section 10)

irrigation, is an even greater factor in the destruction of soil aggregates and lumps. The destruction is caused by both free air in the soil and adsorbed gases, which on being replaced by water penetrate and enlarge the pores of soils. The volume of the replaced air and gas increases, especially at high temperature, for, as is known, the volume increase of gas at high temperatures is greater than at low temperatures.

The method of irrigation is also an important factor in the destruction of soil aggregates and the formation of crusts and fractures. For example, when the soil is completely covered by water, it becomes wet rapidly; and the more rapidly the soil becomes wet, the sooner the air is replaced and the more rapidly the soil disintegrates. Figures 10 and 11 show the effect of the irrigation method in turning soils into mud and in cracking them. As can be seen in the figures, a rapid wetting leads to the destruction of aggregates, mudding of soils, and formation of large cracks after drying out. The thickness of the crust sometimes reaches 20 and 30 cm (fig. 12). A slow wetting does not destroy


FIGURE 12. The size of a crust formed after rapid wetting and drying.

the aggregates and fractures do not develop. The destruction of soil structures by air may be prevented by gradual saturation with water by bringing the water into the soil through capillaries. In this case the air is replaced slowly and does not have a destructive effect. Saturation of soils through capillaries takes place because of adhesion. This binds the soil particles and increase the stability of soil lumps. The significance of capillary forces in binding particles can be illustrated by the following experiment. If we take two glass sheets and put water drops between them, it will be difficult to separate the sheets; they will be kept together by capillary forces. Greater stability of aggregates after capillary saturation has been mentioned in the literature long ago [13].

Slow wetting of soils which can be reached by irrigation along furrows causes gradual swelling of the soils and binding of hard particles by swelling minerals, thereby preventing the destruction of the soil structure. Wetting of soils at lower temperatures also helps to protect soil lumps from destruction, because the adsorbed air expands less at lower temperatures, the water vapor condenses at low temperatures and partially fills in the capillaries. Thus, irrigation in the early morning or at night will contribute toward less destruction of aggregates than irrigation during the day.

If the soil is not too dry and the spaces between the aggregates are filled with water instead of air, the soil will not turn into mud as completely as in the case of wetting a hard crust.

N. E. Bekarevich has measured the hardness of soils in various conditions and found it to depend on the wetness and the speed of saturation. The results of his measurements have been compiled in table 15.

TABLE 15. Hardness of the Soil Crust in Relation to Wetness and Speed of Saturation (averages)
Soil of an Irrigated Meadow, Heavily Crusted, 9 to 10 Grade, (section 10)

| Variety of Experiment | Hardness ($kg/cm^2$) |
|---|---|
| Absolutely dry soil after rapid wetting and drying | 136. 4 |
| Air-dry soil after rapid wetting and drying | 110. 6 |
| Soil wet to its maximum hygroscopic capacity after rapid wetting and drying | 86. 8 |
| Soil of 12. 65 percent wetness after rapid wetting and drying | 70. 0 |
| Soil of 15. 4 to 16. 2 percent wetness after rapid wetting and drying | 65. 6 |
| All soils of previous experiments made slowly wet through capillaries and dried | 47. 0 |

It is interesting to follow the effects of the two interrelated factors: the air content in the soil during a rapid wetting (the more water the less air), and the speed of wetting of the soils. In all cases of rapid wetting, the absolutely dry soil became the hardest if dried out; its hardness was 136. 4 $kg/cm^2$. An increase of the water content prior to the rapid wetting and drying decreased the hardness. Thus, the hardness of crust-building soils declined to 86. 8 $kg/cm^2$ in the sample made wet to its maximum hygroscopic capacity in advance. The hardness of 12. 6 percent and 16. 2 percent of wet soils dropped to 70 and 65. 6 $kg/cm^2$, respectively. In the case of slow saturation

through capillaries, these figures varied from 69.8 to 25.2 kg/cm$^2$, having an average of 47 kg/cm$^2$. (The speed of saturation was slow enough to expel the entire air from the soil freely.)

Thus it is possible to produce different hardnesses in the crust of the same soil by changing either the wetness prior to irrigation or the speed of wetting.

If the soil is made wet through capillaries, the continued wetting by irrigation, for example, does not produce mud and a crust does not develop. We made the following experiment to confirm the above statement. We cut soil in the form of prisms 8 cm high and about 10 cm thick, and we put one of these prisms on wet blotting paper until the sample became slowly saturated through capillaries. The other prism we kept dry.

Then the prisms were put together into two glasses of water. The dry prism broke apart rapidly and turned into a formless mass. The previously saturated prism did not change its form and did not break apart in water; it did not disintegrate, for its air had been expelled previously by saturation with water. The soil particles were kept together by adhesive forces and the soil swelled slowly. The dry prism was destroyed by air expelled from the soil and because of the difference in the volume increase at the edges and the internal parts of the lump. This experiment illustrates clearly how the soil aggregates and lumps disintegrate and how soil turns into mud through rapid irrigation and also shows why wetting along capillaries almost entirely prevents the formation of soil crust. Some authors strongly emphasize the significance of carbonates, which according to them, increase the hardness of soils [17]. It must be mentioned that carbonates are not always the principal factor, although they do contribute to the hardness of soils. For example, soil formed upon the red clays of Araxes have thinner and softer crusts than the soils in the Shirvan steppe, formed upon the gray sediments of the Kura river, although both soils contain great amounts of carbonates. The different behavior of these soils can be explained by the fact that micro-aggregates of the clays of Araxes are covered by films of iron oxides, while the soils formed upon the sediments of the Kura river do not have such films and contain only small amounts of organic substances which affect the soil structure favorably.

The soil salinity also contributes to crust building and to the conversion of soils into mud after irrigation.

The significance of the climate in crust building is related to the fact that high temperatures and wind speed up the drying process in soils. However, slow drying by using mulch[?], for example, does not change the hardness of soils but increases the time of hardening.

## Means of Preventing Crust Building

On the basis of the above experiments, we can formulate means to prevent crust building and decrease the hardness of soils in the following way.

Soil can be preserved in the same condition as when they were prepared after plowing by irrigation with slow streams of water, so that the soil becomes saturated through capillaries. It is desirable that the soil not be too dry at the time of irrigation.

On the basis of popular [farmers] experience concerning suitable irrigation and the results of special studies, we find it possible to recommend the following methods, which are described in a special article in detail by Gorbunov and Bekarevich [7]: 1) artifical showers, first using small, later large, drops; 2) irrigation along furrows by small streams; 3) subsoil irrigation; 4) irrigation at night or early in the mornings.

The above measures of preventing crust building may be applied by first irrigating all soils with unfavorable physical properties, but they can also be used in all other cases, even in soils that hardly form crusts, because these measures protect the soil structure from destruction by water.

Any of these irrigation methods or a combination of them, may be applied in various ways, depending on the conditions on the farm and the duration of vegetation.

It goes without saying that a fundamental improvement in soils requires adding organic substances to the soil and grass cultivation. In the case of soils in salt marshes, it is advisable to add gypsum.

## CONCLUSIONS

1. Some soils in the Kura-Araxes lowland have good structures because of films of crystallized iron oxides on the surfaces of micro-aggregates which increase their stability in water. Besides, the stability in water is caused by capillary forces and by swelling of hydrophilic colloids.

2. Along with the volume increase of soils during irrigation, the nonstructured soils become packed when dry. It is necessary to keep in mind the difference between the volume increase in soils and their actual swelling by irrigation.

3. The crust building must be divided into several stages: swelling of soils, soaking of

soil lumps, their destruction by enclosed or absorbed air, packing of soils, and hardening, with simultaneous shrinkage and cracking.

4. The physical and mineral composition of soils greatly affect the physico-chemical properties of soils and silts, their swelling, their maximum hygroscopic capacity and hardness.

5. Along with the general agrotechnical measures, a slow irrigation along furrows, subsoil irrigation, and rain-making may be recommended in order to prevent crust building.

REFERENCES

1. Aydinyan R. Kh. VYDELENIE POCHVENNYKH KOLLOIDOV BEV KHIMICHESKOI OBRABOTKI [DISCHARGE OF SOIL COLLOIDS WITHOUT TREATMENT]: Kolloidnyi Zhurnal, v. 9, no. 1, 1947.

2. Berestneva, Z. Ya., T. A. Koretskaya, and V. A. Kargin. O MEKHANIZME OBRAZOVANIYA KOLLOIDNYKH CHASTITS GIDROOKISI ALUMINIYA [ON THE DEVELOPMENT MECHANISM OF COLLOID PARTICLES OF ALUMINUM HYDROXIDE]: Kolloidnyi Zhurnal, v. 13, no. 5, 1951.

3. Vasilyev, A. M. OSNOVY SOVREMENNOY METODIKI I TEKHNIKI LABORATORNYKH OPREDELENY FIZICHESKIKH SVOYSTV GRUNTOV [BASIC MODERN METHODS AND LABORATORY TECHNIQUES OF DETERMINING THE PHYSICAL CHARACTERISTICS OF SOILS]: 1949.

4. Gorbunov, N. I. METODIKA RAZDELENIYA POCHV I GLIN NA FRAKTSII DLYA RENTGEMOGRAFICHESKOGO I TERMOGRAFICHES KOGO IZUCHENIYA [METHODS OF DISTRIBUTING SOIL AND CLAY ON FRACTIONS FOR RADIOGRAPHIC AND THERMOGRAPHIC STUDY]: Pochvovedeniye, 1950, no. 7.

5. __________. MINERALOGICHESKY SOSTAV KRASNOZEMOV [MINERALOGIC COMPOSITION OF RED EARTH]: Akademiya Nauk SSSR, Izvestiya-vo Doklad na v Mezhdunarodnom Kongresse Pochvovedov, 1954.

6. Gorbunov, N. I., and N. E. Bekarevich. PRIRODA OBRAZOVANIYA POCHVENNOY KORKI I MERY BORBY S NEY [NATURE OF THE DEVELOPMENT OF SOIL CRUST AND THE OVERWHELMING FIGHT AGAINST IT]: Pochvovedeniye, 1951, no. 4.

7. __________. VZAIMODEYSTVIYE POCHVY, VODY I VOZDUKHA PRI OROSHENII [INTERACTION OF SOIL, WATER AND AIR WITH IRRIGATION]: Khloprovodstvo, 1951, no. 7.

8. Gorbunov, N. I., I. G. Tsyurupa, and E. A. Shurygina. RENTGENOGRAMMY, TERMOGRAMMY I KRIVYYE OBEZVOZHIVANIYA MINERALOV, VSTRECHAYUSHCHIKHSYAV POCHVAKH I GLINAKH [RADIOGRAPHS, THERMOGRAPHS AND DEHYDRATION CURVES OF MINERALS FOUND IN SOIL AND CLAY]: Akademiya Nauk SSSR, Isvestiya-vo, 1952.

9. Zalmanson, E. S., and E. S. Shishova. K METHODIKE VYDELENIYA KOLLOIDNYKH FRÁKTSY IZ KARBONATNYKH GLIN I ILOV [ON THE METHOD OF DISCHARGING COLLOID FRACTIONS FROM CARBONATE CLAY AND SOIL]: Akademiya Nauk SSSR, Izvestiya, Seriya Geologicheskaya, 1950, no. 9.

10. Kachinsky, N. A. METODY MEKHANICHESKOGO I MIKROAGREGATNOGO ANALIZA POCHYV [METHOD OF MECHANICAL AND MICRO-AGGREGATE ANALYSIS OF SOILS]: Akademiya Nauk SSSR, Izvestiya-vo, M.-L., 1943.

11. Kislitsina, L. P. ADSORBTSIYA IONOV VODORODA I ALYUMINIYA DERNOVO-PODZOLISTYMI POCHVAMI I KRASNOZEMAMI [ADSORPTIVE HYDROGEN AND ALUMINUM IONS IN GRASS-PODZOL SOIL AND RED EARTH]: Akademiya Nauk SSSR, Pochv. in-t. (candidate dissertation), 1953.

12. Nefedov, G. F. PADENIYE TVERDYKH CHASTITS V ZHIDKOSTI I MEKHANICHESKY ANALIZ POCHV [PRESSURE STRENGTH OF PARTICLES IN LIQUID AND MECHANICAL ANALYSIS OF ROCKS]: Zhurnal Opytnoy Agronomii, ch. 4, 1902.

13. Pavlov, G. I. METODIKA AGREGATNOGO ANALIZA I AGREGATNYY SOSTAV POCHV [METHODS OF ANALYSIS OF AGGREGATES AND COMPOSITION OF ROCK AGGREGATES]: Ak-Kovkskoy Opytno-orosit Stantsii, Trudy, 1930, no. 6.

14. Rozanov, A. N. SEROZEMY SREDNEY AZII [SULFIDE EARTHS OF CENTRAL ASIA]: Akademiya Nauk SSSR, Izvestiya-vo, 1951.

15. __________. SERO-KORICHNEVYYE POCHVY KURA-ARAKSINSKOY NIZMEN-

NOSTI [BROWN SULFUR EARTH OF THE KURA-ARAXES LOWLAND]: Pochvovedeniye, 1952, no. 12.

16. Rozanov, A. N., and I. D. Sedletsky. FIZIKO-KHIMICHESKIYE PROTSESSY OBRAZOVANIYA SEROZEMOV I BURYKH POCHV [PHYSICO-CHEMICAL PROCESSES OF DEVELOPMENT OF SULFIDE EARTHS AND BROWN SOILS]: Problemy Sovetskogo Pochvovedeniya, 1940, no. 10.

17. Ryzhov, S. N. PRICHINY OBRAZOVANIYA KORKI NA POLIVNYKH ZEMLYAKH SREDNEY AZII I MERY BORBY S NEY [CAUSES FOR THE DEVELOPMENT SOIL CRUSTS ON GLAZED EARTH IN SOUTHERN ASIA AND THE OVERWHELMING FIGHT AGAINST IT]: Voprosy Fiziki, Khimii, Melioratzii Pochv i Udobreniya Khlopchatnika, Soyuztekhizdat, Tashkent, 1932.

18. Shurygina, E. A. ISSELDOVANIYE STARENIYA GELEY GIDROOKISEY ZHELEZA I ALYUMINIYA TERMICHESKIM METODOM [INVESTIGATION OF IRON AND ALUMINUM HYDROXIDES IN AGED GELS BY THE THERMAL METHOD]: Akademiya Nauk SSSR, Mineralogischesky Sosta Pochv i Ikh Fiziko-Khimicheskie Svoystva, Trudy, Pochvennogo Instituta im. V. V. Dokuchaeva, v. 53, 1958.

19. Tsurinov, A. I. NOVOYE O GLINAKH I GLINISTYKH RASTVORAKH [NOTES ON CLAY AND CLAY SOLUTIONS]: 1940.

20. Tsyurupa, I. G. VLIYANIYE STEPENI OKRISTALLIZOVANNOSTI SOEDINENY ZHELEZA NA IKH RASTVORIMOST [EFFECT OF CRYSTALLIZED IRON AGGREGATES ON SOLUTION]: Akademiya Nauk SSSR, Mineralogischesky Sostav Pochv i Ikh Fiziko-Khimicheski Svoystva, Trudy, Pochvennogo Instituta im. V. V. Dokuchaeva, v. 53

21. Puri, A. N. Keen Jour. Agr. Sci., 1925, no. 15.

# THE GENESIS OF $CO_2$ IN GROUND WATER CONTAINING CARBONIC ACID[1]

*by*

*A. A. Smirnov*[2]

*• translated by Dean A. Miller •*

ABSTRACT

Answers to criticisms of a paper concerning the genesis of $CO_2$ made by V. P. Novik-Kachan [1] and A. V. Zhevlakov [2] treat the manufacture of $CO_2$ contained in air and water circulating through tectonic fractures, thermodiffusion of various gases having different molecular weights and under varying degrees of temperature and pressure, and variations in $CO_2$ concentration due to external seasonal variations in temperature and protective snow cover. --Editor.

## INTRODUCTION

In Sovetskaya Geologiya (1956, no. 56), V. P. Novik-Kachan [5] and A. V. Zhevlakov [2] published notes containing remarks critical of me [7]. The following is an answer to both criticisms.

## ANSWER TO NOVIK-KACHAN

Novik-Kachan admits to a lack of familiarith with this particular field of study. Our conclusion on the genesis of $CO_2$ in ground water containing carbonic acid he calls "a theory on the origin of $CO_2$ in air of ground water containing carbonic acid." Actually, we dealt with 1) gas in the atmosphere and in zones of oxidation, 2) $CO_2$ manufactured in soils as a result of oxidation of organic material in tectonic fissures, and 3) $CO_2$ manufactured by the action of sulfuric acid, the product of sulfide oxidation, on carbonates.[1]

Novik-Kachan made the following six points:

1. The concentration of exogenic carbonic acid in water in tectonic fractures which cut folded mountains must correspond to the amount of $CO_2$ in the atmosphere at the earth's surface under normal conditions (0.03 percent), and cannot exceed 0.51 cubic centimeters ($cm^3$) of $CO_2$ per liter (1) of water (1 mg/1), or 1.72 $cm^3$/1 of the total gas in solution.

2. The relative amounts of gas dissolved in water in tectonic fractures must correspond to the relative amounts of gas in the atmosphere at the earth's surface.

We note that Novik-Kachan does not consider $CO_2$ derived from soils and from zones of oxidation. It is known that the concentration of $CO_2$ in gas derived from soil may be 2 or 3 percent or more. Organic material (transported by infiltrating meteroic water) and oxygen (from continuous diffusion of atmospheric gases) enter tectonic fractures, thus facilitating oxidation of organic material and the activity of sulfuric acid (the product of sulfide oxidation) on carbonate components of rocks by which significant quantities of $CO_2$ can be formed. Therefore, $CO_2$ concentration in gas in tectonic fractures can be quite large, higher than the amount usually found in water (even without considering the carbonic acid which is accumulated under conditions resulting from thermodiffusion of gases).

Novik-Kachan's two remarks indicate a lack of comprehension of the discussion of 1) gas-thermodiffusion phenomena, in which gas continually moves in a vertical plane up one wall of a tectonic fracture and down the other while drawing gases from the atmosphere and those, released but not yet dissolved in water, from depth; 2) complete or partial diffusion of gases and the diffusion of their isotopes (especially at great depth); and 3) the concentration of $CO_2$, a heavier gas in the atmosphere, over the zone of oxidation and water when air temperature is higher than water temperature in tectonic fractures (as in spring and summer).

In the given example, continuous influx of air into tectonic fractures is sufficient only for a gradual accumulation of $CO_2$ over the water, but there is no full or partial separation of gases within the mixture. The partial $CO_2$

[1] Translation of Genezis $CO_2$ v sovremennykh uglekislykh podzemnykh vodakh: Sovetskaya Geologiya, 1958, no. 1, p. 159-55.

[2] All-Union Scientific Research Institute of Hydrology and Engineering Geology (VSEGINGEO).

pressure in tectonic fractures under similar conditions may reach 1 atm or more (assuming that $CO_2$ is significantly heavier than air). Under such conditions, free $CO_2$ in water can exceed 1.72 $cm^3/_1$ of total gases dissolved and 0.51 $cm^3/_1$ water, the limits set by Novik-Kachan, and may even be as much as 95 or 100 percent of total gas dissolved and 1,750 $cm^3/l$ water (as much as 3.5 grams per liter g/l) and more. In fact, free-$CO_2$ concentration in ground water containing carbonic acid is 1 to 2.5 g/l, sometimes 3 g/l, and, in exceptional instances, more. In addition to free $CO_2$, a significant amount of $CO_2$ necessary for the solution of carbonates and for the formation of bicarbonates of various metals is present. The $CO_2$ factor in water can be significant (particularly in ground water containing dissolved hydrocarbonates and sodium carbonates); however, the $CO_2$ content exceeds 10 g/l water.

Occasionally, inaccurate measurements result in reports of definitely exaggerated gas content of ground water containing carbonic acid. In 1957, V. N. Kortsenshteyn [4] and K. F. Orfanidi [6] published (in Sovetskaya Geologiya) identical figures for gas content of ground water circulating in dolomites and limestones of the Valangianian stage at Yessentuka bore site. According to their measurements, $CO_2$ content ranged from 20 to 37 g/l. However, the Koltsov expedition of the Ministry of Geology and Mineral Conservation, U. S. S. R., and the hydrogeologic section of the Pyatigorsk Balneological Institute (I. Ya. Panteleev) engaged in a systematic long-term study of ground water at this bore site. Free $CO_2$ did not comprise more than 1 g/l of the water contained in Paleozoic and Mesozoic strata and not more than 4 g/l of total gas dissolved.

Panteleev, on hearing Kortsenshteyn's report at the January 1956 industrial-technical meeting on the results of the 1955 hydrogeologic study of mineral waters at Soviet health resorts, refuted Kortsenshteyn's figures on the grounds that the practical maximum of $CO_2$ concentration in ground water is 3 or 4 g/l water. The measurements presented by Kortsenshteyn and Orfinidi were of water taken from test point PD-03 with a sample selector which is unable to sample gaseous liquids of some level lower than its own. This sample selector is not approved, and its use was discontinued in autumn 1956. Their results contain internal contradictions and also contradict physical laws and experimental data on the solubility of gases at various levels. The magnitude of $CO_2$ content in waters circulating in the rocks of the Valanginian stage are greatly disproportional to the concentration of various metal bicarbonates.

The structure and concentration of gases in low-temperature ground water circulating in tectonic fractures which cut areas of deeply worn erosion networks and permafrost seldom conform to the structure and concentration of atmospheric gases and are, moreover, unstable. The structure and concentration of gases dissolved in water in tectonic fractures vary not only in relation to the amount of organic matter introduced and the degree of organic-material and sulfide oxidation, but also in relation to change in climatic conditions. In spring, summer, and sometimes in fall, when air temperature is higher than water temperature, $CO_2$ accumulates over water in rocks. In late fall and winter, when air temperature is lower than water temperature, light gases, principally nitrogen, are accumulated from the atmosphere and zone of oxidation. Diffusion of gases during winter allows free and semifree $CO_2$ to escape along walls of tectonic fractures into the atmosphere. The probability of this sequence of events is supported by data on gas which is released from ground water containing carbonic acid in tectonic fractures and bottoms of gorges in mountain areas during winter. This same water is resaturated with $CO_2$ during spring and summer. Therefore, the structure and concentration of gas dissolved in water circulating in tectonic fractures vary continuously ( and not only seasonally ) in relation to variations in air temperature and to the duration of temperature variations.

Novik-Kachan ignores the physical phemonena of gas thermodiffusion. He claims that the structure of gas over water is analogous to the structure of air, whereas we are considering the almost continuous variation in gas structures over water, especially in open areas of tectonic fracturing.

3. Novik-Kachan notes that in the winter crust, at a depth of 30 to 40 m, a horizon of constant annual temperatures is observed and that " under normal conditions, the temperature gradient necessary for gas thermodiffusion can exist only above this horizon, "for below it temperature rises. Daily variation in temperature occurs not more than 1 to 2 below this horizon.

This is an obvious misunderstanding. First Novik-Kachan writes that gas thermodiffusion is possible above the horizon of constant annual temperatures because a temperature gradient can exist in tectonic fractures. However, he then notes that "below this horizon thermodiffusion is impossible because the temperature rises." But does temperature rise negate the possibility of a temperature gradient? If a temperature gradient is observed also below the horizon of constant yearly temperature, thermodiffusion inevitably occurs.

In tectonic fractures in folded mountains, the water level is determined by the depth of local erosion, and the depth of water in frac-

tures varies by a fraction of a degree or by a whole degree, but the air temperature ranges from + $30^{o}$ to + $40^{o}$ in summer and from -$30^{o}$ to -$50^{o}$ in winter. Therefore, the insistence on a stable temperature under these conditions at a depth of a 30 to 40 m is equivalent to a denial of gas-molecule movement in the aeration zone in tectonic fractures, which is diametrically opposed to elementary concepts of thermodynamic phenomena. The horizon of relatively constant temperature in tectonic fractures can exist only below the water table.

4. Novik-Kachan finds it difficult to understand the incorporation of carbonic acid in ground water in areas where, during the course of the year (from November to March), a negative temperature of a positive temperature close to zero dominates. Obviously when relative temperatures are dominant, meteoric waters cannot infiltrate tectonic fractures. Therefore, to speak of the genesis in carbonic acid of ground water during this period is impossible.

5. During the summer, at Urchugan spa, surface water, containing carbonic acid is mixed with atmospheric particles and, therefore, contains less $CO_2$ than in winter. Also, the seasonal occurrence of water containing less carbonic acid at points of discharge is limited by water velocity and the distance between the area of gaseous-structure formation and point of discharge. In many instances, water, in its movement between the relatively open area of tectonic fracturing where gaseous-structure formation occurs and area of discharge, passes through a closed (subsurface) fracture or along a permeable strata overlying impermeable sediments (in foothill or intermontane depressions). The subsurface tectonic fracture may be clogged with erosion remnants and minerals precipitated from circulating ground water or may be sealed by a Quaternary cover of considerable thickness. In high altitudes, the fractures may be covered with snow during the winter. Springs containing carbonic acid, especially those in Pyatigorsk, Zheleznovodsk, and at station Nagutskoye in the Caucasian KMV [?] region, are some distance from areas where their gas structures are formed (the small streams Khasaut and Malka, in the Caucasian chain, 60 to 100 km to the south). Ground water containing carbonic acid has no contact with the atmosphere between points of origin and of discharge. Therefore, it is possible that ground water containing a lower concentration of $CO_2$ may be discharged some distance from the areas of gaseous-structure formation during various time of the year.

6. Novik-Kachan maintains that particles, products of the decomposition of rocks in tectonic fractures, absorb gas which would otherwise be dissolved in ground water in fractures. But, if the particles are previously saturated with gas, a process that takes relatively little time, excess gas will be dissolved in the water.

## ANSWER TO ZHEVLAKOV

Zhevlakov, like Novik-Kachan, admits that he did not study gases originating in soils or zones of oxidation. His criticism, that the importance of $CO_2$ genesis in ground water containing carbonic acid by means of metamorphic and post-volcanic processes was disregarded in our article, is denied. Moreover, we have in several papers indicated that the separation of $CO_2$ from rock is possible in areas of magmatic activity. However, we believe that $CO_2$ separation from rock occurs principally in the first stages of volcanism (separation of $CO_2$ from carbonate rock begins in those areas where the temperature of the rock is higher than $450^{o}$ to $1,000^{o}$). Rock metamorphism and thermometamorphism occur everywhere at great depths but, for water occurring in deep tectonic depressions which do not contain $CO_2$ or any other metamorphic gases, it is possible to assume that these gases are not significant in forming a gaseous structure. Frequently, high-temperature water containing nitrogen (nitrogenous hydrothermae) escapes from deep tectonic fractures, but does not contain $CO_2$ (although $CO_2$ is from 50 to 80 times more soluble than nitrogen); low-temperature water containing carbonic acid, not nitrogen, escapes from the vicinity of shallow tectonic fractures. These facts necessitate the revision of the universal hypothesis of the endogenous origin of $CO_2$ in ground water containing carbonic acid and, at the same time, a detailed examination of the role of thermodifussion of various gases in $CO_2$ genesis.

Zhevlakov states that we substantiate the theory of thermodiffusion with data on the release of gas during winter in regions covered with thick sedimentary deposits. Furthermore, he writes that we believe continuous $CO_2$ separation, by means of thermodiffusion, is only possible in springs containing carbonic acid which are located in intermontane and foothill depressions where sediments are very thick. These ideas were not included in our discussions.

Also, Zhevlakov does not understand what continuous $CO_2$ separation in intermontane and foothill depressions is; for, as we have pointed out, $CO_2$ separation occurs in winter in ground water containing carbonic acid only in relatively open regions of tectonic fracturing, which do not have a hard-packed surface, are not overlapped by Quaternary deposits, and are not covered with thick snow during winter. Such conditions exist in southern folded mountains where snow is blown away from crags and is drifted in areas of lower relief. However, in high mountain regions, much of the topography is rather smooth and deposits of unconsolidated material are widespread. Here, the snow cover remains from early fall until spring. The re-

lease of gas from ground water containing carbonic acid does not occur in tectonic fractures in this type region (so past investigations have shown). This is true not only for intermontane and foothill depressions, which are merely examples of geologic structures in which ground water containing carbonic acid is not stripped of gas.

A thick cover of sediments is not necessary for the practical isolation of water in tectonic fractures from the atmosphere. Zhevlakov notes that at Marianske-Lazne spa (Czechosolvia), despite a thick cover of sediments, the $CO_2$ content in ground water containing carbonic acid remains relatively constant. This is a clear contradiction of the thermodiffusion theory of $CO_2$ genesis in ground water containing carbonic acid. The Marinske-Lazne region differs sharply from the studied areas in the Caucasus, the Tien-Shan, and others. It has low relief covered with Quaternary unconsolidated material and, from early fall to spring, a thick blanket of snow. Also the springs containing carbonic acid at Prameny, Farska Kiselka, and others in the Marinske-Lazne region, contain 2,000 mg of $CO_2$/1 of water in winter. These are located in slightly worn hollows close to the watershed, but are points of discharge, not areas of gaseous-structure formation. A sufficiently fuller description of Czechoslovakian ground water containing carbonic acid and its areas of genesis andpoints of discharge would have indicated that this ground water has its source in surrounding high mountains and travels to the points of discharge through tectonic fractures. The ground water containing carbonic acid in the Caucasian mineral-water region is also discharged in foothill depressions tens of kilometers from the area of gaseous-structure formation (in the Caucasian chain).

## CONCLUSIONS

1. The phenomena of the multidirectional gas movements along opposite walls of pipes and fractures, in which temperature gradients occur, and the thermodiffusion of various gases having different molecular weights, objectively exist. These phenomena have been quite fully studied by physicists, and to deny their wide distribution under natural conditions, more expecially in tectonic fractures having significant temperature gradients and zones of aeration from a few tens to 1,000 meters and more in depth, is impossible. The most effective separation of a gas from a mixture of gases occurs in pipes or fractures, assuming temperature gradients, when a gas mixture continually enters the fractures at the surface and at depth [1]. Just such conditions are found in relatively open regions of tectonic fractures in which 1) at depth, low-temperature water circulates, 2) at the surface, gas and carbonic acid from soils and zones of oxidation continually enter, and 3) at depth under warm climatic conditions, $CO_2$ separated from the gas mixture is continually dissolved in water. A high $CO_2$ concentration in water occurs when air temperature exceeds water temperature (during heavy spring, summer and autumn rains); gas is released from ground water containing carbonic acid, which is located in areas of tectonic fracturing, during winter (without dilution of water).

Among other investigators, A. L. Kozlov [3] cites an example of the extremely strong multidirectional movement of air along a tectonic fracture.

2. Criticism by Novik-Kachan and Zhevlakov does not lessen the cogency of our conclusions on the genesis of $CO_2$ in ground water containing carbonic acid or the facts we offer in support of these conclusions.

## REFERENCES


1. Johns, K., and V. Ferry. RAZDELENIYE IZOTOPOV METODOM TERMODIFFUZII (perev. s. Angl.) [THE SEPARATION OF ISOTOPES THROUGH THE THERMODIFFUSION METHOD (trans. from English)]: Gos. Izd. -vo. Inostr. Moscow, 1947.

2. Zhevlakov, A. V. K VOPROSY O PRIRODE $CO_2$ YGLEKISLYKH PODZEMNYKH VOD [ON THE QUESTION OF THE NATURE OF $CO_2$ IN GROUND WATER CONTAINING CARBONIC ACID]: Sovietskaya Geologiya, 1956, no. 56.

3. Kozlov, A. L. PROISKHOZHDENIYE VECHNOY MERZLOTY NA G. RAZBALKA PYATIGORYA I GENEZIS ISTOCHNIKOV MASSIVOV TRESHCHINOVATYKH POROD [THE ORIGIN OF PERMA-FROST IN THE RAZVALKA PYATIGORYA MOUNTAINS AND THE GENESIS OF SPRINGS IN FRACTURED ROCK MASSES]: MOIP, Otdelenie Geologiva, Bull., v. 32, no. 2, 1957.

4. Kortsenshteyn, V. N. NOVYYE DANNYYE PO GAZONASYSHCHENNOSTI MEZOZOYSKYKH VODONOSNYKH GORIZONTOV KAVKAZSKYKH MINERALNYKH VOD [NEW DATA ON THE GAS SATURABILITY OF MESOZOIC WATER-BEARING HORIZONS IN CAUCASIAN MINERAL WATERS]: Akademiya Nauk SSSR, Doklady, v. 113, no. 4, 1957.

5. Novik-Kachan, V. P. O PROISKHOZHDENII UGLEKISLOGOGAZA V PODZEMNYKH VODAKH [ON THE ORIGIN OF CARBON WATERS]: Sovietskaya Geologiya, 1956, no. 56.

6. Orfanidi, K. F. UGLEKISLOTA V PODZEMNYKH VODAKH [CARBON DIOXIDE IN GROUND WATER]: Akademiya Nauk SSSR, Doklady, v. 115, no. 5.

7. Smirnov, A. A. O PRIRODE $CO_2$ UGLEKISLYKH PODZEMNYKH VOD [ON THE NATURE OF $CO_2$ IN GROUND WATER CONTAINING CARBONIC ACID]: Sovietskaya Geologiya, 1955, no. 4.

8. Smirnov, A. A. O ROLI PODZEMNYKH VOD V FORMIROVANII ZALEZHEY GAZOV PREIMUSHCHESTVENNO UGLEVODORODNOGO, AZOTNOGO, GELIYEVO-AZOTNOGO I UGLEKISLOGO SOSTAVA [ON THE ROLE OF GROUND WATER IN THE FORMATION OF STRATA-BORNE GASES: PRIMARILY OF A HYDROCARBONIC, NITRIC, HELIONITRIC AND CARBONIC STRUCTURE]: Questions of Hydrogeology and EngineeringGeology, no. 14, Gosgeoltekhizdat, 1956.

# Review Section

THE GEOLOGY OF THE U. S. S. R. VOLUME XXII: THE TURKMEN SOVIET SOCIALIST REPUBLIC. PART I. GEOLOGICAL DESCRIPTION. Luppov, N. P., ed., Sukocheva, M. P., and Neronova, L. V., assoc. ed: Ministry of Geology and Mineral Conservation, 658 p., Moscow, 1957. A Review by Mark Burgunker.

The Turkmen Soviet Socialist Republic is of interest because it is an area of great sedimentary thicknesses. The structures may represent continuations of the paleoenvironments in which the petroleum deposits of Azerbaidzhan, Dagestan, and the Stavropol uplift evolved. It must be pointed out at the outset, however, that the Alpine structures do not represent a continuation of the Caucasian system, in spite of the fact that this is suggested very strongly by topographic maps.

All visible structures in the area were produced by the Alpine orogeny; this holds for the intensely deformed geosynclinal Kopet-Dag ranges in the southwestern portions of the area, as well as for the gentle folds in the northern and northeastern portions. Drilling has not reached the Paleozoic basement in the Kopet-Dag as yet. This basement, however, outcrops in a few localities in the cratonic portions of the region.

The Kopet-Dag folded belt, strictly speaking, is the Turkmen segment of the great Khurasan-Turkmen arc which swings around the southern side of the Caspian Sea. The system has a dominant northwest strike east of Nokhur and a northeast strike west of it. The Kopet-Dag front-range anticline continues northwestward toward Krasnovodsk.

The most intense orogenic movements in the Kopet-Dag seem to have occurred in the Pliocene. This seems to be the time of the great thermal spring line thrust (to the northeast) of the front-range anticline.

Igneous rocks play a very minor role in the lithology of the Kopet-Dag. Sediment is 6, 000 to 8, 000 m thick, and most of these sediments are marine (of Upper Cretaceous and Cenozoic). It can be pointed out more specifically that the lithology of the Oligocene in the western portions of the mountain system is dominated by marine clays of the Oligocene segment of the Maikop sequence. Oligocene lithology in the central and eastern portions of the system is dominated by the red beds of the Karagaudan molasse.

The major tectonic units of the Kopet-Dag System are as follows:

The Kopet-Dag foredeep: The structure is defined, at least in part, by an area with a 90 mgal gravity anomaly near Ashkhabad. The foredeep is divided into two basins by a large uplift in the pre-Mesozoic basement near Kyzyl-Arvat; the smaller basin is the northwestern and the larger is the southeastern. The foredeep possesses an overall asymmetry. The basement rises gently northeastward (this is treated as the shelf of the Kara-Kum craton), and the southwestern flank of the basement rises much more steeply. The maximum depth of the top of the Mesozoic is estimated to be 7, 000 m; the maximum width of the Kara-Kum shelf (at Ashkhabad) is estimated to be 100 km.

The Kopet-Dag front-range geanticline: This geanticline is a line of elongated domes striking northeast. Deformation is believed to have resulted from the northeastward pressure of the more plastic Kopet-Dag mobile belt against the stiffer Kara-Kum craton. Specifically, the main components in this line of domes are: the Kyurendag anticline which is asymmetrical to the northeast, with a complete Cretaceous and Paleogene section outcropping on its southern flank; the west Kopet-Dag front-range anticline, which has an overthrust southeastern flank (the thermal spring line thrust); the Archman-Nokhur complex, which consists of two anticlines, one following the dominant strike of the system and the other, represented by the Ekiz and Kiasa-Kori ranges, following the dominant trent for a certain distance, then making a 90° turn to the northeast and plunging; the central Kopet-Dag front-range anticline, which extends from Bakharden to Ashkhabad, and which is characterized by a subordinate syncline on its northern flank; the Giaur anticline, perhaps the largest fold in the Kopet-Dag complex, which is entirely linear, northwest striking and plunging; and the east Kopet-Dag front-range anticline following the Soviet Iranian border for 20 km, which is entirely linear and is dominated by continental sediments of Neogene age.

The surface, or surfaces, along which the thermal spring line thrust was displaced dips at relatively high angles. Overthrusting of very early Cretaceous rocks over very late Cretaceous and Paleogene rocks indicate displacements of approximately 4, 000 m. This thrust, of course, cuts the Kopet-Dag front-range anticline. The strata in the lower wing of the recumbent are stretched and thinned at a number of localities.

The Khurasen-Turkmen arc finds expression in the inner Kopet-Dag anticlinorium. The apex of the system is in the Archman area. It should be noted that most of the folds belong to the eastern arm of the arc, i. e., the overall trend is northwest. A great many folds in the anticlinorium are either box folds or folds which have been squeezed at their "necks". It is pointed out that a box fold which has been tilted to the northeast and partly buried will appear to be a normal-type anticline slightly overturned to the southwest if the upper northeast edge is beneath the surface of the ground. This is given as the explanation for the apparent southwestward asymmetry of many of the folds. In the Kopet-Dag, slip faults make acute angles with the folds of both the front ranges and the folds of the Khurasan-Turkmen arc and the strike of the faults in the arc parallels that of the folds.

The overall stratigraphy of the Kopet-Dag possesses the following characteristics: the oldest sediments in the folded system are Upper Jurassic: these sediments consist of approximately 450 m of limestone and marl with very subordinate layers of gypsum and anhydrite. These sediments are succeeded by the Cretaceous sequence which consists of approximately 230 m of Barremian limestone and 1,250 m of Aptian and Albian clastics in the Kyurendag; just over 750 m of Hauterivian and Barremian limestone and as much as 1,300 m of Aptian and Albian clastics in the western Kopet-Dag; and as much as 1,300 m of Valanginian, Hauterivian, and Barremian limestone and marl overlain by 1,400 meters of Aptian, Albian, and later clastics. The carbonates-clastics sequence is reversed in Upper Cretaceous time; between 400 and 500 m of arenaceous claystones and argillaceous sandstones are succeeded by as much as 800 m of argillaceous marls; the former are Cenomanian, and the latter are Campanian. The Upper Cretaceous in the eastern Kopet-Dag is dominated by some 400 m of Turonian, Santonian, Campanian, and Maastrichtian marls and limestones; the section is capped by between 60 and 170 m of red beds which include gypsum. The lithology of the Tertiary is dominated as by as much as 1,680 meters of upper Eocene and lower Oligocene arenaceous clays in western Kopet-Dag.

The other two dominant i. e., regional structural complexes are the Kara-Kum craton and the Turkmen section of the Caspian lowlands.

The thick cover of horizontal Quaternary deposits on the first group of structures has prevented any appreciable degree of tectonic mapping. It seems to be a very shallow basin of great extent which opens, on the south, into Kopet-Dag foredeep. A very small number of exploratory wells indicates a possible maximum of 250 m for the Quaternary cover. The earliest known sediments seem to be of Cenomanian and Turonian age; the former consists of some 55 m of sands and clays, while the latter consists of approximately 30 m of calcareous clays. The Miocene is represented by as much as 2 m of Konka (middle Miocene) gypseous clays and over 35 m of Sarmatian (upper Miocene) calcareous clays.

The Turkmen section of the Caspian lowlands, the sections of the lowlands to the north, are characterized by low gravity values and enormous thicknesses of Quaternary deposits. A number of subordinate structures have been mapped in the basement. These include the Kara-Tepe anticline. This structure strikes northeast; and the northern flank is steeper than the southern. Maximum dip (mapped on the sediments of Baku age) is $6^{o}$. The anticline is cut by a large number of transverse faults. The Cheleken anticline is another structure in the basement. The strike of the fold is east-northeast, a considerable portion of the northern flank of the fold is exposed at the surface, and this flank dips to the north-northwest at an angle of $7^{o}$. The southern flank, on the other hand, is characterized by a dip which increases from $12^{o}$ at the outcrop to $20^{o}$ at depth. These relationships, however, do not exist in the mud volcano section of the anticline. Here, each volcano is situated at the center of a structural basin with an area between 5 and 10 $km^2$ and constant dips in all radial directions.

The (known) stratigraphic record in the Turkmenian section of the Caspian basin begins with middle Miocene clastics (the red beds). These are represented by 1,850 m of sand-clay deposits in the Nebit-Dag, 1,150 m of sands and clays (nine producing pools in a 140-m sand unit) at Kum-Dag, approximately 130 m of sands and clays at Cheleken, and between 70 and 75 m of similar sediments at the Boia-Dag. The Quaternary is represented by between 150 and 160 m of chocolate clays of Baku age, between 100 and 120 m of pink Khazar sandstones, as much as 15 m of Khvalinskoe sands.

Finally, the tectonics of the Krasnovodsk plateau are that of a syncline between the Kuba-Dag uplift on the southwest and the Tuarkyr anticline on the northeast. The strike of the syncline is governed by a structural boundary (the strike is west-northwest). The syncline is 40 to 45 km wide at its eastern end, and 65 to 75 km wide at its western end. The earliest sediments studied in the area are Teriary; 34 m of Paleocene and lower Eocene marls, 25 m of upper Eocene calcareous clays, and 190 to 220 m of later Eocene and Oligocene clays. There is a Pliocene sand-clay-conglomerate-gravel complex followed by 80 m of (dominately) carbonates; the maximum thickness of lower Pliocene clastics is 125 m.

# Notes on international scientific meetings

**REVIEWS OF SOVIET PAPERS PRESENTED AT THE**

**INTERNATIONAL ASSOCIATION OF VOLCANOLOGY**

**Toronto, September 1957**

The Academy of Sciences of the U. S. S. R. has published for its National Committee for Geodesy and Geophysics the following abstracts of papers presented by Soviet scientists at the September 1957 meeting of the International Association of Volcanology held in Toronto during the XI General Assembly of the International Union of Geodesy and Geophysics. Translation of abstracts by Paul Broneer.[1]

Gorshkov, G. S. GIANT ERUPTIONS OF VOLCANO BEZYMYANNAYA. On October 22, 1955, after a series of volcanic earth tremors which lasted three weeks, the volcano Bezymyannaya erupted for the first time in recorded history. The volcano is located at the center of the Klyuchevskaya chain; crater coordinates are 55 58' N. and 106 35' E. Its height before eruption was 3,085 meters (m) above sea level. Until recently, this volcano, a double massif whose western part is a large extrusive dome and whose eastern part is a younger stratified volcano, was little studied.

The eruption began with relatively weak explosions. In the middle of November, the explosions became stronger and a cloud of ash rose 6.5 kilometers (km) above the crater. Ash fell heavily within a 100-km radius of the volcano; on November 16 through 17, at Klyuchi volcanologic station, 11.5 millimeters (mm) or more than 7.5 kilograms per square meter ($kg/m^2$) of ash was accumulated during 24 hours of complete darkness. As a result of the November explosion, a crater 700 to 800 m in diameter developed approximately 200 m from the point of original eruption. For the next few months, pressure caused the dome to slowly rise. This growth was accompanied by a moderately strong avalanche of blocks and glowing ashes.

On March 30, 1956, an intensive eruption demolished the volcano's summit, completely changing its shape and the relief of the surrounding countryside. A cloud of ash rose more than 40 km above the volcano. Ash fell as much as 400 km to the northeast; at Klyuchi. 20 mm or 24.5 $kg/m^2$ of ash fell. The darkness was such that the local inhabitants had difficulty finding their houses. The ash falls were accompanied by strong, stormy discharges.

Toward the east, as much as 20 km from the crater, a fan-shaped spout of hot ash burst with great force, burned dry tree trunks, and stripped away bark. The eastern part of the volcano was affected by this explosion, and torrents of burning agglomerate filled the Sukhaya Khapitsa river valley and its tributaries for 18 km. Mudflows, formed as a result of melting snow, passed through the Bolshaya Khapitsa river valley and destroyed everything in their path. These flows spurted into the Kamchatka river, 80 km from the crater. Large masses of mud caused a 35 centimeter (cm) rise in the water level of this river for five days.

As a result of the explosion, the volcano height was lowered 200 to 300 m and a large east-facing, semicircular crater was formed. Pressure, continuing until autumn 1956, caused rebirth of the dome in the crater cavity.

A thousand secondary fumaroles vented at the surface of the agglomerate and formed the "Kamchatka valley of ten thousand smokes". During the intense melting of the glaciers and during torrential rains, the burning agglomerates, falling into water, gave rise to violent "secondary eruptions". Ash clouds rose 0.5 km and the ring of ash precipitation extended for several kilometers.

During the first few months of eruption, falling ashes were composed of hypersthenic andesite; these appeared to be products of the destruction of the ancient volcanic structure. Pumice debris of the fresh lavas flowing from the agglomerate and lava from the new dome were amphibolitic andesite. The overall volume of eruption products is grossly estimated at 3 $km^3$. The gas from the secondary fumaroles contained $H_2S$, $SO_2$, HCl, and $CH_4$. The temperature of the fumaroles in August 1956 was from $100^o$ to $200^o$.

More than 10,000 unusual volcanic earth tremors were felt during the eruption period. The amplitude of displacements in the Klyuchi mountains in some instances exceeded 1,000 $\mu$. No direct link between the explosions and earth tremors can be observed; however, at times, the tremors may have triggered explosions.

The March 30 explosion was accompanied by tremors and by an explosion wave which was recorded on common barographs at distances greater than 1,000 km. In the Klyuchi mountains, the amplitude of the explosion wave was

[1] Department of Geology, Columbia University, New York

23.5 millibars. The speed of diffusion, depending upon direction, was from 0.8 to 1.1 times the speed of sound. Seiches, as great as 12 cm, were recorded in the mouth of the Kamchatka river.

The energy of the March 30 explosion, defined by various means, was equal to $5 \times 10^{22}$ erg. The quantity of heat in the agglomerate torrent was not less than $5 \times 10^{24}$ erg.

In general, the eruption of the Bezymyannaya volcano most closely resembles the 1912 eruption; the study of its results allows the understanding of many of the Katmai phenomena and of the formation of the Valley of the Ten Thousand Smokes. In particular, it casts doubt on the formation of more basic magma by acid-magma assimilation of morainal material; also, the existence of a fissure in the valley through which the material which filled Katmai Valley was injected, is questionable.

Vlodavets, V. I. ON THE DEEP-SEATED STRUCTURES OF CERTAIN KAMCHATKA VOLCANOS. From the geologic structure of volcanos and of their surroundings, as well as from their surface shapes, an idea of their deep-seated structure can be formulated.

Mouths of volcanic channels (principal and lateral), marked by craters, explosion holes, domes, and dikes; fault structures; and other features revealed by erosion, aid in the determination of the structure, at depth of a given volcano.

Numerous examples exist of simple, and also more or less complex forms of volcanic structures, even in a single volcanic region or in one of its projections. In the northern Kamchatka, volcanos with various surface shapes have different deep-seated structures. This condition (a more complex deep-seated structure) is attributed to the active volcanos Klyuchevskaya, Plosky Tolbachi, Tsentralny Semlyachik, Shiveluck, Uzon, Maly Semlyachik, Karymskaya, and others.

The basaltic volcano Klyuchevskaya is a slightly truncated cone with multiple lateral craters on its northeast, east, and southeast flanks, located chiefly on 12 radii and hypothetically on three arcs. These radii are from 6 to 18 km long and have 3 to 11 craters and explosion holes. The arcs are 4 to 20 km long and each arc includes from 5 to 9 cones. In addition, some cones have no relation to the radii and arcs. A radial dike also occurs.

Tsentralny Semlyachik,is a demolished basaltic cone, containing and surrounded by 16 lava cones (domes) composed chiefly of andesites. These are located on five parallel lines trending northeast, with two northwest-trending branches.

Shiveluch, an andesite and basalt volcano, has a fairly gently sloping cone with a sectorial graben in its southern part. In the graben are radially aligned basalt dikes and laterally aligned andesite domes. The domes also occur on the southwest flank of the principal cone and are located on a line trending north northeast, roughly paralleling the southwest flank of the fault of the sectorial graben. There is a dome at the end of the southeast flank of the fault of the same graben.

The dacite cone-shaped volcano Karymskaya is in a caldera of the volcano Dvor. Dvor consists of lavas ranging in composition from basalt to andesite. In the central part of Dvor, on the wall of the fault formed by the caldera, a small tubular outcrop of dacite appears to be a lateral branch of the Karymskaya volcano's principal conduit.

If the problem of the deep-seated structure of simple volcanic elements is in general resolved simply and uniformly, the question of the roots of complex volcanos is harder to resolve and frequently has alternate solutions.

Generally, the paths taken by the volcano conduits are determined chiefly by local volcanic-tectonic dislocations and in part by regional tectonic faults.

In this article, an attempt is made only to discover the deep-seated structure of the active volcano Klyuchevskaya, based on location and time of lava extrusion in relation to successive variations in the lava composition, assuming the general concept of normal differentiation of basaltic magma, (the formation of relatively more acid derivatives in the upper parts of the column and more basic derivatives in the lower parts). It is generally admitted that feeders of lateral formations (craters, cones, domes, or even groups of these) of a complex volcano can be 1) branches of the principal conduit, 2) independent pipes that come from the volcanic magma chamber, or 3) branches closer to the principal conduit. But the farthest-removed lateral feeders are connected directly to the magma chamber.

When the lateral craters of the Klyuchevskaya volcano erupted in 1938, the acidity of the extruded lavas increased almost directly with the rise in elevation of the point of issue, the extruded lavas from the lowest point (in the Bilukai crater) during the course of year gradually became more acid.

On the basis of changes in lava composition over space and time, and of the correlation of extrusion loci, it is concluded that the lateral feeders are directly connected with the magma chamber of the Klyuchevskaya volcano and not with its principal conduit.

Naboko, S. I. THE GASES OF CERTAIN VOLCANOS OF THE KAMCHATKA-KURIL REGION AND THE PRODUCTS OF THEIR REACTION WITH ATMOSPHERE, WATER, AND ROCK. As the result of the study of gases in lava masses in different cooling stages, of the composition of their products from reaction with atmosphere, water, and rocks; of the formation of contemporaneous hot springs; of deposits precipitated from thermal waters; and also of the disposition of certain elements in post-volcanic processes of certain volcanos of the Kamchatka-Kuril region, the following conclusions are made:

1. Eruptive magmas, in general, contain the same volatile components. The composition of gases depends on the stage of eruption and cooling of lava masses. During the initial stage, at high temperature, all the volatile components are present in the gases from the Klyuchevskaya.

During lava cooling, the halogen-gas content of water vapor first decreases, then sulfureous gas, and finally carbonate gas, which partially reflects the initial gas content in the magma (gases in water vapor, in decreasing abundance, are the C, S, Cl and F groups).

2. Sixty-seven minerals from the fumaroles in the Kamchatka volcanos have been studied. The composition of the sublimates and discolorations partially reflects the composition of the lava.

3. The character and the degree of influence of the volcanic ejecta on the composition of the thermal waters depends on the state of the extruded magma, and on the temperature and depth at which condensation and dissolution in meteoric waters is produced.

4. Mineral precipitation is related to change in thermodynamic conditions during thermal-water emanation. However, the composition of these deposits only partially reflects the composition of thermal waters.

5. The nature of the post-volcanic change in the rocks depends, in general, on the acidity and concentration of the solutions. The process of post-volcanic change in the rocks is always accompanied by surface formation of metallic sulfates, which are brought into solution as a result of the acid dissolution of the rocks. The sulfates are , at a certain depth, changed to sulfides, which are deposited when descending solutions of iron sulfates leached from the rocks come in contact with ascending solutions rich in the sulfide ion.

6. The most intense distillation of volatiles takes place during the initial high-temperature lava phase. The gases are richest in metals.

As a result of post-volcanic processes, elements are regrouped: some dispersed, others concentrated.

Ivanov, V. V. CONTEMPORARY HYDROTHERMAL ACTIVITY WITHIN THE LIMITS OF THE KURIL-KAMCHATKA ISLAND ARC AND ITS RELATION TO VOLCANIC PHENOMENA.

The Kuril-Kamchatka zone of contemporary volcanism, which represents the northwesternmost part of the Pacific island-arc system, is characterized by very intensive and varied hydrothermal activity. The character and genesis of the Kamchatka and Kuril Islands hot springs are different in principle from those of hot springs formed in other regions of the Soviet Far East.

The far-reaching investigations made in recent years in the U. S. S. R. (by B. I. Piip, V. I. Vlodavets, V. V. Ivanov, T. I. Ustinov, S. I. Naboko) on the geologic conditions of the emanation and composition of volcanic gases and thermal waters in this zone allow definite proposals for their genesis and their comparison with known hot springs in Iceland, Alaska, New Zealand, and other regions.

The formation and special distribution of the different types of hot springs of Kamchatka and the Kurile Islands is determined by a series of factors: 1) by recent phenomena of active volcanism, 2) by deep thermometamorphism of rocks, 3) by a broad development of the most recent tectonic fractures, and 4) by strongly anomalous geothermal conditions.

Contemporary hydrothermal activity within the limits of recent volcanism of the Kuril-Kamchatka region is manifest in three general ways: 1) eruptions of hot volcanic gases of two principal types: a) high-temperature (hundreds of degrees) gases circulating under geothermal conditions which eliminate their reciprocal action with water in the liquid phase (containing Cl, $CO_2$, $SO_2$, $H_2S$, and a series of other gases), and b) relatively low-temperature ($100^o$ to $150^o$ gases), which are intermingled with, to some degree, by subterranean water (containing generally $CO_2$ and $H_2S$); 2) thermal springs which are fed by waters of different genetic types: a) sulfureous carbonate waters (from fumaroles) formed in the upper zone of oxidation under the immediate influence of volcanic gases; b) carbonate springs, whose formation is generally linked with deep thermometamorphic processes; c) nitrogenous-alkaline waters that are formed at depth under reducing conditions and high temperatures, and whose genesis is not related to volcanic and thermometamorphic processes; 3) jets of steam which are formed as a result of vaporization of ascending superheated charged waters or of descending

cold subterranean water which comes in contact with rocks at high temperature.

All the enumerated hot springs are formed generally from the infiltration of waters of atmospheric origin; however, metamorphosed ancient marine water plays a part in the formation of water contained in marine sedimentary rocks at great depth. Some water in fumarole hot springs is a condensation of volcanic gases.

Hot springs of the Kuril-Kamchatka volcanic zone are distributed with definite horizontal and vertical zonality. The region of active contemporary volcanism that embraces the Kuril Islands and southeastern Kamchatka and the region of lower Quaternary volcanism of the central and northern parts of the Medial mountain chain of Kamchatka are the largest and most important volcanic zones in terms of hydrothermal activity.

One of the regions of most intense contemporary hydrothermal activity in Kamchatka is the Valley of the Geysers; more than 20 large geysers and many hot springs are fed by superheated alkalic-silicic sources.

The sulfur-carbonate and carbonate hot springs of Kamchatka and the Kurils,just like the analogous thermal waters of other regions of Recent volcanism, should be considered contemporary metalliferous hydrothermal solutions which ensure the transport and, under changing geochemical and thermodynamic conditions, the deposition of various metals (Fe, Al, As, Mg, and for example, Ca ).

The many-sided study of the composition and conditions of formation of hot springs in regions of contemporary volcanism of great interest in determining the relationship between the processes of contemporary volcanism, of thermometamorphism, and of mineral formation. Hot springs also have great practical importance as sources of thermal energy, as well as their use as very valuable medicinal waters.

Ustiev, E. K. ANUY VOLCANO AND QUATERNARY VOLCANISM OF NORTHEAST ASIA. Later Quaternary volcanic phenomena in the southern Anuy mountain chain (Prikolymskoye Zapolyare) are related to the valley of the Monni river. The initial eruptions consisted of large linear flows discharged from tectonic fissures paralleling the valley, the mountain chain, and the folded structures. A lava flow as much as 50 m thick covers the whole valley floor for 60 km.

An interesting peculiarity of the fissure phase was the creation of many lava lakes which remained liquid even after the largest part of the flow was covered with a hard crust. Many tunnels cutting the lava at the bottom of the lakes indicate the presence of high gas and steam pressure under the bed of the flow. Apparently, the lava lakes were formed as a result of an explosion of vapors caused by the melting of the ice. Floods of lava marking a second volcanic phase, were discharged at the intersection of several tectonic fissures which diverged from the line of inital discharge. A new magma chamber of the central type was formed.

The volcano, named by the author the "Anuy volcano", was formed in a massive granodiorite intrusive and is characterized by repeated eruptions chiefly of the explosive type. The life of this volcano ended with a large and relatively calm discharge of a great mass of a great mass of lava, which flowed down the Monni valley and covered older lava. The average length of the flow is 16 km, of which 12 km are in the Monni valley.

The total lava volume discharged in the two eruption phases is almost 3 $km^3$. The recent age of these eruptions is indicated a) by the lava filling a contemporary valley, whose head was sculptured by a mountain glacier; b) by the lack of river-network or acclimation to new conditions and, especially, by lava-dammed lateral tributaries of the Monni river; c) by the preservation of the morphologic pecularities of the lava-flow surface; d) by the preservation of the volcano's cone.

Legends still preserved among the Lamuts intimate that Anuy erupted within historical time.

Shirinyan, K. G., GENERAL FEATURES OF RECENT VOLCANISM IN ARMENIA.

The Soviet Socialist Republic of Armenia is a classic region of extinct Recent volcanos. The volcanic products in this country --various lavas. tuffs and tuffaceous lavas, pumices, scorias, obsidians, trasses, pozzuolanas are of great interest for science and industry.

Volcanic activity in Armenia characterizes all the epochs of its geologic evolution, from the early Paleozoic to Recent inclusive. Recent volcanism, like that of more ancient epochs, is influenced by the geotectonic development of this region and of the entire Little Caucasus.

The present-day complex structure of Armenia resulted from Caledonian, Hercynian, and Alpine orogenies. In early Pliocene, isolated consolidated rigid regions (the Argats massif, the Gegamsky mountain area, the Daralagezsky anticlinorium, the southern Shakhdagsky mountain chain separated by comparatively limited synclinal valleys between the mountains were formed. The Little Caucasus was differentially uplifted, especially within the Armenian geanticline.

Differential tectonic movements (elevation of rigid blocks and relative synclinal submergence between the mountains has stimulated, at the junctures of separate structures and at the vaulted parts of rigid blocks, the formation of large tectonic fractures, to which subaerial (terrestrial) volcanism is related. The deep tectonic faults fracture the earth's surface more easily in areas of ancient, rigid, metamorphosed rock. During Pliocene and post-Pliocene time, important block uplifts, in many instances, caused a spatial connection between the separate chambers of magma and the spurts of lava from the ancient substructure.

Within the limits of Armenia and the adjacent parts of the Little Caucasus, the following structural geomorphic zones and spatially related magma chambers can be determined a) the Akhalkalakskoye plateau, the most elevated part of the Somkhetsky-Kafansky anticlinorium, b) the Argats volcanic shield, c) the Akhmagan volcanic plateau, d) the southern Shakhdagsky mountain chain; and e) the Karabakhskoye highland.

The Aragats volcanic shield and the volcanos of the Akhalkalaskoye mountain region are located along an assumed deep-seated fracture extending from Mt. Ararat to the Dzhavakhetsky mountains; along a similar fissure in the southerly direction are the volcanic centers of the Akhmagan plateau and the volcanic cones of the Karabakhskoye highlands. Certain volcanic structures are situated along a deep-seated fracture extending between the cis-Araksian (to the southwest) and Armenian (to the north), tectonic zones of the Little Caucasus.

The Plio-Pleistocene volcanic cones of Armenia are subdivided, on the basis of origin, morphology, and rock composition, into scoriaceous lava cones, stratified-lava cones (resulting from one or more flows), stratovolcanos, and plug domes of obsidian and rhyolite. These are the result of Hawaiian, Strombolian, and Vulcanian phases of activity, as well as fissure flows.

The magma chambers which, during the upper Pliocene, were located in the center of the uplifts were gradually displaced toward the periphery. In the Quaternary, they are generally located along fractures in the Pliocene volcanic shields. Magma gradually changed from basalt to dacite and rhyolite during the Pliocene and post-Pliocene. In particular cases, this successive change in composition was more complex. Magma, extruded in the Armenian volcanic region, is increasingly alkaline from the Cambrian to Recent.

The mineralogic composition of all Plio-Pleistocene volcanics is rather constant. The more acidic volcanics contain various feldspars, augite, and hypersthene; olivine is present in the lavas of basic composition. In the acid vitreous extrusives the groundmass is more acid than the phenocrysts.

Two periods of intense volcanic activity, corresponding to the Aktchagyl and the Apsheron, are distinguished in the upper Pliocene; from two to five are distinguished from correlation of lava flows and erosion terraces in the Quaternary. Tuffs and tuffaceous lavas (ignimbrites) of Quaternary age occur only in the Argats mountain region. The fissures in the flanks of Mt. Argats and, in certain cases, scoriaceous-lava structures, served as eruption centers for these tuffs and tuffaceous lavas.

Investigations of the magnetic properties of the Pliocene and post-Pliocene lava flows show that these lavas are differentially magnetized and that the Tertiary lavas are in abnormal and Quaternary lavas in normal relation to the magnetic field of the earth.

Afanasev, G. D. SPECIFIC PROPERTIES OF COMPOSITION AND THE MECHANISM OF PENETRATION OF THE CENOZOIC VOLCANIC ROCKS OF THE CAUCASUS. Magmatic activity in the interval between the Eocene and post-Pliocene (absolute age almost 60 million years) terminated the development of the Mesozoic geosyncline in the northern Caucasus. The complexity of tectonic processes resulted in the outcrop on the Cenozoic surface of plutonic and volcanic rocks of various ages, related to the evolution of the general magmatic source.

The Cenozoic volcanics have similar mineral assemblages and overall chemical composition. Granitoid intrusions of the Tyrnyauz type occur as hypabyssal equivalents of the Cenozoic effusives. Highly alkaline rocks (five mountain trachyrhyolites and trachytes of the far-western Caucasus) compose transitional facies within effusive blankets. Roots of young effusives are composed of andesite and rhyolite-dacite. Younger lavas and tuffaceous lavas (ignimbrites) of post-Pliocene age are found in the northern forelands. Rocks of andesite to dacite composition were discharged from volcanic structures of the central-vent type (Elbruz, Kazbek).

Drilling has shown that small outcrops of Tertiary intrusives (about 10 $km^2$) extend more than 1.5 km below the surface.

Oligocene argillites contain widely distributed extrusive bodies and fractures and sediments near the surface due to their incompetency at depth. Cretaceous sediments outcrop adjacent to post-Pliocene volcanics near a tectonic fracture. Drilling 2,000 m revealed a water horizon with temperatures near $100^o$.

Recent volcanic activity in this region has probably influenced the composition of this water and its temperature. A high Clark value

for radioactive and certain dispersed elements in a post-effusive rhyolite is one of the specific geophysical features of post-Pliocene volcanism in the northern caucasus.

Cenozoic volcanism in the northern Caucasus occurred in the region of folding which, during the Paleozoic and Mesozoic, was also an area of intense volcanic and plutonic activity. Therefore, it has been a zone of extreme tectonic and volcanic activity for about 500 million years.

Lebedev, A. P., THE TUNGUSKA PALEOVOLCANIC FORMATION.

The Tunguska depression (a synclise, according to N. S. Shatskiy), which forms the western part of the Siberian platform was, during the upper Paleozoic and lower Mesozoic, a region where volcanic activity took place under platform tectonic conditions. The type of the volcanic processes, their succession and intensity, was determined by contemporary tectonic conditions of the Siberian platform and the adjacent geosynclines.

The younger phases of volcanic activity, whose products covered almost the whole surface of the Tunguska depression, were explosive and resulted in the deposition of considerable quantities of pyroclastic material with almost total absence of lavas. The eruptions were made through structures of the central type and partially of the fissure type.

The succeeding phases of volcanic activity, dating from the Lower Triassic consisted of basaltic magma flows from fissures, and resulted in the formation of typical flow bodies (lava blankets), as well as of hypabyssal bodies (stratiform injections) mainly in the northwest part of the platform.

The Tunguska volcanic rocks, related to a typical geological platform situation, are distinguished from well-studied volcanic formations in fold provinces by the following:

1. Volcanic activity continued for a considerable length of time in response to slow oscillatory movements of the platform. As a result, transportation of the pyroclastic material by streams and other agents played a major role in the formation of the rocks of this phase. Volcanics and sediments are finely interrelated or form rocks of a mixed composition.

2. The more recent fissure flows are characterized by an extremely close interrelation and by reciprocal passage between volcanic formations belonging, on the one hand, to typical effusive facies and, on the other, to hypabyssal facies of basaltic magma. A series of small basaltic injections are parallel to subaerial basalt blankets near the surface; these abundantly saturate the horizontal sedimentary deposits of the upper level of the platform. Also, both effusive and hypabyssal rocks are similar in appearance and in petrographic composition.

3. Intensive development of post-magmatic mineralization is related genetically to hydrothermal derivatives of the basalt effusions and also to the influence of more recent traprock intrusions which cut the entire volcanic field of the Siberian platform.

4. The periodic character of the traprock intrusion of the upper structural level of the platform, in view of the uniformity (mean) of the chemistry of the magmatic material, suggests that the magma arose periodically from the basalt substratum under the rocks of the platform basement. At the same time, certain provincial peculiarities in the composition of the rocks of the formation and of its post-magmatic derivatives observed in various areas of the platform indicate certain difference in the composition of the basalt substratum and, possibly, the presence of several intermediary chambers.

Afanasev, G. D. THE LAWS OF THE EVOLUTION OF MAGMATIC PROCESSES IN FOLDED REGIONS, EXEMPLIFIED BY THE GREAT CAUCASUS, IN THE LIGHT OF INVESTIGATIONS OF ABSOLUTE AGE.

The investigations of the absolute age of the magmatic and in part sedimentary formations of the Great Caucasus were made by applying the K/Ar accelerated mass-spectrographic method, based on the principle of isotope dilution. This method has, during a short time, permitted us to obtain a significant quantity of dependable figures (close to 200) on absolute ages.

The evolution of the magmatic processes accompanying the development of the geosyncline is represented by a complex series of magma formation. As a result, rocks and auxiliary minerals have contained an essentially uniform composition. The Great Caucasus are an example of repeated magmatic activity within the limits of the evolving geosynclinal regions.

In the Cambrian to Silurian periods, ophiolite, (a spilitic-keratophyric association of gabbro-amphibolites and ultrabasics), containing intrusions of plagioclase and later subject to sodic metasomatism, was developed. This stage corresponds to the geosyncline developed during the Caledonian in the contemporary northern Caucasus region. An upper Paleozoic complex composed of magmatic and metasomatic formations with pronounced potassic metasomatism corresponds to the terminal Hercynian stage

stage of the development of the northern Caucasus geosyncline. The incomplete magmatic cycle of the northern Caucasus geosyncline, beginning with the injection of the plagioclase-granite intrusions which mark the end of ophiolite development and ending with the Paleozoic granitoids of essentially potassic composition, lasted 150 million years.

A geosyncline was formed in the Trans-Caucasus, during the Jurassic and Lower Cretaceous. Magmatic activity accompanying the development of this geosyncline also resulted in ophiolite formation, which terminated with the plagioclase-granite intrusions. During the Upper Cretaceous, more granite was intruded in alkaline granitoids and proper alkaline rocks (nepheline syenites, epileucitic rocks). The alkaline rocks of the Trans-Caucasus are in age and magma type similar, close to the alkaline rocks of the Apennine peninsular. According to the data on absolute age, the time of formation of the Mesozoic-Cenozoic geosyncline is calculated to be between 120 million and 130 million years ago.

Within the region of terminal development of the development of the northern Caucasus Paleozoic geosyncline indications of effusive and intrusive magmatic activity representing the echo of the magmatic processes that accompanied the development of the Trans-Caucasian geosyncline during the Mesozoic and Cenozoic eras, are present.

Researchers into the absolute age confirm the great importance of alkaline metasomatism as a stage in the development of the magmatic source which led to the formation of certain varieties of granites.

Field and experimental investigations indicate the possibility of migration of radiogenic argon during reheating of already cooled rocks. This may facilitate the use of the argon method in deciphering the petrogenic processes in the complex history of the development of geologic formations. Data resulting from petrologic and chronologic investigations of the Caucasus, the Urals, and the Far East allow comparison of the evolution of magmatic activity in these regions of folding.